TESIS DE DOCTORADO

THEORETICAL AND COMPUTATIONAL STUDY OF IONIC LIQUIDS CONFINED IN TOPOLOGICALLY COMPLEX MICRO AND NANO STRUCTURES

Hadrián Montes Campos

ESCUELA DE DOCTORADO INTERNACIONAL

PROGRAMA DE DOCTORADO EN CIENCIA DE MATERIALES

SANTIAGO DE COMPOSTELA

2020

USC
UNIVERSIDADE
DE SANTIAGO
DE COMPOSTELA

DECLARACIÓN DEL AUTOR DE LA TESIS

Theoretical and computational study of ionic liquids confined in topologically complex micro and nano structures

D. Hadrián Montes Campos

Presento mi tesis, siguiendo el procedimiento adecuado al Reglamento, y declaro que:

1) *La tesis abarca los resultados de la elaboración de mi trabajo.*
2) *En su caso, en la tesis se hace referencia a las colaboraciones que tuvo este trabajo.*
3) *La tesis es la versión definitiva presentada para su defensa y coincide con la versión enviada en formato electrónico.*
4) *Confirmo que la tesis no incurre en ningún tipo de plagio de otros autores ni de trabajos presentados por mí para la obtención de otros títulos.*

En Santiago de Compostela., 21 de Septiembre de 2020

Fdo.: Hadrián Montes Campos

USC
UNIVERSIDADE
DE SANTIAGO
DE COMPOSTELA

AUTORIZACIÓN DEL DIRECTOR / TUTOR DE LA TESIS

Theoretical and computational study of ionic liquids confined in topologically complex micro and nano structures

D. Luis Miguel Varela Cabo, catedrático del área de Física da Materia Condensada, del Departamento de Física de Partículas de la Universidade de Santiago de Compostela,

INFORMA:

Que la presente tesis, corresponde con el trabajo realizado por D/Dña. Hadrián Montes Campos, bajo mi dirección, y autorizo su presentación, considerando que reúne los requisitos exigidos en el Reglamento de Estudios de Doctorado de la USC, y que como director de ésta no incurre en las causas de abstención establecidas en Ley 40/2015.

En Santiago de Compostela, 21. de Septiembre de 2020

Fdo.: Luis Miguel Varela Cabo

USC
UNIVERSIDADE
DE SANTIAGO
DE COMPOSTELA

Resumo

Os líquidos iónicos (LIs), ou sales fundidas a temperatura ambiente, son considerados hoxe en día como un dos materiais avanzados máis prometedores e están a atraer moita atención nas últimas dúas décadas debido as súas interesantes propiedades. Os LIs son materiais formados unicamente por ións que se atopan en estado líquido a temperaturas inferiores a 100 °C. É xeralmente admitido que esta baixa temperatura de fusión obtense debido as grandes asimetrías entre anións e catións, as cales debilitarían a enerxía de rede evitando así obter un sólido cunha lata simetría. As súas propiedades, tales como a súa baixa presión de vapor, a súa nano estructuración ou a sía gran resistencia a diferencias de potencial os fan desexables para aplicacións tales como a catálise, fluídos térmicos, lubricantes ou dispositivos electroquímicos. É nesta última aplicación a que será obxecto de estudo preferente nesta tese. Ademais, os LIs son considerados *disolventes de deseño*, debido a que é posible combinar diferentes anións e catións dando lugar a millóns de combinacións posibles. Debido a isto é posible escoller a combinación que reúna as propiedades óptimas para unha tarefa en concreto.

O interese do uso de LIs en dispositivos electroquímicos debese a que teñen unha gran ventá electroquímica, é dicir, se manteñen estables baixo un amplo rango de diferencias de potencial. Esto debería permitir en teoría a fabricación de dispositivos electroquímicos con un rango de voltaxe de funcionamento maís amplo e, no caso concreto de dispositivos para o almacenamento de enerxía, permitiría unha maior potencia e capacidade. Nestas aplicacións a rexión do espazo onde ten lugar as interaccións maís relevantes é na interfase eléctrodo-líquido. Ademais, para conseguir un rendemento maior é frecuentemente desexable traballar con eléctrodos que teñan un cociente superficie volume grande. Polo tanto, resulta imprescindíbel coñecer detalladamente como se comportarán os LIs cando se atopen confinados en recintos con poros nanométricos. Este será polo tanto o obxectivo principal da tese, o análise da estructura e dinámica d LIs baixo condicións de nano-confinamento. O estudo do confinamento será realizado por partes, comezando polo es-

tudo de como a propia nano estruturación inherente dos LIs afecta a súa estrutura, pasando polo análise da estrutura dos LIs en interfases planas e rematando co estudo de LIs próticos e apróticos confinados dentro de unha nano estructura topoloxicamente complexa.

Para obter istos resultados foron utilizadas ferramentas computacionais, isto nos permite ter una ccesaccesoo directo ás propiedades microscópicas dos LIs. Para este estudo utilizaremos diferentes técnicas dependen da da precisión coa que necesitemos traballar. En concreto as dúas ferramentas que foron maís utilizadas foron a simulación por dinámica molecular clásica (MD) e a simulación usando a teoría do funcional densidade cuántica (DFT). As simulacións por MD foron as utilizadas para para estudar as propiedades dos LIs en escalas espaciais de decenas de nm e temporais de decenas de ns. Neste método non se incluen de forma os electróns dos átomos e polo tanto se asume que non hay unha variación das densidades electrónicas durante o transcurso da simulación. Para a realización destas simulacións se utilizou a suite de simulación de código aberto GROMACS[1] xunto co campo de forzas OPLS-AA,[2] o cal é amplamente utilizado para simulacións de líquidos. Pola outra banda, os cálculos DFT foros os empregados para a obtención e caracterización de estruturas de equilibrio cunha gran precisión en escalas espaciais subnanométricas. O programa escollido para á realización de ditos cálculos DFT foi o programa comercial VASP.[3] Este programa resolve as ecuacións de Kohn-Sham utilizando unha expansión da densidade electrónica do sistema en ondas planas. Para á execución deste programa empregáronse diferentes funcionais de intercambio e correlación dependendo do sistema a estudar, en concreto empregáronse os funcionais PBE e B3LYP.

[1] **Mark James Abraham, Teemu Murtola, Roland Schulz, Szilárd Páll, Jeremy C Smith, Berk Hess, and Erik Lindahl,** GROMACS: High performance molecular simulations through multilevel par allelism from laptops to supercomputers, *SoftwareX,* **1**(19–25), 2015 (.)

[2] **William L Jorgensen, David S Maxwell, and Julian Tirado -Rives,** Development and testing of the OPLS all-atom force field on con formational energetics and properties of organic liquids, *J. Am. Chem. Soc.,* **118**(45), 11225–11236 (1996).

[3] **GeorgKresse and Jürgen Furthmüller,** Efficient iterative schemes for ab initio total energy calculations using a planewave basis set, *Phys. Rev. B,* **54**(16), 11169 (1996).

Comezamos o estudo da estructura baixo confinamento dos LIS no Capítulo 4 cunha avaliación da validez do campo de forzas a empregar durante os seguintes estudos. En concreto se avaliaron as diferencias na estructura en na dinámica dunha mistura de bis-(trifluorometilsulfonil)-amida (TFSI) 1-butil-3-metilimidazolio (BMIM) con bis-(trifluorometilsulfonil)-amida de litio. Para elo realizaronse simulacións MD con campos de forzas polarizables e non-polarizables. O campo de forzas non-polarizable que escollimos para o estudo foi o OPLS-AA, mentras que para o campo de forzas polarizable escollimos o APPLE&P.[4]Ademais, se engadiu unha versión do campo de forzas APPLE&P cos términos de polarización desactivados (APPLE&P-NP), pero se modificar ningún outro parámetro do potencial co fin de avaliar se é preciso recalcular os parámetros de un campo de forzas ao acender ou apagar os termos de polarización. A escolla de este sistema debeuse a que, debido ña elevada densidade electrónica presente non ións de litio, a polarizabilidade do campo de forzas debería xogar un papel moi importante nas propiedades deste sistema. Para istos sistemas analizáronse tanta a estructura como a dinámica monoparticular. A primeira avaliáronse a través da función de distribución radial (RDF) e a súa integral, a cal se corresponde co número de coordinación a unha determinada distancia. A dinámica, polo outra banda, avaliouse utilizando os desprazamentos cadráticos medios, a función de autocorrelación da caixa de solvatación a función de autocorrelación de velocidades e a súa transformada de Fourier, a densidade vibracional de estados. A estructura mostrou estruturas moi similares para os dous campos de forzas completamente optimizados (OPLS-AA e APPLE&P), mostrando só pequenas diferencias nas distancias de equilibrio entre o litio eo LI. Pola outra banda, o campo de forzas APPLE&P-NO mostrou unha coordinación do litio moi diferente á obtida mediante os outras campos de forzas. No tocante á dinámica a polarizabilidade xoga un papel moi relevante, con grandes diferencias no desprazamento cadrático medio entre o campo de forzas polarizable e o non-polarizable. A propiedade máis afectada resultou ser a función de correlación da caixa de solvatación. Dita fun-

[4]**O. Borodin,** Polarizable force field development and molecular dynamics simulations of ionic liquids, *J. Phys. Chem. B,* **113**(33), 11463–11478 (2009).

ción amosa un tempo de residencia do litio na súa caixa de solvatación ordes de magnitude maiores no caso do campo de forzas non-polarizable fronte ao polarizable, o cal pode asociarse a unha maior forza promedio na configuración de equilibrio. Non obstante, un análise da densidade vibracional de estados amosa que ámbolos dous campos de forzas producen distribucións simulares, pero con corremento cara o azul para o campo de forzas non-polarizable. Este estudio permítenos concluír que os campos de forzas non-polarizables son adecuados para o estudo da estructura, pero non para o estudo da dinámica. Ademais tamén nos permite concluír que tras engadir a polarización a un campo de forzas é preciso recalcular os seus parámetros.

Co noso campo de forzas debidamente validado continuamos o noso estudio analizando a nano estructura inherente ao LI (Capítulo **??**). Esta nano estructura impón un confinamento en rexións polares e apolares intrínseco ao LI. Dito confinamento da lugar ao paradigma da solvatación nano-estructurada, segundo o cal outras moléculas son disoltas nas diferentes rexións do seno do LI atendendo a súa polaridade. Polo tanto as moléculas polares se disolverán nos nano dominios polares do LI e as apolares nos nano dominios apolares. Para comprobar este paradigma se realizaron simulacións de MD de nitrato de etilamonio (EAN) e nitrato de butilamonio (BAN) misturado con 1-propanol, 1-butanol e 2-pentanol. A particularidade de estes alcohois ñe que amosan unha cabeza polar e unha cadea alquílica apolar. Dado que son moléculas anfifílicas, segundo o paradigma da solvatación nanostructurada deberían ser disoltas na interfase entre os nano dominios polar e apolar. Ademais, este comportamento anfifílico o comparte xunto co catión do LI, polo que deberíamos ver unha competición entre ambas moléculas pola mesma rexión do seno do LI. Para avaliar esta competición estudamos a estructura e a dinámica monoparticular de ditas misturas. A estructura foi avaliada utilizando a RDF, a función de distribución espacial e o número de enlaces de hidróxeno por molécula.A dinámica foi avaliada utilizando a función de correlación de velocidades e a súa transformada de Fourier. As RDFs mostraron cambios significativos ao engadir alcohol fronte á distribución do LI puro. Pola outra banda, a función de distribución espacial mostrou que, efectivamente, tanto o alcohol como

o catión compiten pola mesma rexión do espazo ao redor dos anións, coa salvedade de que a capacidade de formar múltiples enlaces de hidróxeno do catión permítelle acceder a unha configuración bidentada. O análise do número de enlaces de hidróxeno por molécula corroborou dita imaxe mostrando un reemprazo gradual das moléculas do catión por moléculas de alcohol a medida que a concentración de alcohol aumenta. Pola outra banda, a dinámica non amosou diferencias significativas para o LI puro e o misturado con alcohol. Esto nos permitiu concluír que a imaxe proposta pola solvatación nano-estructurada é correcta e que en LIs con unha amplia rede de enlaces de hidróxeno esta interacción é tan importante como a interacción de Coulomb entre anións e catións.

A continuación procedimos a estudar a interfase eletrodo-LI para sistemas con eléctrodos planos (Capítulos 6, 7 y 8). Comezamos estudando a estructura da interfase nas direccións paralelas á interfase (Capítulo 6). Para o estudo utilizamos simulacións de [BMIM][BF_4] (un LI prótico) misturado con diferentes aditivos confinados entre dous eléctrodos de grafeno. O análise da estructura en ditas direccións mostrou a existencia de dúas conformacións diferentes para os anións situados máis preto do ánodo. Dependendo da composición exacta da mistura LI máis aditivo, este se configuraba en patróns hexagonais ou de bandas. Para o estudo de dito fenómeno plantexamos un modelo teórico baseado na teoría fenomenolóxica de Landau-Brazovskii. Este modelo predí a existencia de diferentes fases, incluíndo patróns de bandas, hexagonais e unha fase homoxénea. A configuración final do sistema segundo este modelo debería depender só da densidade de carga efectiva na interfase. Polo tanto o tipo de patrón obtido debería ser independente da composición do eléctrodo e do LI. Ademais, para confirmar estos resultados realizamos simulacións de Monte Carlo de modelos xenéricos de ións distribuídos sobre unha rede. Utilizando este modelo puidemos obter un diagrama de fases de que patrón debería ser o resultante dependendo das interaccións anión-catión e cuxos resultados estaban en acordo cos resultantes de MD, Estos resultados teórico-computacionais predín polo tanto a existencia de polo menos dous patróns posibles para os ións na interfase electrodo-LI. Ademais, ditos patróns deberían ser modificables externamente por calquera interacción que poida modificar a densidade

efectiva no eléctrodo.

Co fin de estudar como se produce o cambio entre estos patróns, no Capítulo 7 realizamos un estudo extensivo das propiedades dos patróns para unha mistura de [BMIM][BF_4] con $LiBF_4$ confinada entre dous eléctrodos de grafeno. A estos eléctrodos se lles engadiron unha fracción de defectos de vacantes co fin de crear modificacións locais da densidade de carga na interfase. Estos cambios nas densidades de carga deberían, según o concluído no estudio anterior, ser capaces de modificar a estructura bidimensional da interface. Para elo comezamos realizando un estudo de como se ve modificada a estructura e a distribución de carga do grafeno ao engadir vacantes. Este estudo preliminar mostrou que o grafeno se mantén plano tras quitar un dos seus átomos, en oposición ao que defendían algúns estudios previos da bibliografía. Ademais, usando ditos resultados puidemos crear un modelo sinxelo de redistribución da carga da vacante entre os seus átomos veciños. Utilizando este modelo realizamos simulacións de MD con diferentes fraccións de defectos distribuídos aleatoriamente polo eléctrodo. Os resultados de ditas simulacións foron analizados utilizando a distribución da densidade, tanto na dirección perpendicular como nas direccións paralelas á interfase, funcións de correlación da densidade e distribucións de enerxía potencial no eléctrodo. Ademais, se utilizou o algoritmo de Otsu para dividir a interfase en rexións con e sin presenza de anións para unha avaliación maís profunda das propiedades dos patróns. Este estudio mostrou que os defectos non son capaces de alterar de forma significativa a estructura do LI na dirección perpendicular á interfase. Ademais, este cambio non se produce de forma gradual, se non que se produce de forma repentina unha vez se supera unha fracción crítica de defecto. Este estudo amosou ademais que a transición entre patróns bidimensionais pode modificar propiedades macroscópicas do sistema.

Acabamos o estudo de interfases planas no Capítulo 8 estudando misturas de [BMIM][BF_4] con $LiBF_4$ entre dous eléctrodos de borofeno. Estos eléctrodos teñen a particularidade de ser rugosos a nivel atómico. Este estudo foi pioneiro no estudo de interfases de borofeno con LI e nos permite avaliar oss efectos que as rugosidades poden ter nas propie-

dades do LI. Comezamos o estudo con un cálculo DFT da distribución de cargas de unha monocapa de borofeno cargado. Estas distribucións de carga utilizáronse a continuación para realizar simulacións de MD do sistema. Nestas simulacións analizamos a estructura do LI a través das distribucións de densidade (tanto na dirección perpendicular á interfase de borofeno como nas direccións paralelas) e a distribución da orientación dos ións na interfase. Ademais, a dinámica monoparticular foi analizada usando a densidade vibracional de estados. A distribución da densidade na dirección perpendicular ña interfase e a orientación dos ións amosou resultados moi similares ao das simulacións de grafeno, o cal indica que a estrutura é, a grandes rasgos, similar ña do LI confinado entre eléctrodos de grafeno. O análise da densidade bidimensional amosou non obstante notables diferencias entre amos sistemas cunha transición de un patrón hexagonal para o grafeno a un patrón de bandas no borofeno. Este cambio parece esta inducido polas nano-rugosidades do eléctrodo. Polo tanto podemos concluír que as rugosidades do eléctrodo afectan tan só á primeira capa de LI xunto á interfase, pero que non producen efecto algún no seno do fluído.

Antes de proceder ao estudo de LIs dentro dunha estrutura topoloxicamente complexa realizamos un modelo teórico para explicar o transporte en LIs (Capítulo 9). Este modelo intenta explicar as diferencias experimentais para a condutividade predita polo modelo de Bahe-Varela[5] para altas concentracións de materia iónica. O noso modelo modela o seno do fluído como unha mistura de rexións con alta e baixa mobintroducimosilidade, da mesma forma que o modelo orixinal de Bahe-Varela. Non obstante, introducimos unha dependencia extra para as frecuencias de salto entre rexións. Mentras que no modelo orixinal as frecuencias dependían unicamente do tipo de cela inicial, no noso novo modelo dependen tanto da celcelaa inicial como da final. Esto conleva a inclusión de un novo termo na teoría que ten en conta o exceso de frecuencia de salto entre as celas de diferente tipo. Este modelo pode ser utilizado para explicar a condutividade de misturas de LIs e disolventes moleculares e

[5] **L M Varela, J Carrete, M García, L J Gallego, M Turmine, E Rilo, and O Cabeza,** Pseudolattice theory of charge transport in ionic solutions: Corresponding states law for the electric conductivity, *Fluid Phase Equilibria,* **298**(2), 280–286 (2010)

de disolucións electrolíticas en xeral en todo o rango de concentracións con éxito.

Finalmente procedimos ao estudo do comportamento de LIs próticos e apróticos dentro de estruturas topolóxicamente complexas con múltiples poros interconectados (Capítulo 10). Para elo realizamos simulacións de MD de un LI prótico (EAN) e un LI aprótico ([EMIM][BF_4]) dentro de nanotubos de carbono (CNT) e dentro dunha estrutura de carbono temperado en zeolita (ZTC). Esta estructura ZTC contén poros en diferentes direccións do espazo que se interconectan formando cavidades. Esto confírelle un gran cociente superficie volume, o cal é desexable en eléctrodos reais. O estudo incorporou dúas partes. Na primeira parte se analizaron as propiedades estruturais e dinámicas dos LIs dentro de CNT de diferentes radios para o seu uso como referencia das propiedades dos mesmos LIs dentro da ZTC. Para as propiedades estruturais se utilizou a densidade, a RDF, así como a súa integral tanto para os LIs dentro dos CNT como para dentro da ZTC. Ademais, para os sistemas de CNTs se estudou o seu factor de estructura e a densidade radial de partículas. Para a dinámica monoparticular se estudaron os desprazamentos cadráticos medios e as densidades vibracionais de estado. A estructura de ambos LIs dentro dos CNTs amosa dous rexímenes ben diferenciados, un primeiro cando o radio do CNT é inferior ao tamaño típico dun par iónico e un segundo cando o radio é superior. No primeiro reximen, o correspondente aos CNTs maís estreitos, a estructura está dominada por efectos estéricos e ambos LIs amosan estruturas puramente unidimensionais. Cando se supera o tamaño típico dun par iónico as interaccións coulombianas entre o anión e o catión comezan a ser relevantes e se aprecian diferencias estruturais entre ambos LIs a medida que se incrementa or radio e a estructura deixa de ser unidimensional. Os LIs dentro de CNT amosan ademais unha dinámica acelerada con respecto ao seno do fluído, con un desprazamento cadrático medio maior e un desprazamento cara o azul da densidade vibracional de estados. Pola outra banda, os mesmos LIs dentro da ZTC amosa unha estrutura máis parecida á existente no interior do fluído, o cal deixa entrever que o aumento da dimensionalidade dentro de ditas estruturas xoga un rol fundamental. Ademais,

a estrutura do LI prótico é máis parecida á do seno do fluído que a do LI aprótico. Esta recuperación acelerada da estructura do interior do LI libre parece estar causada pola rede de enlaces de hidróxeno presente no LI prótico, que como vimos no segundo estudo desta tese adoita xogar un papel moi relevante na estruturación do LI. A dinámica pola outra banda amosa un comportamento parecido ña dos CNTs para a densidade vibracional de estados con un desprazamento cara o azul con respecto ao espectro do LI libre. O desprazamento cadrático medio, non obstante, mantiveuse en reximen subdifusivo durante todo o rango de estudo, en contraste coa difusión acelerada presente nas simulacións dentro de CNTs. Ademais, propuxemos o estudo da ZTC como unha estructura de dimensionalidade intermedia entre un e tres. Isto nos permite modelar a estructura do LI dentro da ZTC como a combinación de unha estrutura puramente unidimensional (obtida a partir das simulacións dos LI dentro dos CNTs) e unha tridimensional. Este modelo é capaz de predir a densidade do sistema e a coordinacións dos ións utilizando a distribución de tamaño de poro da estrutura ZTC. A dinámica, sen embargo, non é sinxela de calcular utilizando este modelo e é preciso desenrolar traballo adicional nesta dirección (similar ao presentado no Capítulo 9).

A tese finaliza con unhas conclusións xerais á toda a tese e listando diferentes liñas de investigación futuras (Capítulo 11). A tese consta tamén de unha listaxe de publicacións relacionadas, pero non contidas, na tese.

USC
UNIVERSIDADE
DE SANTIAGO
DE COMPOSTELA

Resumen

Los líquidos iónicos (LIs), o sales fundidas a temperatura ambiente, se consideran hoy uno de los materiales avanzados más prometedores y han ganado mucha atención en las últimas dos décadas debido a sus interesantes propiedades. Los LIs son materiales formados únicamente por iones que se encuentran en estado líquido a temperaturas inferiores a 100 °C. Es generalmente admitido que esta baja temperatura de fusión se obtiene debido a las asimetrías entre aniones y cationes, las cuales debilitarían la energía de red evitando obtener un sólido con alta simetría. Sus propiedades, tales como su baja presión de vapor, su nanoestructuración o su gran resistencia a diferencias de potencial los hacen deseables para aplicaciones tales como la catálisis, fluidos térmicos, lubricantes o dispositivos electroquímicos. Es esta última aplicación la que será objeto de estudio preferente en esta tesis. Además, los LIs son considerados *disolventes de diseño*, debido a que es posible combinar diferentes aniones y cationes dando lugar a millones de combinaciones posibles. Debido a esto es posible escoger la combinación que reúna las propiedades óptimas para una tarea en concreto.

El interés del uso de LIs en dispositivos electroquímicos se debe a que tienen una gran ventana electroquímica, es decir, se mantienen estables bajo un amplio rango de diferencias de potencial. Esto debería permitir en teoría la fabricación de dispositivos con un mayor voltaje de funcionamiento y, en el caso de dispositivos para almacenamiento de energía, una mayor potencia y capacidad. En estas aplicaciones la región del espacio donde tienen lugar las interacciones mas importantes es la interfase electrodo-líquido. Además, para conseguir una mayor rendimiento es frecuentemente deseable trabajar con electrodos con un amplio cociente superficie-volumen. Por lo tanto, resulta imprescindible conocer como se comportarán los LIs cuando se encuentren confinados en recintos nanoporosos. Este será por lo tanto el objetivo principal de la tesis, el análisis de la estructura y dinámica de LIs nano-confinados. El estudio del confinamiento será realizado por partes, empezando por como la propia nano-estructuración de los LIs afecta a su estructura, pa-

sando por el análisis de la estructura de los LIs en interfases planas y finalizando con el estudio de LIs próticos y apróticos confinados dentro de una nano-estructura topológicamente compleja.

Para obtener estos resultados utilizaremos herramientas computacionales, que nos permiten un acceso directo a las propiedades microscópicas de los LIs. Para el estudio utilizaremos diferentes técnicas según la precisión con la que necesitemos trabajar. En concreto las dos herramientas que más hemos utilizado fueron la simulación por dinámica molecular (MD) y la simulación usando la teoría del funcional densidad cuántica (DFT). Las simulaciones por MD fueron utilizadas para estudiar los LIs en escalas espaciales de decenas de nm y temporales de decenas de ns. En este método no se incluyen de forma explícita los electrones de los átomos y se asume que no hay variación de las densidades electrónicas en la simulación. Para realizar estas simulaciones se usó la suite de simulación de código abierto GROMACS[1] y el campo de fuerzas OPLS-AA,[2] el cual es ampliamente utilizado para simulaciones de líquidos. Por otro lado, los cálculos DFT fueron utilizados para la obtención y caracterización de estructuras de equilibrio con gran precisión en escalas subnanométricas. Para la realización de dichos cálculos DFT hemos utilizado el programa comercial VASP.[3] Este programa resuelve las ecuaciones de Kohn-Sham utilizando una expansión de la densidad electrónica en ondas planas. Se han utilizado diferentes funcionales de intercambio y correlación dependiendo del sistema de estudio, en concreto se ha utilizado los funcionales PBE y B3LYP.

Comenzamos el estudio de la estructura bajo confinamiento de los LIs en el Capítulo 4 con una evaluación de la validez de los métodos

[1] **Mark James Abraham, Teemu Murtola, Roland Schulz, Szilárd Páll, Jeremy C Smith, Berk Hess, and Erik Lindahl,** GROMACS: High performance molecular simulations through multilevel par allelism from laptops to supercomputers, *SoftwareX,* **1**(19–25), 2015 (.)

[2] **William L Jorgensen, David S Maxwell, and Julian Tirado -Rives,** Development and testing of the OPLS all-atom force field on con formational energetics and properties of organic liquids, *J. Am. Chem. Soc.,* **118**(45), 11225–11236 (1996).

[3] **GeorgKresse and Jürgen Furthmüller,** Efficient iterative schemes for ab initio total energy calculations using a planewave basis set, *Phys. Rev. B,* **54**(16), 11169 (1996).

utilizados. En concreto se evaluaron las diferencias en la estructura y la dinámica de una mezcla de bis-(trifluorometilsulfonil)-amida (TFSI) 1-butil-3-metilimidazolio (BMIM) con bis-(trifluorometilsulfonil)-amida de litio usando simulaciones MD con campos de fuerza polarizables y no-polarizables. El campo de fuerza no-polarizable utilizado fue el OPLS-AA, mientras que el polarizable fue el APPLE&P.[4] Además, se añadió una versión del campo de fuerzas APPLE&P con la polarización apagada (APPLE&P-NP), pero sin modificar ningún otro parámetro del potencial con el fin de evaluar si es necesario recalcular los parámetros de un campo de fuerza al encender o apagar los términos de polarización. Este sistema fue escogido ya que, debido a la elevada densidad electrónica de los iones de litio, la polarizabilidad del campo de fuerzas debería jugar un papel muy importante en las propiedades del sistema. Para estos sistemas se analizaron la estructura y la dinámica monoparticular. La primera fue evaluada a través de función de distribución radial (RDF) y su integral, la cual nos da el número de coordinación a una determinada distancia. La dinámica, por otro lado, fue evaluada utilizando desplazamientos cuadráticos medios, la función de autocorrelación de la caja de solvatación, la función de autocorrelación de velocidades y su transformada de Fourier, la densidad vibracional de estados. La estructura mostró estructuras muy similares para los dos campos de fuerzas completamente optimizados (OPLS-AA y APPLE&P), con solo pequeñas diferencias en las distancias de equilibrio del litio. Por otro lado, el campo de fuerzas APPLE&P-NP mostró una coordinación del litio muy diferente a la obtenida con los otros campos de fuerzas. En lo tocante a la dinámica la polarizabilidad juega un papel muy relevante, con grandes diferencias en el desplazamiento cuadrático medio. La propiedad más afectada es la función de correlación de la caja. Dicha función muestra un tiempo de residencia del litio en su caja de solvatación órdenes de magnitud mayor en el caso del campo de fuerzas no-polarizable que en el del polarizable. La función de autocorrelación de velocidades muestra un menor tiempo de colisión en el caso del campo de fuerzas no-polarizable, lo cual puede asociarse con una mayor fuerza promedio

[4] **O. Borodin,** Polarizable force field development and molecular dynamics simulations of ionic liquids, *J. Phys. Chem. B,* **113**(33), 11463–11478 (2009).

en la configuración de equilibrio. Sin embargo un análisis de la densidad vibracional de estados muestra que ambos campos de fuerza producen distribuciones similares, pero con un corrimiento hacia el azul para el campo de fuerzas no polarizable. Este estudio nos permite concluir que los campos de fuerza no-polarizables son adecuados para estudiar la estructura, pero no la dinámica y que tras añadir la polarización a un campo de fuerzas es necesario recalcular sus parámetros.

Con el campo de fuerzas apropiadamente validado continuamos nuestro estudio analizando la nano-estructura propia del LI (Capítulo 5). Esta nano-estructura impone un confinamiento en regiones polares y apolares intrínseco al LI. Dicho confinamiento da lugar al paradigma de la solvatación nano-estructurada, según el cual otras moléculas son disueltas en las diferentes regiones del seno del LI atendiendo a su polaridad. Por lo tanto moléculas polares se disolverán en los nano-dominios polares del LI y las apolares en los nano-dominios apolares. Para comprobar este paradigma se realizaron simulaciones de MD de nitrato de etilamonio (EAN) y nitrato de butilamonio (BAN) mezclado con 1-propanol, 1-butanol y 2-pentanol. La particularidad de estos alcoholes es que muestran una cabeza polar y una cadena alquílica apolar. Dado que son anfifílicas, según el paradigma de la solvatación nano-estructurada deberían ser disueltas en la interfase entre los nano-dominios polar y apolar. Además, este comportamiento anfifílico lo comparte con el catión del LI, por lo que deberíamos ver una competición entre ambas moléculas por la misma región del seno del LI. Para evaluar esta competición estudiamos la estructura y la dinámica monoparticular de dichas mezclas. La estructura fue evaluada utilizando la RDF, la función de distribución espacial y el número de enlaces de hidrógeno por molécula. La dinámica fue evaluada utilizando la función de correlación de velocidades y su transformada de Fourier. Las RDFs no mostraron cambios significativos al añadir alcohol frente a la distribución del LI puro. Por otro lado, la función de distribución espacial mostró que, efectivamente, tanto el alcohol como el catión compiten por la misma región del espacio alrededor de los aniones, con la salvedad de que la capacidad de formar múltiples enlaces de hidrógeno del catión le permite acceder a una configuración bidentada. El análisis del

número de enlaces de hidrógeno por molécula corroboró dicha imagen mostrando un reemplazo gradual de las moléculas del catión por moléculas de alcohol a medida que la concentración de alcohol aumenta. Por otro lado, la dinámica no mostró diferencias significativas para el LI puro y el mezclado con alcohol. Esto nos permitió concluir que la imagen propuesta por la solvatación nano-estructurada es correcta y que en LIs con una amplia red de enlaces de hidrógeno esta interacción es tan importante como la interacción de Coulomb entre aniones y cationes.

A continuación procedimos a estudiar la interfase electrodo-LI para sistemas con electrodos planos (Capítulos 6, 7 y 8). Comenzamos estudiando la estructura de la interfase en las direcciones paralelas a la interfase (Capítulo 6). Para ello utilizamos simulaciones de [BMIM][BF_4] con diferentes aditivos confinados entre dos electrodos de grafeno. El análisis de la estructura en dichas direcciones mostró la existencia de dos conformaciones diferentes para los aniones en el ánodo. Dependiendo de la composición exacta del LI, este se configuraba siguiendo un patrón hexagonal o uno de bandas. Para estudiar dicho fenómeno planteamos un modelo teórico basado en la teoría fenomenológica de Landau-Brazovskii. Este modelo predice la existencia de diferentes fases, incluyendo patrones de bandas, hexagonales y una homogéneos. La configuración final del sistema según este modelo depende solo de la densidad de carga efectiva en la interfase y el tipo de patrones posibles debería ser, por lo tanto, independiente del electrodo y del LI. Además, para confirmar estos resultados realizamos simulaciones de Monte Carlo de modelos genéricos de iones sobre una red. Usando este modelo pudimos obtener un diagrama de fases de que patrón debería ser el resultante dependiendo de las interacciones anión-catión y cuyos resultados concuerdan con los de MD. Estos resultados teórico-computacionales predicen por lo tanto la existencia de al menos dos patrones posibles para los iones en la interfase eletrodo-LI. Además, dichos patrones deberían ser modificables externamente por cualquier interacción que pueda modificar la densidad de carga efectiva en el electrodo.

Con el fin de estudiar como se produce el cambio entre estos patrones, en el Capítulo 7 realizamos un estudio extensivo de las propiedades

de dichos patrones para una mezcla de [BMIM][BF_4] con $LiBF_4$ confinada entre dos electrodos de grafeno. A estos electrodos se le añadieron defectos de vacantes con el fin de crear modificaciones locales de la densidad de carga en la interfase. Estos cambios en las densidades de carga deberían, según el estudio anterior, ser capaces de modificar la estructura bidimensional de la interfase. Para ello comenzamos realizando un estudio de cómo se ve modificada la estructura y distribución de carga del grafeno al añadir vacantes. Este estudio preliminar mostró que el grafeno se mantiene plano tras quitar uno de sus átomos. Además, usando dichos resultados creamos un modelo sencillo de redistribución de la carga de la vacante entre sus átomos vecinos. Usando este modelo realizamos simulaciones de MD con diferentes fracciones de defectos distribuidos aleatoriamente. Los resultados de dichas simulaciones fueron analizados usando la distribución de la densidad, tanto en la dirección perpendicular como en las direcciones paralelas a la interfase, funciones de correlación de la densidad y distribuciones de energía potencial en el electrodo. Además, se utilizó el algoritmo de Otsu para dividir la interfase en regiones con y sin aniones para una evaluación más profunda de las propiedades de los patrones. Este estudio mostró que los defectos no son capaces de alterar significativamente la estructura del LI en la dirección perpendicular a la interfase. Sin embargo, estos defectos son capaces de modificar el patrón en las direcciones paralelas a la interfase. Además, dicho cambio no se produce de forma gradual, sino que se produce de forma repentina al superar una fracción crítica de defectos. Este estudio mostró además que la transición entre patrones bidimensionales puede modificar propiedades macroscópicas del sistema.

Acabamos el estudio de interfases planas en el Capítulo 8 estudiando mezclas de [BMIM][BF_4] con $LiBF_4$ confinado entre dos electrodos de borofeno. Estos electrodos tienen la particularidad de ser rugosos a nivel atómico. Este estudio fue pionero en el estudio de interfases de borofeno con LI y nos permite evaluar los efectos que las rugosidades puedan tener en el LI. Comenzamos el estudio con un cálculo DFT de la distribución de cargas de una monocapa de borofeno cargado. Estas distribuciones de carga fueron usadas a continuación para realizar simulaciones de MD del sistema. En estas simulaciones analizamos la

estructura del LI a través de las distribuciones de densidad (tanto en la dirección perpendicular a la interfase como en las direcciones paralelas) y de la orientación de los iones en la interfase. Además, la dinámica monoparticular fue analizada usando la densidad vibracional de estados. La distribución de la densidad en la dirección perpendicular a la interfase y la orientación de los iones mostró resultados muy similares a las de las simulaciones de grafeno, lo cual indica que la estructura es a grandes rasgo similar a la del LI confinado entre electrodos de grafeno. El análisis de la densidad bidimensional mostró sin embargo notables diferencias entre ambos sistemas con una transición de un patrón hexagonal para el grafeno a un patrón de bandas en el borofeno. Este cambio parece estar inducido por las nano-rugosidades del electrodo. Por lo tanto podemos concluir que las rugosidades del electrodo afectan solo a la primera capa de LI junto a la interfase, pero que no producen efecto alguno en el seno del fluído.

Antes de proceder al estudio de LIs dentro de una estructura topológicamente compleja realizamos un modelo teórico para explicar el transporte en LIs (Capítulo 9). Este modelo intenta explicar las diferencias experimentales para la conductividad con el modelo de Bahe-Varela[5] para altas concentraciones de materia iónica. Nuestro modelo modela el seno del fluido como una mezcla de regiones de alta y baja movilidad, de la misma forma que el modelo original de Bahe-Varela. Sin embargo, introdujimos una dependencia extra a las frecuencias de salto entre regiones. Mientras que en el modelo original las frecuencias dependían únicamente del tipo de celda inicial, en el nuevo modelo dependen tanto de la celda inicial como de la final. Esto conlleva la inclusión de un nuevo término en la teoría que tiene en cuenta el exceso de frecuencia de salto entre celdas de diferente tipo. Este modelo puede ser utilizado para explicar la conductividad de mezclas de LIs y disolventes moleculares y de disoluciones electrolíticas en general en todo el rango de concentraciones con éxito.

[5] **L M Varela, J Carrete, M García, L J Gallego, M Turmine, E Rilo, and O Cabeza,** Pseudolattice theory of charge transport in ionic solutions: Corresponding states law for the electric conductivity, *Fluid Phase Equilibria,* **298**(2), 280–286 (2010)

Finalmente procedimos al estudio del comportamiento de LIs próticos y aproticos dentro estructuras topológicamente complejas con multiples poros interconectados (Capítulo 10). Para ello hemos realizado simulaciones MD de un LI prótico (EAN) y un LI aprótico ([EMIM][BF_4]) dentro de nanotubos de carbono (CNT) y dentro de una estructura de carbono templado en zeolita (ZTC). Esta estructura ZTC contiene poros en diferentes direcciones del espacio que se interconectan formando cavidades. Esto le confiere un gran cociente superficie volumen deseable en electrodos reales. El estudio incorporó dos partes. En la primera se analizan las propiedades estructurales y dinámicas de los LIs dentro de CNTs de diferentes radios para usar como referencia de las propiedades dentro de la ZTC. A continuación se estudiaron las mismas propiedades dentro de la ZTC. Para las propiedades estructurales se utilizó la densidad, la RDF, así como su integral tanto para los CNTs como para la ZTC. Además, para los CNTs se estudió su factor de estructura y la densidad radial de partículas. Para la dinámica monoparticular se estudiaron los desplazamientos cuadráticos medios y las densidades vibracionales de estado. La estructura de los LIs dentro de los CNTs muestra dos regímenes diferentes, uno cuando el radio del CNT es inferior al tamaño típico de un par iónico y otro cuando es superior. En los CNTs más estrechos la estructura está dominada por efectos estéricos y ambos LIs muestran estructuras puramente unidimensionales. Cuando se supera el tamaño típico de un par iónico las interacciones coulombianas anión-catión empiezan a ser importantes y se aprecian diferencias estructurales entre ambos LIs a medida que se incrementa el radio y la estructura deja de ser unidimensional. Los LIs dentro de CNTs muestran además una dinámica acelerada con respecto al seno del fluido, con un desplazamiento cuadrático medio mayor y un desplazamiento hacia el azul de la densidad vibracional de estados. Por otro lado, los mismos LIs dentro de la ZTC muestran una estructura más parecida a la del interior del fluido, lo cual deja entrever que el aumento de la dimensionalidad dentro de dichas estructuras tiene un papel fundamental. Además, la estructura del LI prótico es más parecida a la del seno del fluido que a la del LI aprótico. Esta recuperación acelerada de la estructura del LI libre parece estar causada

por la red de enlaces de hidrógeno presente en LI prótico. La dinámica por otro lado muestra un comportamiento parecido a la de los CNTs para la densidad vibracional de estados, mientras que en el rango de estudio el desplazamiento cuadrático medio se mantuvo en régimen subdifusivo. Además, proponemos estudiar la ZTC como una estructura de dimensionalidad intermedia entre uno y tres. Esto nos permite modelar la estructura del LI dentro de la ZTC como la combinación de una estructura puramente unidimensional (obtenida de las simulaciones de los CNTs) y una tridimensional. Este modelo es capaz de predecir la densidad del sistema y la coordinación de los iones utilizando la distribución de tamaño de poro de la estructura ZTC. La dinámica sin embargo no es sencilla de calcular utilizando dicho modelo y es necesario desarrollar trabajo adicional en esta dirección (similar al presentado en el Capítulo 9).

La tesis finaliza con unas conclusiones generales y con potenciales lineas de investigación futuras (Capítulo 11). Además se presenta una lista de publicaciones relacionadas, pero no contenidas, en la tesis.

USC
UNIVERSIDADE
DE SANTIAGO
DE COMPOSTELA

Summary

Ionic liquids (ILs), or room temperature molten salts, are considered nowadays as one of the most promising advanced materials and they have attracted a lot of interest during the last two decades due to their interesting properties. ILs are materials formed only by ions which are liquid at temperatures lower than 100 ° C. This low melting temperature is commonly attributed to the asymmetries between anions and cations, which weaken the lattice energy and avoid the formation of a high symmetry solid. Their properties, such as low vapour pressure, their nanostructuration or their great endurance of high voltage differences make them desirable for applications such as catalysis, thermal fluids, lubricants or electrochemical devices. This last application is the one which will be the main object of study of this thesis. Moreover, ILs are considered as *designer solvents*, because it is possible to combine different anions and cations creating millions of different combinations. Thus it is possible to choose the combination which result in the optimal properties for a given task.

The interest of ILs for electrochemical devices is due to their wide electrochemical window, *i.e.* they remain stable under a wide range of voltages. This should allow in theory the creation of new devices with a greater operating voltage and, if applied to energy storage devices, to higher power and capacity. In these applications the region of the space where the more relevant interactions take place is the electrode-liquid interface. Moreover, in order to achieve a better performance it is usually desirable to use electrodes with a large surface to volume ratio. Therefore, it is critical to know how will the ILs behave when they are confined inside nanoporous regions. This will be, therefore, the main objective of this thesis, the analysis of the structure of ILs nanoconfined. This confinement study will be divided in pieces, starting by analyzing how intrinsic nanostructuring of ILs affects their structure, followed by an analysis of the structure of ILs at planar interface and finally studying protic and aprotic ILs confined inside a topologically complex nanostructure.

In order to obtain such results we will use computational tools. These tools grants us a direct access to the microscopical properties of ILs. In these studies we will use different tools depending on the precision required by the task in hand. More specifically the main tools used are molecular dynamics (MD) simulations and quantum density functional theory (DFT) calculations. MD simulations were used to study ILs in spatial scales of tens of nm and temporal scales of tens of ns. In this method the atomic electrons are not explicitly included and it is assumed that no variation in the electronic levels take place during the simulation. In order to perform such simulations we used the open source simulation suite GROMACS[1] and the OPLS-AA force field,[2] which is widely used in liquid simulations. On the other hand, DFT calculation were used in order to obtain and characterize equilibrium structures with great precision in the subnanometric scale. For the realization of such DFT calculation we used the commercial software VASP.[3] This program solves Kohn-Sham equations using a plane wave expansion of the electronic density. Different exchange and correlation functionals were used depending of the system of study, specifically the PBE and B3LYP functionals were used.

We start the study of the structure of ILs under confinement in Chapter 4 with a validation of the used methods. Specifically the differences in the structure and dynamics of a mixture of 1-ethyl-3-methylimidazolium (EMIM) bis-(trifluoromethylsulfonyl)-imide (TFSI) and lithium bis-(trifluoromethylsulfonyl)-imide were evaluated using MD simulations with polarizable and non-polarizable force-fields. The OPLS-AA was selected as the non-polarizable force field and the APPLE&P[4]

[1] **Mark James Abraham, Teemu Murtola, Roland Schulz, Szilárd Páll, Jeremy C Smith, Berk Hess, and Erik Lindahl,** GROMACS: High performance molecular simulations through multilevel par allelism from laptops to supercomputers, *SoftwareX,* **1**(19–25), 2015 (.)

[2] **William L Jorgensen, David S Maxwell, and Julian Tirado-Rives,** Development and testing of the OPLS all-atom force field on con formational energetics and properties of organic liquids, *J. Am. Chem. Soc.,* **118**(45), 11225–11236 (1996).

[3] **GeorgKresse and Jürgen Furthmüller,** Efficient iterative schemes for ab initio total energy calculations using a planewave basis set, *Phys. Rev. B,* **54**(16), 11169 (1996).

[4] **O. Borodin,** Polarizable force field development and molecular dynamics simulations of ionic liquids, *J. Phys. Chem. B,* **113**(33), 11463–11478 (2009).

as the polarizable one. Moreover, a version of the APPLE&P force field with the polarization switched off (APPLE&P-NP), but without modifying any other parameter, was also used in order to evaluate if it is necessary to recalculate the force field parameters after switching on or off the polarization terms. The system was chosen due to their high electronic density of the lithium ions which makes the polarizabilty of the force field very relevant for calculating the system properties. For these system we analyzed the structure and the single-particle dynamics. The former was evaluated using the radial distribution function and its integral, which return the coordination number at a given distance. On the other hand, the dynamics was studied using the mean square displacement, the cage correlation function, the velocity autocorrelation function and its Fourier transform, the vibrational density of states. THe structure showed very similar results for the two fully optimized force fields (OPLS-AA and APPLE&P), with only minor differences in the equilibrium distances of the lithium ion. On the other hand, the APPLE&P-NP force field showed a very different lithium coordination to the obtained with the other force fields. The dynamics, however, is very affected by the polarizability with big differences in the mean square displacement. The property that suffer the greater differences was the cage autocorrelation function. This function show a residence time of lithium in tis solvation cage that is order of magnitude higher in the non-polarizable potential. The velocity autocorrelation function, however, shows a shorter collision time in the non-polarizable force field, which can be associated with stronger average forces in the equilibrium configuration. However, the analysis of the vibrational density of states showed that both force fields produce similar distributions, but with a blue-shift of the non-polarizable one. This study allows us to conclude that non-polarizable force fields are adequate for the study of the structure, but yield a quantitatively incorrect dynamics and that after adding polarization terms to a potential it is required to recalculate its parameters.

With the force field properly validated we continue our study by analyzing the nanostructured inherent to the IL (Chapter 5). This nanostructure impose a confinement in polar and apolar regions intrinsic to the IL. Such confinement in give rise to the nanostructured solvation

paradigm, in which molecules are solvated in bulk IL according to their chemical polarity. Thus, polar molecules will be solvated in the polar nanodomains of the IL and the apolar ones in the apolar nanodomains. In order to check the validity of this paradigm, MD simulations of ethylammonium nitrate (EAN) and buthylammoium nitrate (BAN) mixtured with 1-propanol, 1-butanol and 2-pentanol were performed. The alcohol molecules have a polar head and an apolar alkyl chain, and are, therefore, amphiphilic. Due to being amphiphilic, the nanostructured solvation paradigm dictates that they should be solvated in the interface between the polar and apolar nanodomains. Moreover, this very same amphiphilic behaviour is present in the IL cations and we should, therefore, see a competition between bot molecules for the same region of the bulk IL. In order to evaluate the effects of this competition we studied the structure and single-particle dynamics of such mixtures. The structured was evaluated using the RDF, the spatial distribution function and the number of hydrogen bonds per molecule. The dynamics was studied using the velocity autocorrelation function and its Fourier transform. The RDFs did not show any relevant differences when the alcohols were added compared to the pure IL. On the other hand, the spatial distribution function showed that the IL cation and the alcohol molecules compete for the same region surrounding the anions, with the only difference that the capability of forming multiple hydrogen bonds of the action allow them to access the bidentate configuration. The analysis of the number of hydrogen bonds per molecule corroborated this picture, showing a gradual replacement of cation ions by alcohol molecules as the alcohol concentration increases. On the other hand the dynamics did not show any significant differences for the pure IL and the mixture of IL and alcohol. This allowed us conclude that the picture proposed by the nanostructured solvation in correct and that in ILs with a wide hydrogen bond network this interaction is as important as the Columbic interaction between anions and cations.

We proceed next to the study of the electrode-IL interface for system with planar electrodes (Chapters 6, 7 and 8). We start the study by analyzing the interface in the directions parallel to the interface (Chapter 6). In order to do that, we used simulations of [BMIM][BF_4] with differ-

ent additives confined between two graphene electrodes. The analysis of the structure showed that in those directions there are two different conformations for the anions at the anode. Depending on the exact composition of the IL it was structured following an hexagonal pattern of and stripped one. In order to study this phenomena we created a theoretical model based on the Landau-Brazovskii phenomenological theory. This model predicted the existence of different phases, including the stripped, the hexagonal and an homogenous one. The final configuration of the system according to this model depends only on the effective charge density at the interface and thus, the possible patterns should be independent of te electrode and IL. Moreover, in order to confirm those results, we performed Monte Carlo simulations using a generic model for the IL placed over a lattice. Using these simulations we ere able to create a phase diagram for the resulting pattern depending on the anion-cation interactions, which yielded results in agreement wit the MD ones. These theoretical-computational results predict, therefore, the existence of at least two possible patterns for the ions at the electrode-liquid interface. Moreover, such patterns should be modifiable by any interaction that is able to modify the effective charge density at the electrode.

In order to study how does the change between these patterns happen, in Chapter 7 we perform an extensive study of the properties of the patterns for a mixture of [BMIM][BF_4] with $LiBF_4$ confined between two graphene electrodes. In these electrodes vacancy defects were randomly added in order to create local perturbations of the charge density at the interface. These changes in the charge density should, according to the previous study, be able to modify the two-dimensional structure of the interface. In order to do that, we made a preliminary study of how is modified the charge distribution of graphene when vacancies are added. This preliminary study allowed us show that graphene remains planar with addition of a vacancy and to create a simple model for the redistribution of the charge of the vacancy among its neighbours. Using this model we preformed MD simulations with difference fraction of defects randomly distributed. The results of the simulations were analyzed using the distribution of the density, both in the perpendicual and parallel directions to the interface, correlation functions of he density and po-

tential energy distribution in the electrode. Moreover, Otsu's algorithm was used to divide he interface in regions with and without anions in order to perform a deeper evaluation of the properties of the patterns. This study showed that the defects are not able to significantly modify the IL structure in the direction perpendicular to the interface, However, these defects are able to modify he pattern in the directions parallel to the interface. Moreover, that change is not produced in a gradual way, but it changes suddenly once a critical fraction of defects in achieved. This study showed also that the transitions between the two-dimensional patterns can modify macroscopic properties of the system.

We finish the study of planar interfaces in Chapter 8 with the study of the same mixtures of [BMIM][BF_4] with $LiBF_4$ confined between borophene electrodes. This electrodes have the particularity of having roughness at the atomic level. This study is pioneer in the analysis of IL-borophene interfaces and allow us to evaluate the effects that roughness may have on the IL. We start the study with a DFT calculation fo the charge distribution of a charged borophene layer. This charge distribution is used then to perform MD simulations of the system. In these simulations we analyzed the structure of the IL using the density distribution (both in the perpendicular and parallel directions to the interface) and the orientation of the ions at the interface. Moreover, the single-particle dynamics was analyzed using the vibrational density of states. The density distribution in the directions perpendicular to the interface showed very similar results to the graphene ones, which indicates that the structure is pretty much the same than the one of IL confined between graphene electrodes. The analysis in the parallel direction, however, showed notable differences between both system with a transition from an hexagonal pattern in the case of graphene to an stripped pattern for the borophene. This change sees to be induced by the nano-roughness of the electrode. Thus, we can conclude that the roughness of the electrode only affect to the first layer of IL next to the interface, but they do not produce any effect in the bulk IL.

Before proceeding to the study of IL inside a topologically complex structure, we designed a theoretical model to predict the transport in ILs

(Chapter 9). This model tries to explain the experimental differences of the conductivity with the Bahe-Varela model[5] for high concentrations of ionic matter. Our model treats the IL bulk as a mixture of high and low mobility regions, in the same way than the original Bahe-Varela model. However, we introduce an extra dependence to the jumping frequencies between the regions. While in the original model, jumping frequencies were only dependent on the mobility of the initial region, in this new model they depend on both the initial and final regions. This leads to the inclusion of a new parameter in the theory that accounts for the jumping frequency excess between region of different type. This model can be successfully used to predict the conductivities of mixtures of ILS and molecular solvents and electrolytic mixtures in the whole concentration range.

Finally we proceed to the study of the behaviour of protic and aprotic ILs inside topologically complex structures with multiple interconnected pores (Chapter 10). For this study we performed MD simulations of a protic (EAN) and an aprotic ([EMIM][BF_4]) IL inside carbon nanotubes (CNTs) and inside a zeolite-templated carbon (ZTC) framework. This ZTC framework have multiple pores in different directions that interconnect creating cavities. This gives a large surface to volume ratio with is desirable in real electrodes. The study is split in two parts. In the first one the structural and dynamic properties of ILs inside CNTs of different radii to be used as a reference for the properties inside the ZTC. Then the same properties properties are analyzed inside the ZTC. The structural properties are analyzed using the density, the RDF and its integral fo the ILs inside the CNTs and the ZTC framework. Moreover, inside the CNTs the structure factor and the radial density are also analyzed. The single-particle dynamics of the ILs inside the ZTC and the CNTs is analyzed using the mean squared displacement and the vibrational density of states. The structure of the ILs inside the CNTs show two different regimes, one when the radius of the CNT is smaller than the typical ion pair size and another

[5] **L M Varela, J Carrete, M García, L J Gallego, M Turmine, E Rilo, and O Cabeza,** Pseudolattice theory of charge transport in ionic solutions: Corresponding states law for the electric conductivity, *Fluid Phase Equilibria,* **298**(2), 280–286 (2010).

when it is higher. In the narrower CNTs the structure is dominated by steric effects and both ILs show purely one-dimensional structures. When the radius is higher than the typical ion pair size the anion-cation Coulombic interactions start to be relevant and structural differences between both ILs appear as the CNT radius increases and the structure stops being purely one-dimensional. The ILs inside the CNTs show also an accelerated dynamics with respect to the bulk one, showing a higher mean square displacement and a blue-shift of the vibrational density of states. On the other hand, the same ILs inside the ZTC structure show a structure more similar to he bulk one, which suggest that the increase of dimensionality inside those structures have a fundamental role. Moreover, the structure of the protic IL is closer to its bulk one that the aprotic IL. This accelerated recovery of the bulk structure seems to be caused by the extensive hydrogen-bonding network present in the protic IL. On the other hand, the dynamics shows a behaviour similar to the CNTs for the vibrational density of states, while the mean squared displacement slowed down and showed a subdiffusive regime in the whole range of study. Moreover, we studied the ZTC as an structure with a fractional dimensionality between one and three. This allows us to model the structure of the IL inside the ZTC as a combination of a purely one-dimensiona structure (obtained from the CNT simulations) and three-dimensional one. Using this model we are able t predict the density of the system and the ionic coordination using the pore size distribution of the ZTC framework. The dynamics, however, cannot be calculated easily using that model and more work in this direction (similar to the present in Chapter 9) is required.

The thesis ends with some general conclusions to the thesis and potential future research lines (Chapter 11). Moreover a list of publications related, but not included, in this thesis is presented.

Cargando contenido…
Por favor, manténgase a la espera.

USC
UNIVERSIDADE
DE SANTIAGO
DE COMPOSTELA

Agradecimientos

Esta tesis representa mi trabajo de los últimos 4 años, sin embargo, este no sería posible sin la presencia de personas que me han apoyado durante el camino. Es por ello que quiero dedicar las siguientes lineas a agradecerles su contribución a esta tesis.

- A mi familia, mis padres y mi hermano, por su continuo apoyo, especialmente en los momentos más duros. Sin ellos esta tesis no habría sido posible.

- A Yara, por darme su apoyo y aguantarme con mis estreses, especialmente durante estos últimos meses. Además, por ser una compañera perfecta para el confinamiento.

- A mi director de tesis, Luis, por su apoyo y consejos, tanto científicos como personales.

- A Txema, como compañero de trabajo y amigo. Sin nuestras conversaciones y nuestros planes para automatizar todo hasta niveles absurdos muchos de los resultados de esta tesis no existirían.

- A Víctor y Alex, por sus interminables conversaciones en el despacho.

- A mis amigos, especialmente a Carlos y Adrián, por estar ahí y apoyarme siempre que lo he necesitado, además de las cañas de los fines de semana.

- A Jesús Carrete, por su apoyo, conversaciones y conocimiento sobre cervezas mostrado durante mi estancia en Viena.

- A Luis Javier Gallego, por su apoyo, consejos y discusiones científicas, así como al resto de compañeros de Nafomat (Trini, Borja, Julio, …) por su apoyo constante.

Además, también agradezco la financiación y recursos aportados por las siguientes entidades. Agradezco al Centro de Supercomputación de Galicia los recursos disponibles a mi disposición y al Ministerio de Educación por su financiación mediante una ayuda para formación de profesorado universitario (FPU). Además, la tesis fue realizada con las ayudas de los proyectos MAT2014-57943-C3-1P, MAT-2014-57943-C3-2P, MAT2014-57943-C3-1P, MAT2014-57943-C3-2P, MAT2017-89239-C2-1P, MAT2017-89239-C2-12P, CTQ2015-65816-R and PGC2018-093745-B-I00 y FIS2012-33126 del Ministerio de Economía y Competitividad. Además, esta tesis recibió financiación de la Xunta de Galicia a través de la red gallega de líquidos iónicos (REGALIS CN 2014/1015), AGRUP 2015/11, ED431D 2017/06, ED431E 2018/08 y GRC ED431C 2016/001. También se recibió apoyo de la Unión Europea a través de acciones COST (CM1206 y MP1303). La tesis fue financiada parcialmente con fondos FEDER.

Contents

List of Figures

List of Tables

List of publications included in this thesis

- **Molecular dynamics analysis of the effect of electronic polarization on the structure and single-particle dynamics of mixtures of ionic liquids and lithium salts,** Volker Lesch, Hadrián Montes-Campos, Trinidad Méndez-Morales, Luis Javier Gallego, Andreas Heuer, Christian Schröder, & Luis M Varela, *J. Chem. Phys.,* **145**(20), 204507 (2016). **Journal information:** Impact factor: 2,965. Cathegory: Physics. Atomic, Molecular & Chemical. Ranking inside cathegory: 10/36 (Q2).

- **Nanostructured solvation in mixtures of protic ionic liquids and long-chained alcohols,** Hadrián Montes-Campos, José M Otero-Mato, Trinidad Méndez-Morales, Elena López-Lago, Olga Russina, Oscar Cabeza, Luis J Gallego & Luis M Varela, *J. Chem. Phys.,* **146**(12), 124503 (2017). **Journal information:** Impact factor: 2,843. Cathegory: Physics, Atomic, Molecular & Chemical. Ranking inside cathegory: 13/36 (Q2).

- **Two-dimensional pattern formation in ionic liquids confined between graphene walls,** Hadrián Montes-Campos, José Manuel Otero-Mato, Trinidad Méndez-Morales, Oscar Cabeza, Luis J Gallego, Alina Ciach, & Luis M Varela , *Phys. Chem. Chem. Phys.,* **19**(36), 24505 (2017). **Journal information:** Impact factor: 3,906. Cathegory: Physics, Atomic, Molecular & Chemical. Ranking inside cathegory: 9/36 (Q1).

- **Mixtures of Lithium Salts and Ionic Liquids at Defected Graphene Walls,** Hadrián Montes-Campos, Jose Manuel Otero-Mato, Roberto Carlos Longo, Oscar Cabeza, Luis Javier Gallego, & Luis Miguel Varela, *J. Mol. Liq.,* **289**, 111083 (2019). **Journal information:** Impact factor: 5,065. Cathegory: Physics, Atomic, Molecular & chemical. Ranking inside cathegory: 4/37 (Q1).

- **Borophene vs. graphene interfaces: Tuning the electric double layer in ionic liquids,** Víctor Gómez-González, J

Manuel Otero-Mato, Hadrián Montes-Campos, Xabier García-Andrade, Amador García-Fuente, Andrés Vega, Jesús Carrete, Oscar Cabeza, Luis J Gallego, & Luis M Varela, *J. Mol. Liq.,* **303**, 112647 (2020). **Journal information:*** Impact factor: 5,065. Cathegory: Physics, Atomic, Molecular & chemical. Ranking inside cathegory: 4/37 (Q1).

- **Random-Alloy Model for the Conductivity of Ionic Liquid–Solvent Mixtures,** Hadrián Montes-Campos, Svyatoslav Kondrat, Esther Rilo, Oscar Cabeza, & Luis M Varela, *J Phys. Chem. C,* **124**(22), 11754 (2020). **Journal information:*** Impact factor: 4,404. Cathegory: Materials Science, Multidisciplinary. Ranking inside cathegory: 90/314 (Q2).

- **Structure of protic and aprotic ionic liquid inside carbon nanotubes and zeolite templated carbon structures,** Hadrián Montes-Campos, Trinidad Méndez-Morales, Jose Manuel Otero-Mato, Oscar Cabeza, Luis Javier Gallego, Enrique Lomba, & Luis Miguel Varela, *J. Mol. Liq.,* **318**, 114264 (2020). **Journal information:*** Impact factor: 5,065. Cathegory: Physics, Atomic, Molecular & chemical. Ranking inside cathegory: 4/37 (Q1).

*The journal information for the articles published in 2020 corresponds to the data of 2019 due to the yearly nature of this information.

List of publications related to this thesis

- **Molecular dynamics simulation of the behaviour of water in nano-confined ionic liquid–water mixtures,** Borja Docampo-Álvarez, Victor Gómez-González, Hadrián Montes-Campos, José M Otero-Mato, Trinidad Méndez-Morales, Oscar Cabeza, LJ Gallego, Ruth M Lynden-Bell, Vladislav B Ivaništšev, Maxim V Fedorov & Luis M Varela, *J. Phys.: Cond. Matt.,* **28**(46), 464001 (2016)

- **Solvation of Al 3+ cations in bulk and confined protic ionic liquids: a computational study,** Víctor Gómez-González, Borja Docampo-Álvarez, Hadrián Montes-Campos, Juan Carlos Otero, Elena López Lago, Oscar Cabeza, Luis J Gallego, & Luis M Varela, *Phys. Chem. Chem. Phys.,* **20**(28), 19071 (2018)

- **3D structure of the electric double layer of ionic liquid–alcohol mixtures at the electrochemical interface,** José M Otero-Mato, Hadrián Montes-Campos, Oscar Cabeza, Diddo Diddens, Alina Ciach, Luis J Gallego, & Luis M Varela, *Phys. Chem. Chem. Phys.,* **20**(48), 30412 (2018)

- **GADDLE Maps: General Algorithm For Discrete Object Deformations Based on Local Exchange Maps,** J Manuel Otero-Mato, Hadrián Montes-Campos, Martin Calvelo, Rebeca Garcia-Fandino, Luis J Gallego, Ángel Piñeiro, & Luis M Varela, *J. Chem. Theory Comput.,* **14**(2), 466 (2018)

- **Molecular dynamic simulation, molecular interactions and structural properties of 1-butyl-3-methylimidazolium bis(trifluoromethylsulfonyl)imide + 1-butanol/1-propanol mixtures at (298.15–323.15) K and 0.1 M Pa,** Urooj Fatima, Naushad Anwar, Hadrián Montes-Campos, & Luis M Varela, *Fluid Phase Equilibria,* **472**, 9 (2018)

- **Solvation in ionic liquid-water mixtures: A computational study,** Jose M Otero-Mato, Volker Lesch, Hadrián Montes-

Campos, Jens Smiatek, Diddo Diddens, Oscar Cabeza, Luis J Gallego, & Luis M Varela, *J. Mol. Liq.,* **292**, 111273 (2019)

- **Experimental and MD simulation investigation on thermophysical properties of binary/ternary mixtures of 1-butyl-3-methylimidazolium trifluoromethanesulfonate with molecular solvents,** Urook Fatima, Riyazuddeen, Hadrián Montes-Campos, & Luis M. Varela, *J. Mol. Liq,* **302**, 112481 (2020)
- **Thermo-switchable de novo ionogel as metal absorbing and curcumin loaded smart bandage material,** Muzammil Kuddushi, Nehal K Patel, Santosh L Gawali, Jitendra P Mata, Hadrian Montes-Campos, Luis M Varela, Puthusserickal A Hassan, & Naved I Malek, *J. Mol. Liq.,* **306**, 112922 (2020)
- **Microstructure, dynamics and optical properties of metal-doped imidazolium-based ionic liquids,** Carlos Damián Rodríguez-Fernández, Hadrián Montes-Campos, Elena López-Lago, Raúl de la Fuente, & Luis M Varela, *J. Mol. Liq,* **317**, 113866 (2020)
- **Nanoconfined ionic liquids: A computational study,** José M. Otero-Mato, Hadrián Montes-Campos, Oscar Cabeza, Luis J. Gallego, & Luis M. Varela, *J. Mol. Liq,* **320**, 114446 (2020)

Part I

Introduction and Methods

USC
UNIVERSIDADE
DE SANTIAGO
DE COMPOSTELA

1- Introduction

1.1 Motivation and purpose

Our future is stored inside a battery. Everybody carries at least one battery powered device in their day to day life, and the demand for battery powered consumer gadgets is not going to stop. The beginning of the Internet of Things and an increase in home automation is expected to greatly increase the demand for consumer batteries. This fact alone is enough to put battery related research, including more efficient batteries and recovering and recycling of used batteries, in the center of many research interests. Moreover, there are several challenges associated with the decarbonation of the economy that require bigger and more efficient batteries. Changing from traditional non-renewable energies, like thermoeletricity, to renewable sources like wind energy in which the energy output depends on uncontrollable sources (like wind speed) creates many challenges in order to satisfy an energy demand with daily cycles.[1] In order to solve this mismatch between the harvesting and the consumption of energy, energy storage schemes are required, among which the use of batteries to store energy in low demand times and to supply extra power to the grid under high demand is highly promising. Moreover, the increasing demand of electric vehicles will require safer, more compact and more powerful batteries.

Currently, rechargeable lithium batteries are used for mobile applications, including small consumer devices and consumer electric vehicles; while other technologies like redox flow batteries are being designed targeting large-scale applications, like storing over-production of energy by renewable sources due to their improved scalability and almost unlimited life.[2] Currently, there is an enormous research effort directed towards finding which materials can improve the current lithium batteries or design post-lithium batteries based in different electrolytes.

Among the materials with the most promising properties properties for electrochemical devices, including future batteries, ionic liquids (ILs) play an outstanding role. These materials have been known since 1914,[3] but they have attracted a lot of interest for the past 20 years. As can be seen in Fig. 1.1 the number of publications related to ILs have been increasing for the last two decades. The main properties that make ILs a good candidate for their use in electrochemical devices are their extremely low vapour pressure, high ionic conductivity and their large electrochemical windows. These properties should allow to run electrochemical devices with increased voltage, and therefore, capacity. We will discuss the properties of ILs in a more detailed way in the following section.

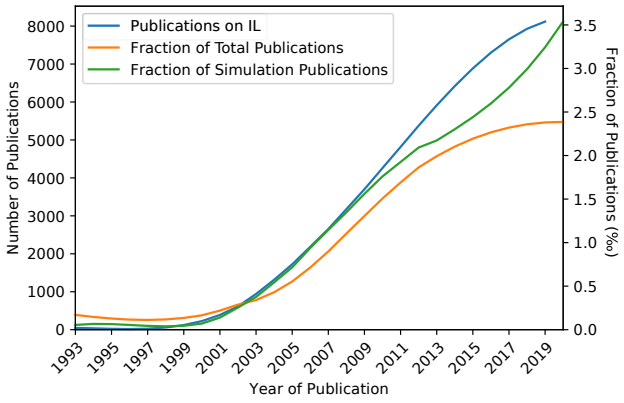

Figure 1.1: Evolution of the publications in ionic liquids since 1993. Blue, the total number of publications with the topic "ionic liquids"; orange, fraction of all the publications in the database whose topic is "ionic liquids"; green, fraction of all the publications about simulations concerning also ionic liquids. The data was extracted from the Web of Science on 2020 July 28 and smoothed for an easier visualization. The total number of articles for 2020 is missing due to limited access to data.

In all electrochemical devices the region where most of the critical interactions happen is in the solid electrolyte interface. However, this region is arguably the less understood one of a battery,[2] which is also true for ILs. Computer simulations, such as molecular dynamics and quantum density functional theory arise as very powerful tools to ana-

lyze the interactions and structure of ILs. They have also the advantage of being relatively cheap, compared to the equivalent experimental setups.

During these last two decades most of the research effort in ILs have been devoted to studying and characterizing, both computationally[4–9] and experimentally,[10–17] bulk systems. However, in the last years an increasing amount on interfacial properties have been reported, specially using computational methods (see Part II of this thesis for the relevant references). A proper study of these interfacial regions is no trivial task however, due to the differences in characteristic times between solids and liquids and considerable difficulties for direct experimental observation. Therefore, most studies of ILs at the interface have been focused on the properties of the IL itself and not on its specific interactions with the electrode.

When and IL is placed at a charged interface, it forms an electric double layer (EDL). This EDL presents charge oscillations that spam for a 1-2 nm that can be explained by overscreening or crowding effects.[18] These charge oscillations have been extensively studied by many research groups (see for example Refs. 19–26). However, these studies focus on the structure of the interface in the direction perpendicular to the electrode's surface. However, the EDL has indeed a three-dimensional structure,[27] an the structure in the directions parallel to the surface must be studied also. However, the number of studies that take into account the structure in these directions is much lower.[28–31] Despite this lack of research, some results indicate that there is a rich structure is these directions, and that there are at least two different configurations for the IL at the interface.[31] In this thesis we will carefully analyze the existence and behaviour of those patterns and the driving force of these structures.

All these studies dealt with ILs confined between ideally planar interfaces (see Ref. 32 for a review of simulations for non-planar interfaces). However, real world electrodes are not planar. In particular, for energy storage devices, e.g. EDL capacitors, materials with a large surface to volume ratio are desirable.[33;34] Moreover, in order to achieve high values of intensity is such devices it is also necessary to have struc-

tures with different pore sizes in order to be able to quickly access the narrower pores which have a higher surface to volume ratio.[35] There are several materials that can be used to fulfill this task such as carbide-derived carbons;[36;37] ordered mesoporous carbons CMK-3,[38] CMK-5,[39] and CMK-8;[38] or zeolite-templated carbon (ZTC).[40] Moreover, experimental measurements of capacity inside ordered mesoporous carbons show that the capacity has a maximum when the pore size is close to the typical ion pair size.[41]

However, there is only a handful of studies that focus in studying the properties of ILs inside topologically complex nanopores.[42;43] This thesis tries to fill this gap of knowledge in this matter by shedding light on the behaviour of ILs inside this topologically complex nanostructures. Specifically, we will focus in a ZTC framework. These frameworks have a pore size radius of the order o the typical ion pair size of some the most widely used ILs (as we will see later in chapter 10).

Therefore, the **main objectives** of this thesis are:

1. Understanding the effect of confinement in IL, including their nanostructuration, confinement in two-dimmensional and one-dimensional geometries.

2. Analyzing the properties of the three-dimensional EDL, including the effect of defects and roughness of the interface.

3. Characterizing the structure and dynamics of ILs inside topologically complex nanostructures. These properties will be analyzed for both protic and aprotic ILs and will be compared to the properties of ILs confined in *simple* geometries.

In order to achieve these objectives we will use different computational tools. The main one will be molecular dynamics, which will used to simulate the properties of the IL. However, we will use also quantum density functional theory when calculations of charge distributions at shorter length or time scales are required, and Monte Carlo methods to efficiently map the phase space of theoretical models.

The remaining of Part I contains a summary of the properties of ILs and a chapter with the description of the methodology used in this thesis. In Part II (including Chapters 4-10) of this thesis the results of these thesis are detailed and discussed. Finally in Chapter 11 the main conclusions of this thesis and future research topics are indicated.

1.2 Properties of ionic liquids

The first definition of an IL was given by Paul Walden in 1914 described then as "materials composed of cations and anions, that melt around 100 °C or below as a arbitrary temperature limit".[44] This definition has been pretty much unchanged up to present day. There are several synonyms for materials that fall under this definition[45;46] such as "room temperature molten salt", "low temperature molten salt", "ambient temperature molten salt", "ionic fluid", "liquid organic salt", "room-temperature ionic liquid" or "nonaqueous ionic liquid". In this thesis we will use the term "ionic liquids" to refer to these materials. Their low melting points compared to "common" ionic material are considered to be due to asymmetries between the anions and cations, which prevent the formation of a proper ionic coordination and, therefore, produce low lattice energies. It has been estimated that with the current available anions and cations (some of which are represented in Fig. 1.2) that form ILs it is possible to generate around a million of different binary ILs and 10^{18} ternary ILs.[47] This number makes finding a set of properties common to every IL a very difficult task. We can, however, find some properties that are common to most ILs.[48;49]

ILs are usually composed of small inorganic anions, such as PF_6^-, NO_3^- and BF_4^-, and relatively large (compared to the anions) organic cations, such as the alkyl-ammonium and the imidazolium families. There are, however, notable exceptions to this rule, like the bis(trifluoromethane)sulfonimide anion, widely used for electrochemical applications, which is an organic molecule and is relatively large compared to other common anions. Other like $C_n$min-alkylsulfate show complex anions linked to short-chained cations. There is also a

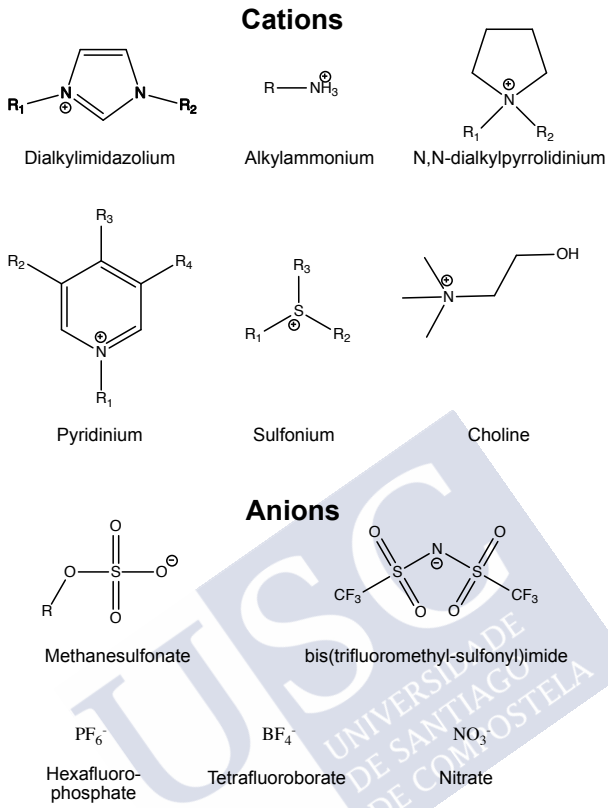

Figure 1.2: Some of the most common cations and anions that form ILs.

very relevant classification of ILs that arise from the method used in their synthesis. When the IL is created by a proton-transfer reaction between an acid and a base without any solvent in the process, it is called a protic ionic liquid,[50;51] in contrast with aprotic ILs which are synthesized with different methods. Protic ILs usually present many hydrogen-bonds which heavily modify their properties.[52].

Most of these novel solvents show interesting and unique properties as:

- **Very low vapour pressure/volatility:** Due to strong interactions

inside the IL, and to the requirement of forming ionic pairs before vapourizing, their vapour pressure is very low, almost undetectable. Experimental measurements of ILs from the imidazolium family show vapour pressures lower that 1 Pa,[53;54] *i.e.* less than one thousand that of water. This makes ILs good candidates for their use as thermal fluids and in situations in which temperature increases are expected.

- **Low toxicity:** ILs have a toxicity in line with other organic materials.[55] However, their extremely low vapour pressures make them safer to handle and avoids toxic emissions to the atmosphere. Moreover, when used in catalytic processes they can be recovered by distillation.[56] For these reason they are usually classified as *green solvents*.

- **High viscosity:** ILs have in general higher viscosities than other common solvents due to being a highly charged medium. Their viscosities range between 10 and 500 cP. This magnitude usually shows a strong dependence with temperature. For instance, the viscosity of [BMIM][PF_6] changes from 286 cP at 293 K to 29 cP at 343 K.[57].

- **Great thermal stability:** Due to the previously discussed low vapour pressure, ILs remain in liquid state for a very broad range of temperatures, compared to other molecular solvents. Their maximum temperature of practical operation is usually controlled not by evaporation but by chemical instability.

- **High electrochemical stability and good ionic conductivity:** Due to being composed only by ions and to their large liquid range, ILs are capable of redistributing their charges under an electric find allowing a fast migration of ions which provide a good ionic conductivity. Moreover, they show high redox potential, and, therefore, they are able to withstand high voltages. The range of voltage than an IL can withstand is generally much higher than other common solvents like water, with electrochemical windows of more than 6 V having been reported.[12] Their

conductivities are also greater than for most common solvents ($\sim 10^{-1}$ S/m). Moreover, in protic ILs the Grotthuss mechanism may be present[58] greatly enhancing electrical conductivity. These two properties are they key ones for their use in electrochemical devices, such as batteries, super-capacitors or fuel cells.

- **Solvation and variable chemical polarity:** The large number of cations and anions that form ILs provides a wide range of chemical polarities and chemical groups to choose in order to design an IL. This large number of possibilities allows tuning ILs to solvate a huge variety of molecules. Moreover, most ILs contain both polar and apolar regions which generates a nanostructuration inside the bulk IL. This nanostructure is composed of two segregated nanodomains with clearly defined chemical polarities. This amphiphilicity is the reason behind the high adaptability of ILs to solvate a great number of substances. Moreover, it is possible to tune the ability to solvate a specific material in order to make it fully miscible or immiscible.[46] This property grants ILs the title of *designer solvents*, and it is behind the huge increase of the number of available solvents.

- **Nanostructured Solvation:** Due to the previously discussed segregation in two nanoregions with different chemical polarities, the solvation of molecules inside ILs is selective.[59] The nanodomains inside ILs are quite stable and therefore solvated materials must accommodate to this underlying structure. Moreover, the highly polar/apolar character of these nanodomains, forces the solute to be placed in a nanodomain with similar polarity. The presence of a robust hydrogen-bond network in many ILs also conditions the ability to solvate other molecules. For example water may create clusters in ILs that lack such hydrogen-bond network,[60] while it is easily accommodated into the polar domains of hydrogen-bonded ILs.[61] This nanostructure also endows ILs with the ability to solvate amphiphilic molecules without significant impact on the IL structure itself, as we will see later in the results of this thesis.

2- Methods

In this chapter we will detail the main aspects of the methods used in this thesis. The chapter is divided in two subsections: in the first one we will detail the different computational tools (which are the main tools used in this thesis), and in the second one we will show the basis of the pseudolattice theory of ionic transport which will be used later in Chapter 9.

2.1 Computational tools

The main computational tools used in this thesis can be classified as computer simulations. Computer simulations are complementary tools to experimental measurements that allow us to access properties that are not directly accessible using experiments. Moreover, computer simulations can also be used as a cheap alternative to screen the properties of a given set of materials due to the low cost of replicating the simulation for different materials. Computer simulations can be used to study systems in almost any scale, from nuclear reactions[62] to gravitational waves.[63] However, the time-scale that computer simulations are able to deal with is strongly tied to the spatial resolution (see Fig. 2.1). Therefore, in order to simulate systems during long times, the spatial resolution must be very low. This means that in all simulations we must find a compromise between the length and time scales involved.

All the computer simulations in this thesis can be classified as *atomistic simulations*. In this kind of simulations the length scale goes from pm, when making quantum simulation of the electronic density of atoms and molecules, to μm in coarse grained molecular dynamics simulations. On the other hand, time scales go from some ps for quantum simulations to μs for molecular dynamics simulations. In this thesis the following simulation methods were used and will be discussed in the following pages:

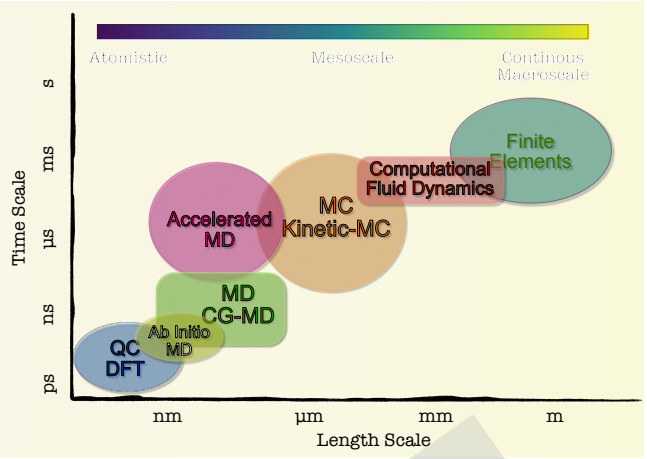

Figure 2.1: Most widely used computer simulation methods according to their time and length scales of application.

- Molecular dynamics.
- Quantum density functional theory.
- Monte Carlo simulations.

2.1.1 Molecular dynamics

Molecular dynamics (MD) is the main technique used in this thesis, in particular classical MD. In classical MD we obtain the time evolution of the motion of a series of atoms through numerical integration of Newton's classical equations of motion. Despite the apparent simplicity of MD, the method allows for a lot of flexibility including the implementation of barostats, thermostats, algorithms for setting constraints (e.g. SHAKE algorithm),… Moreover, there are several open source packages that allow for an easy setup of MD simulations, include tools for the analysis of the results and allow to parallelize the

simulations. Among these simulation packages we want to highlight **GROMACS**[64;65] (GROningen MAchine for Chemical Simulations) for its simplicity, great performance and built-in tools for postprocessing and **LAMMPS**[66] (Large-scale Atomistic/Molecular Massively Parallel Simulator) for its modularity and flexibility to add and modify atomic interactions. For these reasons, we chose GROMACS as our reference suite for this thesis.

In order to follow the motion of the atoms we must discretize the simulation time. The usual approach is to divide the whole simulation in timesteps of constant size. Therefore, at the end of the simulation we will have a trajectory consisting of different snapshots of the system. These frozen images of the system are obtained in an algorithmic way by numerical integration of the Newton equation of motion:

$$\frac{d^2\vec{r_i}}{dt^2} = \frac{\vec{F_i}}{m_i} = -\frac{1}{m_i}\frac{\partial V}{\partial \vec{r_i}}\,, i = 1, \ldots, N\,, \tag{2.1}$$

where V is the potential energy of the system comprising all the relevant interactions in it. There are several integration algorithms that can be used in order to obtain the next snapshot of the trajectory. One of the most frequently used is the *Velocity Verlet* algorithm. In this algorithm the positions and velocities are updated from the previous configuration using the following transformations:

$$\vec{a_i}(t) = -\frac{1}{m_i}\frac{\partial V(\vec{x_i}(t))}{\partial \vec{r_i}} \tag{2.2}$$

$$\vec{x_i}(t+\Delta t) = \vec{x_i}(t) + \vec{v_i}(t)\Delta t + \frac{1}{2}\vec{a_i}(t)\Delta t^2 \tag{2.3}$$

$$\vec{v_i}(t+\Delta t) = \vec{v_i}(t) + \frac{1}{2}\left[\vec{a_i}(t) + \vec{a_i}(t+\Delta t)\right]\Delta t\,. \tag{2.4}$$

Note that before updating the velocities we must recalculate the accelerations using the updated positions for recalculating the forces. Another common algorithm, and the one we will be using in the simulations contained in this thesis, is the *leap-frog* algorithm. This algorithm has the particularity that velocities are calculated at half timestep, *i.e.* they are

not evaluated for same simulation time than the positions. However, this is not usually a problem because the velocities are not stored in the trajectory for all the simulation frames. The equations for updating the positions and velocities in this algorithm are:

$$\vec{a_i}(t) = -\frac{1}{m_i}\frac{\partial V(\vec{x}_i(t))}{\partial \vec{r_i}} \tag{2.5}$$

$$\vec{v_i}\left(t + \frac{\Delta t}{2}\right) = \vec{v_i}\left(t - \frac{\Delta t}{2}\right) + \vec{a_i}(t)\Delta t \tag{2.6}$$

$$\vec{x_i}(t + \Delta t) = \vec{x_i}(t) + \vec{v_i}\left(t + \frac{\Delta t}{2}\right)\Delta t\,. \tag{2.7}$$

The basic algorithm for an MD simulation with a generic integration algorithm is summarized in Fig. 2.2. There are, however, some topics that must be taken into account before performing a MD simulation.

In order to start our simulation, we need an initial configuration with well defined positions and velocities. This is no minor task, as this might very well condition the results of the simulation. A usual approach for simulating liquids is to start with a random distribution of molecules inside a volume, such that there is no overlapping between the atomic van der Waals spheres, and a distribution of velocities that follows Maxwell's distribution for the desired temperature. The volume is chosen such that the system has a density similar to the expected one. After that, an energy minimization is performed in order to avoid configurations with unrealistic energies. Finally, an MD simulation in the NPT ensemble is performed in order to relax the system. Usually a good value for the density is achieved in less than 1 ns and in less than 10 ns the system is usually fully relaxed. The final configuration obtained from this last simulation can now be used to perform the production simulation run.

Another important topic are border effects. In order to avoid having borders in our simulation and being able to simulate bulk material, periodic boundary conditions are applied. These conditions create an infinitely replicated system where the molecules that exit the simulation box through one side reenter the system by the opposite one.

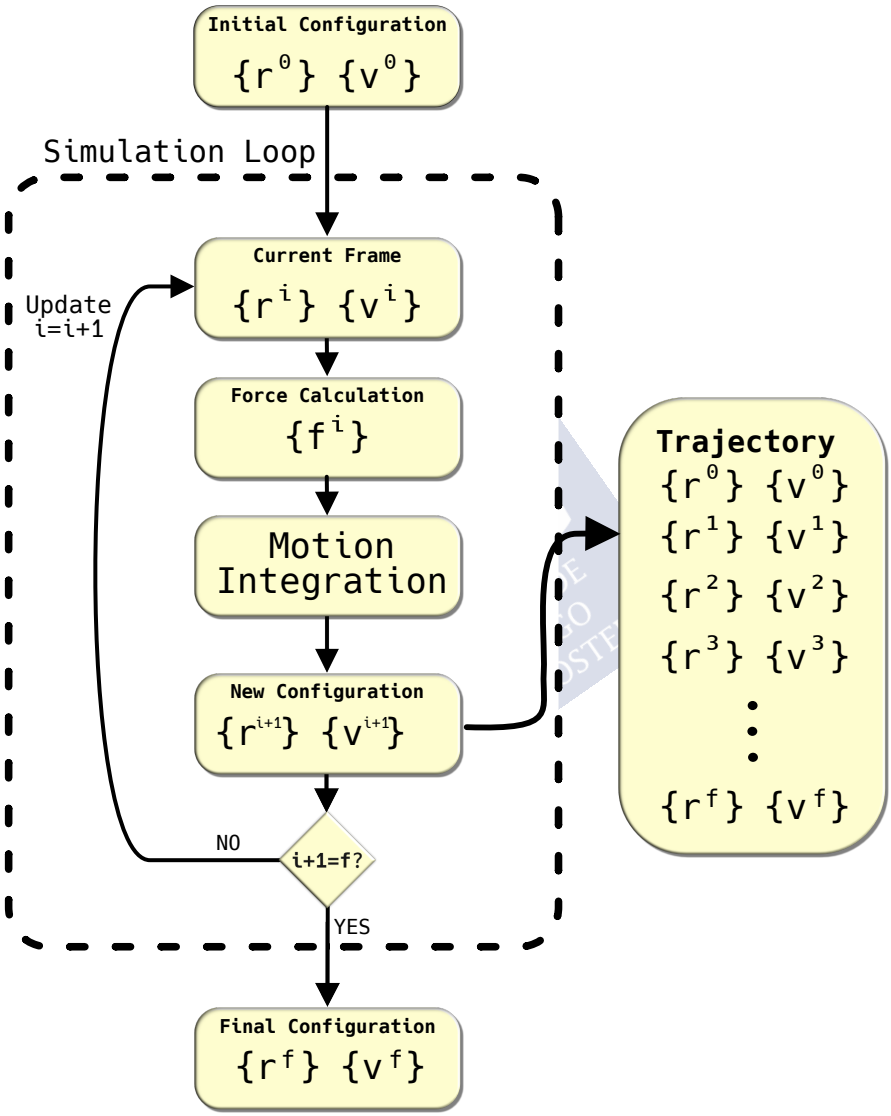

Figure 2.2: Scheme of the basic algorithm for MD simulations.

Finally, the choice of a proper model for the potential energy, and therefore the interactions, of the system is a crucial part of a classical MD simulation, as the accuracy of the results is directly conditioned by the accuracy of the force field modeling of the interactions in the system. This potential energy must include all the interactions present in the system (see Fig. 2.3 for a scheme of the most usual interaction present in MD simulations of classical liquids). The collection of physical models and the parameters used to define the potential energy of the system is what constitutes a force field. There are several force fields available in the literature including OPLS,[67;68] CL&P,[69] APPLE&P,[70] GROMOS,[71] AMBER,[72] CHARMM.[73] In this thesis, our reference force field will be the OPLS-AA[68] (Optimized Potentials for Liquid Simulations, All-Atom), whose components will be summarized in the following. Note that these models are not exclusive of this force field, but are shared by many of the other force fields.

The OPLS-AA force field includes intermolecular and intramolecular interactions defined as:[68]

$$V = V_{\text{bonded}} + V_{\text{nonbonded}} \tag{2.8}$$

$$V_{\text{bonded}} = V_{\text{bonds}} + V_{\text{angles}} + V_{\text{dihedrals}} \tag{2.9}$$

$$V_{\text{nonbonded}} = V_{\text{LJ}} + V_{\text{Coulomb}} \,. \tag{2.10}$$

The bonded interactions are made up of the interactions between two bonded atoms separated a distance r

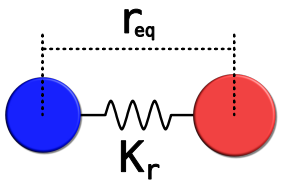

$$V_{\text{bonds}} = \sum_{\text{bonds}} K_r \left(r - r_{\text{eq}}\right)^2 \,, \tag{2.11}$$

the interactions between three atoms forming an angle θ

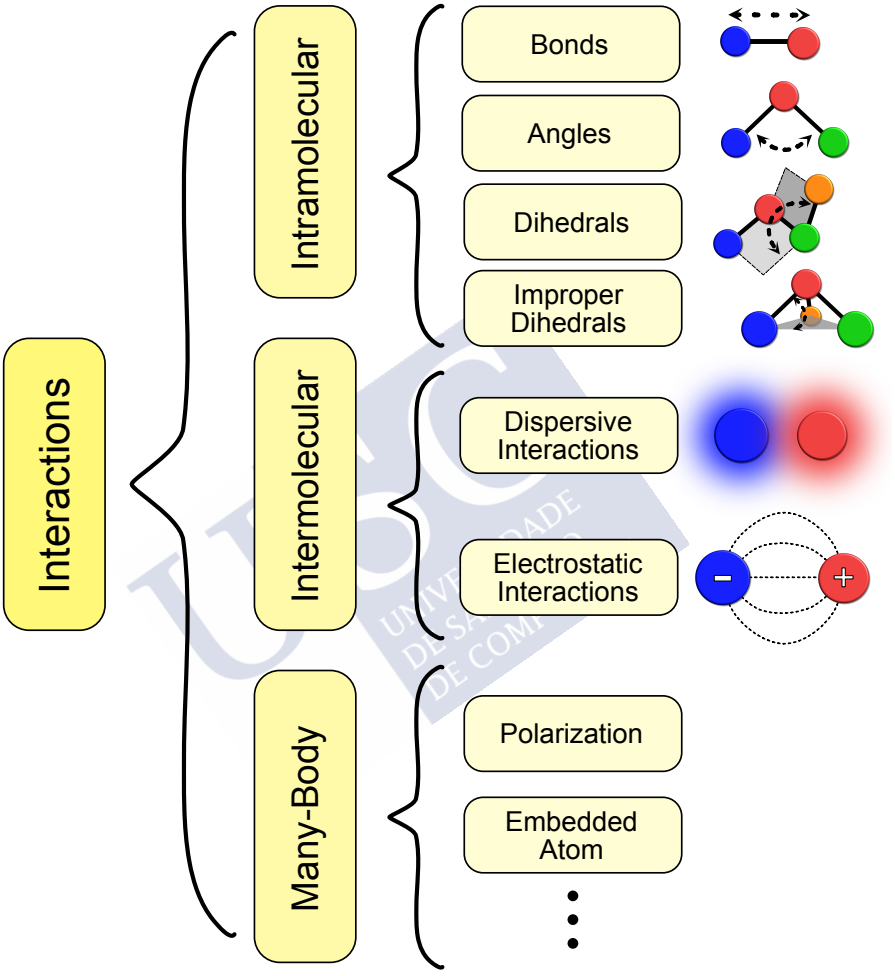

Figure 2.3: Scheme of the most common interactions present in a classical MD simulation.

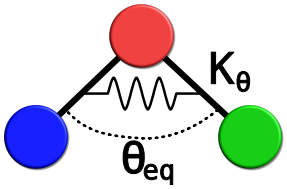

$$V_{\text{angles}} = \sum_{\text{angles}} K_\theta \left(\theta - \theta_{\text{eq}}\right)^2 , \tag{2.12}$$

and the interactions between four atoms forming a dihedral angle ϕ

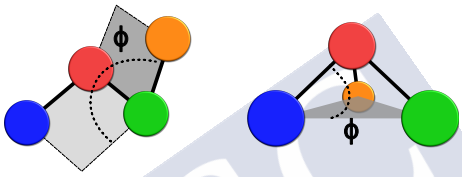

$$V_{\text{dihedrals}} = \sum_{\text{dihedrals}} \frac{V_1}{2}\left[1 + \cos\left(\phi + f_1\right)\right] + \frac{V_2}{2}\left[1 - \cos\left(2\phi + f_2\right)\right] + \frac{V_3}{3}\left[1 + \cos\left(3\phi + f_3\right)\right] . \tag{2.13}$$

On the other hand $V_{\text{nonbonded}}$ is computed only between atoms that are separated by three or more bonds. Moreover, in the special case where the atoms are separated by exactly three bonds the interaction is scaled by a fudge factor $f_{ij} = 0.5$. The nonbonded interactions can be divided into dispersive interactions, modeled by means of a 12-6 Lennard-Jones potential

$$V_{\text{LJ}} = \sum_i \sum_{j \neq i} 4\epsilon_{ij} \left[\left(\frac{\sigma_{ij}}{r_{ij}} \right)^{12} - \left(\frac{\sigma_{ij}}{r_{ij}} \right)^{6} \right] f_{ij} , \tag{2.14}$$

and electrostatic interactions, computed by the Coulomb law

$$V_{\text{Coulomb}} = \sum_i \sum_{j \neq i} \frac{q_i q_j}{r_{ij}^2} f_{ij} . \tag{2.15}$$

For both expressions the fudge factor f_{ij} has a value of 0.5 for atoms that are separated by exactly three bonds and a value of 1 for atoms that are separated by at least four bonds (including atoms in different molecules). This factor is empirically added in order to be able use the same parameters for the calculation of intra- and inter-molecular non-bonded interactions.[74]

However, the OPLS-AA force field does not include any many body interaction. One of the relevant interactions in ILs is the polarization of the electronic densities. This polarization can be modeled with a many body potential, and it is included in the APPLE&P force field, which has been used in this thesis. There are multiple ways of modeling this interaction, the used in the APPLE&P potential is based on including induced dipoles in the simulation with fixed polarizabilities. Therefore, the potential energy due to the polarization is calculated as:[70]

$$V_{\text{pol}} = -\frac{1}{2}\sum_i \vec{\mu}_i \vec{E}_i^0 \,, \tag{2.16}$$

where $\vec{E}_i^0$ is the total electrostatic field at the atomic site i due to permanent charges and $\vec{\mu}_i$ is the induced dipole at the atomic site i. These are calculated as:

$$\vec{\mu}_i = \alpha_i \vec{E}_i^{\text{tot}} \,, \tag{2.17}$$

where α_i is the isotropic polarizability and $\vec{E}_i^{\text{tot}}$ is the total electric field (produced both by fixed charges and induced dipoles) at the atomic site i. Note that in order to prevent the so-called "polarization catastrophe" when two dipoles get too close to each other (including intramolecular interactions of dipoles) a Thole screening is applied,[75] which smears the induced dipoles.

Moreover, due to the previously mentioned need for periodic boundary conditions, there are infinite possible images for a given particle. In order to avoid interactions with these replicas a cutoff range for the interaction is set, so for each pair of atoms there is only one image with a nonzero contribution to the energy. This can be easily done for the Lennard-Jones potential, but it is not possible for the

Coulomb potential due to its infinite interaction range. However, if we evaluate this interaction in the Fourier space, we find that it is possible to evaluate it and therefore we compute the resulting interaction of the infinite images of the atoms. In order to make this computation of the electrostatic interactions methods like the particle mesh Ewald method (PME)[76] or the particle-particle-particle-mesh (P3M).[77]

2.1.2 Quantum mechanical simulation: density functional theory

Despite the usefulness of classical MD, this level of theory is not always enough for accurately describing the interactions in the system. Moreover, classical MD discards any explicit information about the electronic interactions and the electronic states. In order to take into account the electronic degrees of freedom one must use the quantum hamiltonian:

$$\begin{aligned}\hat{H} = &-\frac{\hbar^2}{2m_e}\sum_i \nabla_i^2 + \frac{1}{4\pi\epsilon_0}\sum_i\sum_{j>i}\frac{e^2}{|\vec{r_i}-\vec{r_j}|} \\ &- \frac{1}{4\pi\epsilon_0}\sum_i\sum_\alpha \frac{Z_\alpha e^2}{|\vec{r_i}-\vec{r_\alpha}|} \\ &- \frac{\hbar^2}{2}\sum_\alpha \frac{\nabla_\alpha^2}{M_\alpha} + \frac{1}{4\pi\epsilon_0}\sum_\alpha\sum_{\beta>\alpha}\frac{Z_\alpha Z_\beta e^2}{|\vec{r_\beta}-\vec{r_\alpha}|}\,, \end{aligned} \quad (2.18)$$

where the latin indexes correspond to electronic coordinates and the greek ones to nuclear coordinates. The terms in the hamiltonian can be easily interpreted as the kinetic energy of the electrons, the interaction between electrons, the electron-nucleus interaction, the interaction between nucleii and the kinetic energy of the nucleii. Using the Born-Oppenheimer approximation,[78] it is possible to decouple the nuclear degrees of freedom from the electronic ones, which simplifies the hamiltonian retaining only the first three terms. However, even after this approximation, computing the wavefunction for systems with many

electrons is too demanding making it unsolvable for modern computing capabilities.

A different approach to this many-body problem is given by the Hohenberg-Kohn theorems.[79] These theorems state that:

1. The external potential energy (and therefore the total energy) is a unique functional of the electronic density.

2. The electronic density which minimizes the total energy is the density of the ground state.

These theorems effectively turns solving the Schrödinger equation into a minimization problem. However, they do not provide a way for calculating such energy from the electronic density. This problem was solved by Kohn and Sham introducing quasi-electrons. These quasi-electrons behave as non-interacting particles on an effective potential (V_{eff}) and have the same density than the real electrons.[79] The introduction of these quasi-particles results in the Khon-Sham equations, which can be written as:

$$\left(-\frac{\hbar^2}{2m}\nabla^2 + V_{\text{eff}}(\vec{r})\right)\phi_i(\vec{r}) = \epsilon_i\phi_i(\vec{r})\,, \tag{2.19}$$

where the i index correspond to each of the quasi-electrons and ϕ_i to their orbitals. These equations effectively reduces one many-body problem to many one-body problem. The effective potential can be divided in three contributions:

$$V_{\text{eff}}(\vec{r}) = V'(\vec{r}) + V_H(\vec{r}) + V_{xc}(\vec{r})\,, \tag{2.20}$$

where V' is the external potential (including the electrostatic potential created by the nucleii), V_H is the Hartree term for the electron-electron repulsion and V_{xc} is the exchange and correlation potential. The Hartree term can be written as:

$$V_H(\vec{r}) = \int \frac{e^2}{|\vec{r} - \vec{r}'|}\rho(\vec{r}')d^3\vec{r}'\,, \tag{2.21}$$

where $\rho(\vec{r})$ is the total electronic density the system, which can be calculated from the Kohn-Sham orbitals as:

$$\rho(\vec{r}) = \sum_i |\phi_i(\vec{r})|^2 \ . \tag{2.22}$$

This total density has the property of being equal to the density of the real electrons. On the other hand, the exchange and correlation term (V_{xc}) includes all the many body interactions, which are not included in the other terms. Despite being a formally exact theory, a functional form for this term is not provided. However, there are several approximations to this functional, which we will cover later. From Eqs.(2.19) and (2.20) it is also possible to calculate the total energy of the system as:

$$E\left[\rho\right] = T_{ks} + \int V'(\vec{r})\rho(\vec{r})d\vec{r} + \int V_H(\vec{r})\rho(\vec{r})d\vec{r} + E_{xc}\left[\rho\right] \tag{2.23}$$

where E_{xc} is the exchange and correlation energy, and T_{ks} is the Kohn-Sham kinetic energy, which is calculated as:

$$T_{ks} = \int d\vec{r} \sum_i \vec{\nabla}\phi_i^\dagger(\vec{r})\vec{\nabla}\phi_i(\vec{r}) \ . \tag{2.24}$$

Therefore, the calculation of the energy of a configuration involves a self-consistent loop where the density which yields the minimum energy is searched.

As previously commented, there are several approximations to the exchange and correlation functional that provide quantitatively correct results. Some of the most used families for approximating this functional are the local density approximation (LDA), the generalized gradient approximation (GGA) and the hybrid functionals.

- **Local density approximation (LDA):** In this approximation, the value of the exchange and correlation energy depends only upon the value of the electronic density at each point of the space. Moreover, the usual approach is to model the interaction as a homogeneous electron gas. With this approach, the exchange and

correlation energies are treated separately, so the total exchange an correlation energy can be written as:

$$E_{xc} = E_x + E_c\,, \tag{2.25}$$

and, therefore, the exchange and correlation potential are also additive:

$$V_{xc} = V_x + V_c = \frac{\partial E_x}{\delta\rho(\vec{r})} + \frac{\partial E_c}{\delta\rho(\vec{r})}\,. \tag{2.26}$$

In this approximation, the exchange energy can be calculated analytically using a generalization of the homogeneous electron gas as:

$$\begin{aligned} E_x &= \int \rho(\vec{r})\epsilon_x^{LDA}\left[\rho(\vec{r})\right] d\vec{r} \\ &= -\frac{3}{2\pi}\left(3\pi^2\right)^{1/3}\int \rho(\vec{r})^{4/3} d\vec{r} \end{aligned} \tag{2.27}$$

$$V_x = \frac{\delta E_x}{\partial\rho(\vec{r})} = -\frac{2}{\pi}\left[3\pi^2\rho(\vec{r})\right]^{1/3}\,, \tag{2.28}$$

while the correlation energy can be numerically calculated under the same approximation. This approximation should work well with smooth electronic densities.

- **Generalized gradient approximation (GGA):** In this family of approximations, instead of having an functional that depends only on the local value of the electronic density, as in the LDA approximation, a dependency on the first derivative of the electronic density is added. Therefore, the general expression for the exchange and correlation energy is:

$$E_{xc} = \int \rho(\vec{r})\epsilon_{xc}^{GGA}\left[\rho(\vec{r}), \vec{\nabla}\rho(\vec{r})\right] d\vec{r}\,. \tag{2.29}$$

There are versions of this approximation, known as meta-GGA, which also takes into account the second derivative of the electronic density in the exchange and correlation energy calculation.

$$E_{xc} = \int \rho(\vec{r})\epsilon_{xc}^{MGGA}\left[\rho(\vec{r}), \vec{\nabla}\rho(\vec{r}), \vec{\nabla}^2\rho(\vec{r})\right] d\vec{r}\,. \tag{2.30}$$

- **Hybrid functionals:** This functionals are composed by an empirical mixing of exact energy given by Hartree-Fock's theory and one (or several) of the previously mentioned functionals. For instance, one of the most widely used hybrid functionals, the B3LYP hybrid functional, is calculated as:

$$E_{xc}^{B3LYP} = E_x^{LDA} + a_0\left(E_x^{HF} - E_x^{LDA}\right) + a_x\left(E_x^{GGA} - E_x^{LDA}\right) + E_c^{LDA} + a_c\left(E_c^{GGA} - E_c^{LDA}\right), \quad (2.31)$$

with $a_0 = 0.20$, $a_x = 0.72$ and $a_c = 0.81$. The GGA energy is computed using the exchange functional Becke 88[80] and Lee's exchange functional,[81] while the LDA correlation is computed using the VWN functional.[82]

Note that there are spin polarized versions of these approximations that instead of using the total electronic density in the ϵ_{xc} depend on the *up* and *down* electronic spin densities:

$$\epsilon_x^{LDA}[\rho] \rightarrow \epsilon_x^{LDA}[\rho_\uparrow, \rho_\downarrow] \quad (2.32)$$

$$\epsilon_{xc}^{GGA}\left[\rho(\vec{r}), \vec{\nabla}\rho\right] \rightarrow \epsilon_{xc}^{GGA}\left[\rho_\uparrow, \rho_\downarrow, \vec{\nabla}\rho_\uparrow, \vec{\nabla}\rho_\downarrow\right] \quad (2.33)$$

$$\epsilon_{xc}^{MGGA}\left[\rho, \vec{\nabla}\rho, \vec{\nabla}^2\rho\right] \rightarrow \epsilon_{xc}^{MGGA}\left[\rho_\uparrow, \rho_\downarrow, \vec{\nabla}\rho_\uparrow, \vec{\nabla}\rho_\downarrow, \vec{\nabla}^2\rho_\uparrow, \vec{\nabla}^2\rho_\downarrow\right]. \quad (2.34)$$

In this thesis we have used the commercial software VASP[83;84] for the DFT calculations. Moreover the PBE GGA functional[85] and the B3LYP hybrid functional[86] were chosen as the exchange and correlation functionals.

2.1.3 Monte Carlo simulations

Monte Carlo (MC) simulations, and Monte Carlo methods in general, are a collection of techniques based on random processes that are widely used for integration and simulation processes. The common characteristic of these methods is that instead of exploring the phase space in a deterministic manner, it is done in an stochastic one. These methods are specially powerful to analyze the phase space of multidimensional system as the convergence ratio is $\mathcal{O}(N^{-1/2})$ independently of the dimensionality of the data. This makes MC simulations a very interesting method to study systems with a large number of degrees of freedom.

MC simulations are used in material science in order to simulate different properties. The resulting values from MC simulations converge to the results from MD simulations if the ergodicity of the system is granted. In general terms, a system can be said to be ergodic if after a long enough time a system in evolution is able to reach any point in the phase space. If this condition is met, then the average value measured following the time evolution of the system and integrating over the phase space coincide.

In a conventional MC simulation we are going to produce an stochastic trajectory in the phase space in order to calculate average values,* these values will be equivalent to the ones that would be calculated using a time dependent method (see Fig. 2.4 for a visual representation of the equivalence of deterministic and stochastic trajectories). However, for these values to be equivalent, we must traverse the phase space in a way that preserves the probability distribution of the points in it. For physical systems coupled to a thermostat the probability of a state l of the phase space is given by the Boltzmann

*It is possible to produce a trajectory which reproduces the correct time evolution using Kinetic MC as we will discuss later.

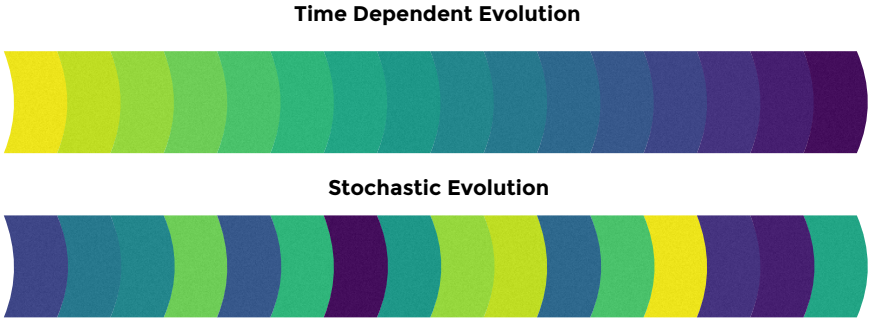

Figure 2.4: Example of the equivalence between an deterministic and a stochastic evolution for an ergodic process.

distribution

$$P_l \propto e^{-E_l/k_B T} \,. \tag{2.35}$$

The Metropolis-Hastings algorithm [87;88] gives an implementation to generate configurations that follows a given distribution. The sequence of samples is obtained by simulating a Markov chain. [88] Let $W = \{w_{ij}\}$ be the transition probability matrix of an irreducible Markov chain and P_i the probability of the state i. If this matrix is to represent the probabilities of a stationary configuration, then it must hold that:

$$\frac{dP_i}{dt} = \sum_j \left[P_i w_{ij} - P_j w_{ji}\right] = 0 \,. \tag{2.36}$$

A sufficient condition for this is:

$$P_i w_{ij} = P_j w_{ji} \,, \tag{2.37}$$

which is known as the detailed balance condition and is based on the microscopic time reversibility. [88]. We can write the transition probability between both states as:

$$w_{ij} = q_{ij}\alpha_{ij} \tag{2.38}$$

where q_{ij} is the probability that a system in the state i tries to go from state i to state j and α_{ij} is the probability of success of such transition. Obviously, Eq. (2.37) implies that this probability of success must verify:

$$\frac{\alpha_{ij}}{\alpha_{ji}} = \frac{P_j}{P_i}\frac{q_{ji}}{q_{ij}} \,. \tag{2.39}$$

A way of fulfilling this relation is to use the following acceptance ratio:

$$\alpha_{ij} = \min\left(1, \frac{P_j}{P_i}\frac{q_{ji}}{q_{ij}}\right) \,, \tag{2.40}$$

which warrants than either α_{ij} or α_{ji} is 1. If we assume that $q_{ij} = q_{ji}$ and using the Bolztmann distribution we obtain that in order to generate random configurations that follow the Boltzmann distribution at a given temperature T the acceptance ratio must be:

$$\alpha_{ij} = \min\left(1, e^{-\frac{E_j - E_i}{k_B T}}\right) \,, \tag{2.41}$$

where E_i and E_j are the energies of the i and j configurations respectively. With this acceptance ratio, the Metropolis-Hastings algorithm[†] produces a Markov chain in which the following element of the chain is produced from a given configuration i using the following rules:

1. Select one of the accessible configurations j with a probability of q_{ij}.
2. Calculate the energy of configuration j.
3. Accept the change from i to j with a probability given by Eq. (2.41).
4. If the change is accepted j becomes the next element of the chain. If it is rejected, then i is added to the chain.

[†]Note that the detailed balance condition allows the determination of the stationary distribution P_i if w_{ij} are known (ensemble theory) and of w_{ij} if P_i is known (Metropolis-Hastings algorithm).

This process is repeated the desired number of times in order to map the phase space. It is important to note that following this algorithm, and most MC algorithms, the time evolution information is completely missing and no dynamic properties can be observed. There are however some algorithms that include time dependent information that can be used to analyze dynamical properties.[89] However, these algorithms usually need be fed with accurate transition times for all the possible process in the system in order to match actual chronological trajectories and reproduce the dynamics.

Further details about the specific methods used in each of the studies are given in their corresponding methods section.

2.2 PSEUDOLATTICE THEORY OF CHARGE TRANSPORT IN IONIC SOLUTIONS

The pseudolattice theory of charge transport in ionic solutions[90] aims to explain and predict the ionic conductivity of ionic solutions in systems for ionic solutions with high concentrations of ionic matter. This theory extends the concentration range beyond the classical Deby-Hückel theory,[91] which is not suitable to study mixtures of ILs and solvents due their inherent high charge density.

This theory consider the mixture of $N = N_+ + N_-$ IL molecules[‡] and N_0 solvent molecules as a 3D pseudolattice with coordination number s, lattice constant a and $M = N + N_0$ nodes. Ions are embedded in this pseudolattice and move between adjacent cells by means of hops activated by the action of an external electric field $\vec{E}$. These hops are considered statistically independent and, therefore, there is no correlation between two consecutive hops. Two adjacent cells are considered to be separated by an energy barrier. Due to the ergodic nature associated to the short characteristic times present in liquid systems, these energy barriers are the product of averaging all the possible molecular environments. In this model only two different kind of ionic environment are considered: β-cells, where no ions are present in the adjacent cells; and

[‡]We will consider only binary ILs for simplicity.

α-cells, where ions are present in the adjacent cells. These cells have two different potential well depths, ϵ_β for the β-cells and ϵ_α for the β ones.

The distribution of α and β cells is considered to be random and no correlation between them is imposed. Therefore the probabilities of having an α or β cells are given by:

$$\chi_\alpha = \phi_\alpha \, , \; \chi_\beta = \phi_\beta \, , \tag{2.42}$$

where ϕ_α and ϕ_β are the volume fractions of ions and solvent respectively. The volume fractions are used instead of the molar ones to take into account the size differences between substances.

In the absence of an electric field, the probability per unit time that an ion jumps a barrier is:[92]

$$\bar{\nu}_i = \frac{1}{3} \frac{(k_B T)^3}{h^3 \nu_{si}^2} e^{-\epsilon_i / k_B T} \; ; \; i = \alpha, \beta \, , \tag{2.43}$$

where h is Planck's constant and ν_{si} is the vibrational frequency of an ion in the two directions of the saddle point perpendicular to the flow in a cell of i type. Under the effect of an electric field $\vec{E}$ these hopping frequencies are altered in the direction parallel to the electric field by an ammount:

$$\begin{aligned} \bar{\nu}_{pi} = \frac{1}{3} \frac{(k_B T)^3}{h^3 \nu_{si}^2} \left[e^{-(\epsilon_i - (aqE/2))/k_B T} - e^{-(\epsilon_i + (aqE/2))/k_B T} \right] \\ = 2 \bar{\nu}_i \sinh \left(\frac{aqE}{2 k_B T} \right) \; ; \; i = \alpha, \beta \, , \end{aligned} \tag{2.44}$$

where q is the charge of the ions. This expression can be easily approximated for weak electric fields as:

$$\bar{\nu}_{pi} \approx \bar{\nu}_i \frac{aqE}{k_B T} \; ; \; i = \alpha, \beta \, . \tag{2.45}$$

Using this expression and the probabilities given by Eq. 2.42, it is possible to calculate the weighted average excess probability of jumping

in the direction parallel to the field as:

$$\bar{\nu}_p = \sum_{i=\alpha,\beta} \phi_i \bar{\nu}_{pi} = \frac{qa}{k_B T} \left(\phi_\alpha \bar{\nu}_\alpha + \phi_\beta \bar{\nu}_\beta\right) E \,. \tag{2.46}$$

Each ionic jump has an associated polarization qa. Thus, the total current density is given by $j = n_\alpha q a \bar{\nu}_p$, where n_α in the number density of ions. This number density can be approximated, due to the low excess volume of ILs, as $n_\alpha \approx \phi_\alpha / V_\alpha$, where V_α is the ionic volume. Therefore the ionic conductivity is finally given by:

$$\kappa = \frac{q^2 a^2}{V_\alpha k_B T} \left[\phi_\alpha^2 \bar{\nu}_\alpha + (1 - \phi_\alpha)\, \phi_\alpha \bar{\nu}_\beta\right] \,. \tag{2.47}$$

Moreover, if the values from this expression are normalized by the maximum conductivity (κ_{max}) and the volume fraction at which this maximum appears (ϕ_{max}), the resulting expression has no parameters and, therefore, it defines a universal behaviour for the conductivity. This universal conductivity can be written as:

$$\bar{\kappa} = 2\bar{\phi}\left(1 - \frac{\bar{\phi}}{2}\right) \,, \tag{2.48}$$

where $\bar{\kappa} = \kappa / \kappa_{max}$ and $\bar{\phi} = \phi_\alpha / \phi_{max}$. As can be seen in Fig. 2.5, this model correctly predicts the conductivity at low and medium concentrations of IL. However, at nearly pure ILs, the experimental values of the conductivity deviate from the prediction of the model. In Chapter 9 we will present an extension of this model with 2-cell dependences of the jumping frequency in order to improve the predictions at nearly pure ILs.

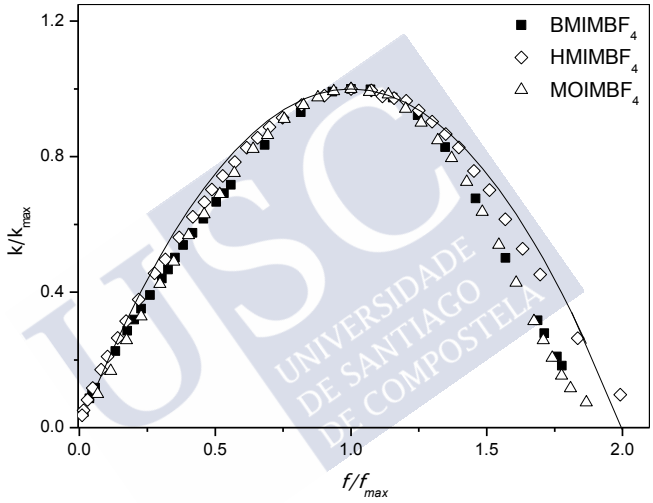

Figure 2.5: Normalized conductivity vs. scaled concentration for IL-ethanol mixtures. Reproduced from Ref.[90]

USC
UNIVERSIDADE
DE SANTIAGO
DE COMPOSTELA

Part II

Results

USC
UNIVERSIDADE
DE SANTIAGO
DE COMPOSTELA

3- Summary of the Results

In this chapter we will present a detailed description of the results contained in this thesis. The long term goal of this thesis was obtaining a detailed description of the structure and the dynamics of ILs under confinement. However, in order to achieve a proper understanding of the effects that the confinement has on the ILs, we need to study also their structure and dynamics in other scales. Therefore, we will start analyzing the structure and dynamics of bulk ILs, as their nanostructure plays the role of as an intrinsic confinement in the IL segregating it into two types of nanodomains. Then, we will study the IL at the solid-liquid interface with an special focus on the structure near a charged interface, which is the most interesting region for electrochemical applications. Finally, we will analyze the properties of ILs inside nanoporous media with different dimensionality. On the other hand, in order to have a proper understanding of how do the interactions between anions and cations affect the overall structure of the IL, specially hydrogen bonding, we will analyze both protic and aprotic ionic liquids. In these studies we used the alkyl-ammonium family as the prototypical protic cations and the alkyl-methyl-imidazolium family as the prototypical aprotic cation.

More specifically, we started validating the usefulness of non-polarizable force fields for predicting the structure and dynamics of ILs and their mixtures. In order to that we compared the results of three fully atomistic force fields: a polarizable force field, APPLE&P; the same force field with the polarization turned off; and a non-polarizable force field, OPLS-AA. These force fields were used to simulate a mixture of 1-ethyl-3-methylimidazolium bis-(trifluoromethylsulfonyl)-imide and lithium bis-(trifluoromethylsulfonyl)-imide. The large charge density of the lithium cation can induce a strong polarization of the anion electronic cloud. This makes this system particularly sensitive to the usage of a non-polarizable force field and, therefore, makes it a good candidate for evaluating the effect of polarization in the force field. These simulations allowed us to conclude, that both polarizable

and non-polarizable force fields predict the same equilibrium structure and the polarizability seems to affect mainly to the system dynamics. Moreover, we concluded that, while the single particle dynamics resulting of simulating with a non-polarizable force field is quantitative incorrect, it qualitative predicts the same single particle dynamics.

With the limitations of non-polarizable force fields well determined, we started our study of the structure of nano-confined ILs testing the nanostructured solvation paradigm,[93] the selective solvation that takes place when molecules are solvated in a protic IL. In order to do that, mixtures of alcohols with different chain lengths (1-propanol, 1-butanol and 2-pentanol) and protic ILs (ethylammonium nitrate and butylammonium nitrate) were simulated. These simulations revealed that, despite being neutral molecules, alcohols were able to replace the cations in the IL structure. This result is in accordance with the nanostructured solvation paradigm, as alkyl-ammonium cations and alcohols are both amphiphilic, they should both be located at the border between both nanodomains of the bulk IL.

With the bulk structure properly characterized and our force field adequately validated, we started our study of the solid-liquid interface. In particular, we were interested in the study of the lateral and 3D structure of the innermost layers of the electric double layer. The structure in these directions has been much less studied, and it was not properly characterized. We found that there was, at least, two different structures that the IL could adopt at the interface, that might be tuned modifying the composition of the IL mixture. Moreover, we developed a theoretical model based on the Landau–Brazovskii phenomenological theory which was able to explain those structures.

In order to gain a deeper insight of the properties of those 2D structures, we simulated a butyl-methyl-imidazolium tetrafluoroborate mixture with lithium tetrafluoroborate in the presence of 2 graphene electrodes with varying fractions of randomly distributed point vacancy defects. These vacancy defects acted as a source of local charge perturbations. These perturbations were not able to significantly change the composition of the IL at the interface, but they were able to change

its structure from one 2D conformation to the other. This allowed us to carefully characterize the similarities and differences between both structures in a controlled environment. Moreover, we concluded that the change between these two conformations could significantly alter some macroscopical properties such as the amount of lithium adsorbed at the interface.

Following these studies of the IL at graphene interfaces, we studied the effect of changing the electrode material. In order to do that, we compared our previous results of 1-butyl-3-methyl-imidazolium tetrafluoroborate mixtured with lithium tetrafluoroborate at a graphene interface, to the same system at a borophene interface. Borophene is, like graphene, a new promising 2D material, but with the difference that it is non-planar, *i.e.* there are some roughnesses in its surface. This resulted in the same overall image of the structure if the IL, but with some important differences at the interface, that can have a great impact on potential applications of such electrodes.

In parallel to our computational analysis, and in order to provide some theoretical framework to describe the calculated dynamics of the ILs we developed a theoretical model for the transport in ILs. This model is based on the proposed by Varela *et al.*[90] based on a pseudolattice structural model which is able to explain ionic conductivity up to very high concentrations. However, this model showed failures at nearly pure ILs. In order to extend the predictions to the whole concentration range, we extended it by considering hopes in a 2-cell model in contrast to the 1-cell model of Varela *et al.* This model is able to correctly predict the ionic conductivity of ionic mixtures throughout the whole concentration range and predicts the evolution of it with temperature.

Finally, we concluded our studies by analyzing both protic and aprotic ILs inside carbon nanotubes prior to introducing them in a zeolite-templated carbon framework. These two systems share the property that they are completely made up of interfaces, *i.e.* they contain no bulk-like region. This last study is, therefore, the culmination of all our previous work and a first step towards studying the IL inside more realistic, complex electrodes. In this study we were able to model

the IL inside the zeolite-templated carbon as mixture of 1D and 2D IL which should theoretically allow us to have very fast estimates of the IL structure inside other frameworks without having to simulate them. The dynamics, however, was not easily understandable by any existing simple model, and a more complex one, with hopping probabilities between the different pores (similar to the presented in our previous study), is required.

In the following chapters we detail the contents of all the studies included in this thesis. For each one of them a short introduction to the article is presented followed by the article in its published format and a transcription of the published article for a more comfortable reading. It must be noted that due to the aggregation of all the references, the number of the references in the transcripted texts may not correspond to the actual number in the published article.

4- Molecular dynamics analysis of the effect of electronic polarization on the structure and single-particle dynamics of mixtures of ionic liquids and lithium salts

Before starting our studies on the properties of nanoconfined ILs, a proper validation of the force field was required. In order to do so, we compared the results of an state of the art polarizable force field (APPLE&P) and a widely used classical one (OPLS-AA). We chose to simulate a mixture of 1-ethyl-3-methylimidazolium bis-(trifluoromethylsulfonyl)-imide and lithium bis-(trifluoromethylsulfonyl)-imide because in this system a large polarization of the electronic density of the anion appears due to the high charge density of the lithium ion. Therefore, this system is particularly sensitive to the polarization effects and it should show remarkable differences between polarizable and non-polarizable force fields.

In this study we thoroughly analyzed the differences in the structure and single particle dynamics between both force fields. We concluded that the main effect of the electronic fluctuations is a perturbative weakening of the Coulomb interactions in the bulk system. The structure does not show great differences between the polarizable and non-polarizable force fields. However, the single particle dynamics shows clear differences between both force fields. The main effect of the suppression of the electronic polarization is the increase of the caging effect of the lithium ions in the bulk, which leads to a much slower diffusion of lithium ions and very long times before reaching the diffusive regime. The velocity correlation function, on the other hand, shows a faster dynamics of the lithium cation compatible with a stronger force in the solvation cage with the non-polarizable force field. This leads to a blue-shift of the normal modes of the density of states, but without notable differences in the number of normal modes present.

Moreover, we also analyzed the effect of switching off the polarization of the polarizable force field without modifying any other para-

meters. This analysis showed that after switching off the polarization the structure and dynamics of the IL is severely impacted. Therefore we conclude that in order to add polarizability to a non-polarizable force field, the rest of its parameters must be re-fitted in order to obtain accurate results.

The contribution of the author of this thesis to this publication, using the CRediT contribution classification,[94;95] was: Conceptualization, Methodology, Software, Validation, Formal Analysis, Investigation, Data Curation, Writing - Original Draft, Writing - Review & Editing, Visualization.

THE JOURNAL OF CHEMICAL PHYSICS **145**, 204507 (2016)

Molecular dynamics analysis of the effect of electronic polarization on the structure and single-particle dynamics of mixtures of ionic liquids and lithium salts

Volker Lesch,[1,2,a),b)] Hadrián Montes-Campos,[3,a)] Trinidad Méndez-Morales,[3] Luis Javier Gallego,[3] Andreas Heuer,[2,4] Christian Schröder,[5] and Luis M. Varela[3,b)]
[1]*Helmholtz-Institute Münster (IEK-12): Ionics in Energy Storage, Forschungszentrum Jülich, Corrensstrasse 46, 48149 Münster, Germany*
[2]*Institute of Physical Chemistry, Westfälische Wilhelms-Universität Münster, Corrensstrasse 28/30, 48149 Münster, Germany*
[3]*Grupo de Nanomateriais e Materia Branda, Departamento de Física da Materia Condensada, Universidade de Santiago de Compostela, Campus Vida s/n, E-15782 Santiago de Compostela, Spain*
[4]*Center for Multiscale Theory and Computation, Corrensstrasse 40, 48149 Münster, Germany*
[5]*Department of Computational Biological Chemistry, University of Vienna, Währingerstrasse 17, A-1090 Vienna, Austria*

(Received 20 June 2016; accepted 9 November 2016; published online 30 November 2016)

DOI: https://doi.org/10.1063/1.4968393

USC
UNIVERSIDADE
DE SANTIAGO
DE COMPOSTELA

5- Nanostructured solvation in mixtures of protic ionic liquids and long-chained alcohols

With the limitations of non-polarizable force fields correctly characterized, we started our study of nanoconfinement of ILs analyzing their internal nanosegregation. The nanosegregation of the IL in polar and apolar nanodomains acts as an intrinsic nanoconfinement of the IL. In this study we analyzed the applicability of the nanostructured solvation paradigm to the solvation of amphiphilic molecules inside the IL. According to this paradigm, molecules are relatively solvated inside the ionic liquid according to their chemical polarities. Therefore, polar molecules are solvated in the polar domains, the apolar in the apolar ones and amphiphilic molecules place themselves in the border between these two regions. In order to test this, we simulated alcohols with different chain lengths (1-propanol, 1-butanol and 2-pentanol) solvated in two protic ionic liquids with different cation sizes (ethylammonium nitrate and butylammonium nitrate). These cations have a marked amphiphilic behaviour and will, therefore, compete with the alcohol molecules in order to be located at the border between the polar and apolar nanodomains.

Our study concluded that the structural results were compatible with the nanostructured solvation paradigm. This picture was further proven by analyzing the hydrogen bonding between the anions and both the cations and the alcohol molecules. The hydrogen bonding revealed that alcohol molecules are able to replace the IL cations in the structure and, therefore, adding alcohol does not significantly alter the properties of the pure IL. Moreover, experimental small angle x-ray scattering measurements of these mixtured showed large scale structural heterogeneities (ca. 10 nm). Due to the size of these heterogeneities their study is outside the scope of this thesis, but work towards simulating this effect is currently planned.

The contribution of the author of this thesis to this publication, using the CRediT contribution classification,[94;95] was: Conceptualization,

Methodology, Software, Validation, Formal Analysis, Investigation, Data Curation, Writing - Original Draft, Writing - Review & Editing, Visualization.

THE JOURNAL OF CHEMICAL PHYSICS **146**, 124503 (2017)

Nanostructured solvation in mixtures of protic ionic liquids and long-chained alcohols

Hadrián Montes-Campos,[1,a)] José M. Otero-Mato,[1,a)] Trinidad Méndez-Morales,[1] Elena López-Lago,[1] Olga Russina,[2] Oscar Cabeza,[3] Luis J. Gallego,[1] and Luis M. Varela[1,b)]

[1]*Grupo de Nanomateriais, Fotónica e Materia Branda, Departamentos de Física de Partículas e de Física Aplicada, Universidade de Santiago de Compostela, Campus Vida s/n, E-15782 Santiago de Compostela, Spain*
[2]*Dipartimento di Chimica, Sapienza Università di Roma, Piazzale Aldo Moro 5, I-00185 Roma, Italy*
[3]*Facultade de Ciencias, Universidade da Coruña, Campus A Zapateira s/n, E-15071 A Coruña, Spain*

(Received 5 January 2017; accepted 7 March 2017; published online 29 March 2017)

DOI: https://doi.org/10.1063/1.4978943

USC
UNIVERSIDADE
DE SANTIAGO
DE COMPOSTELA

6- Two-dimensional pattern formation in ionic liquids confined between graphene walls

In this paper we started the study of the solid-liquid interface. This study will span for three articles, in which efforts were devoted to properly characterize the structural properties of the interface, specially in the directions parallel to the electrodes. The structure of this interface is of key importance for any electrochemical device, as it is the region where reactions and/or the charge start to happen. However, this lateral structure has been much less studied that in the direction perpendicular to the interface. Moreover, previous experimental and computational results had suggested the possibility of two different arrangements of anions and cations in these directions.

In this first study of the interface we will analyze the possible structural conformations that can appear at the electrode. Analyzing the structure in the lateral direction for different composition of the electrolyte showed that two different patterns can arise: one with the ions arranged in an hexagonal pattern and another one creating stripes. These results are backed up by a theoretical model based on the Landau–Brazovskii phenomenological theory which predicts the same structures. Moreover, Monte Carlo simulations of a simple IL model are able to replicate the same conformations. We finally conclude that the pattern that the IL will should adopt depends on the charge density of the first layer of IL at the interface and therefore, we can tune the structure of this layer by modifying any external parameter that couples to such density.

The contribution of the author of this thesis to this publication, using the CRediT contribution classification,[94;95] was: Conceptualization, Methodology, Software, Validation, Formal Analysis, Investigation, Data Curation, Writing - Original Draft, Writing - Review & Editing, Visualization.

USC
UNIVERSIDADE
DE SANTIAGO
DE COMPOSTELA

PCCP

PAPER

Cite this: *Phys. Chem. Chem. Phys.*, 2017, **19**, 24505

Two-dimensional pattern formation in ionic liquids confined between graphene walls

Hadrián Montes-Campos, [a] José Manuel Otero-Mato, [a] Trinidad Méndez-Morales,[a] Oscar Cabeza, [b] Luis J. Gallego,[a] Alina Ciach [c] and Luis M. Varela *[a]

DOI: https://doi.org/10.1039/C7CP04649A

7- Mixtures of Lithium Salts and Ionic Liquids at Defected Graphene Walls

Following the results from our previous article, we analyzed how to induce changes in the IL structure at the interface from the hexagonal pattern to the striped one. In order to do so, we randomly added point defects to a graphene electrode in order to add local perturbations of the electric field. These perturbations should in theory, according to our previous study, be able to induce transitions between conformations. On the other hand, these perturbations were expected to be weak enough so they will not have any relevant impact in the composition of this first IL layer. Therefore, with this setup we can analyze the structures without significantly altering the composition of the interface. Using these simulations we were able to properly characterize the structure and energetics of the patterns. These patterns are compatible with an underlying common structure. Moreover, we find that the change from one conformation to the other is not a progressive one and for one set of external conditions the IL will restructure itself into one of these two patterns. Finally, we were also capable of correlating transitions between the patterns with macroscopical properties such as the amount of lithium cations adsorbed at the interface and, therefore, we are confident that this effect could be used to further tuning of the IL properties at the interface.

The supplementary information for this article can be found on appendix A.1.

The contribution of the author of this thesis to this publication, using the CRediT contribution classification,[94;95] was: Conceptualization, Methodology, Software, Validation, Formal Analysis, Investigation, Data Curation, Writing - Original Draft, Writing - Review & Editing, Visualization.

USC
UNIVERSIDADE
DE SANTIAGO
DE COMPOSTELA

Journal of Molecular Liquids 289 (2019) 111083

Contents lists available at ScienceDirect

Journal of Molecular Liquids

journal homepage: www.elsevier.com/locate/molliq

Mixtures of lithium salts and ionic liquids at defected graphene walls

Hadrián Montes-Campos[a], José Manuel Otero-Mato[a], Roberto Carlos Longo[b], Oscar Cabeza[c], Luis Javier Gallego[a], Luis Miguel Varela[a,*]

[a]Grupo de Nanomateriais, Fotónica e Materia Branda, Departamento de Física de Partículas, Universidade de Santiago de Compostela, Campus Vida s/n E-15782, Santiago de Compostela, Spain
[b]Department of Materials Science & Engineering, The University of Texas at Dallas, Richardson, TX 75080, USA
[c]Mesturas Group, Department of Physics and Earth Sciences, University of A Coruña, A Coruña 15071, Spain

DOI: https://doi.org/10.1016/j.molliq.2019.111083

USC
UNIVERSIDADE
DE SANTIAGO
DE COMPOSTELA

8- Borophene vs. Graphene Interfaces: Tuning the Electric Double Layer in Ionic Liquids

In this last article centered in the study of the solid-liquid interface changed the material of our electrode in order to see which differences may arise. Thus, we replicated the simulations of 1-butyl-3-methyl-imidazolium tetrafluoroborate mixed with lithium tetrafluoroborate in the presence of graphene electrodes, but replacing the graphene electrode with a borophene one. Borophene is a 2D material similar to graphene but with a non-planar interface, *i.e.* it has a rough surface. This was, to the best of our knowledge, the first time that simulations of ILs in contact with borophene electrodes were reported.

In this study we first characterized the charge distribution of the atoms in a charged Pmmn8 borophene sheet, analyzing specifically the two inequivalent atomic positions in the structure. Using these results, we performed MD simulations of IL between two walls of Pmmn8 borophene. We analyzed both the direction perpendicular to the electrode and the parallel ones. We found that changing to a borophene wall has little effect on the direction perpendicular to the electrode. This result suggests that the structure in this direction is very resilient to changes in the electrode and that the strong interactions present in the first layers of IL quickly destroy the information about the electrode roughness. However, the roughness of the electrode's surface has a deep impact in the lateral direction. The existence of a privileged direction in the borophene electrode translates into the appearance of a privileged direction in the IL. Therefore, the ionic liquid settles into a very marked striped conformation. On the other hand, lithium ions seem to be able to reach closer distances to the borophene electrode than to the graphene one. This may be due to enhanced influence of the borophene wall on the anion-cation complexes that form close to the electrode.

The contribution of the author of this thesis to this publication, using the CRediT contribution classification,[94;95] was: Methodology, Soft-

ware, Formal Analysis, Writing - Original Draft, Writing - Review & Editing, Visualization.

Journal of Molecular Liquids 303 (2020) 112647

Contents lists available at ScienceDirect

Journal of Molecular Liquids

journal homepage: www.elsevier.com/locate/molliq

Borophene vs. graphene interfaces: Tuning the electric double layer in ionic liquids

Víctor Gómez-González[a,1], J. Manuel Otero-Mato[a,1], Hadrián Montes-Campos[a], Xabier García-Andrade[a], Amador García-Fuente[b,f], Andrés Vega[c], Jesús Carrete[d], Oscar Cabeza[e], Luis J. Gallego[a], Luis M. Varela[a,*]

[a]Grupo de Nanomateriales, Fotónica y Materia Blanda, Departamento de Física de Partículas, Facultade de Física, Universidade de Santiago de Compostela, Campus Vida s/n, Santiago de Compostela E-15782, Spain
[b]Departamento de Física, Universidad de Oviedo, Oviedo E-33007, Spain
[c]Departamento de Física Teórica, Atómica y Óptica, Universidad de Valladolid, Valladolid E-47011, Spain
[d]Institute of Materials Chemistry, TU Wien, Vienna A-1060, Austria
[e]Departamento de Física y Ciencias de la Tierra, Facultade de Ciencias, Universidade da Coruña, Campus A Zapateira s/n, A Coruña E-15071, Spain
[f]Nanomaterials and Nanotechnology Research Center CINN, CSIC-Universidad de Oviedo, El Entrego, Spain

DOI: https://doi.org/10.1016/j.molliq.2020.112647

USC
UNIVERSIDADE
DE SANTIAGO
DE COMPOSTELA

9- Random-alloy Model for the Conductivity of Ionic Liquid–Solvent Mixtures

The following work tries to close the gap in the understanding of transport in ILs and other ionic systems. It is well-known that for systems with low ionic concentrations, Debye-Hückel equilibrium theory can be used to explain the transport, which leads to Onsager's limiting law for ionic conductance, which predict a conductance proportional to the square root of the ionic concentration. However, ILs and other charged fluids fall completely outside the range of applicability of this theory. An alternative approach to this model was proposed by Varela et al.[90] based on a pseudolattice structural model of the ionic fluid, which models the liquid as a random mixture of low and high mobility cells. This theory is able to explain ionic conductivity up to very high concentrations, but it showed failures at nearly pure ILs.

In order to account for the deviations that the model proposed by Varela *et. al.* had at extremely large ionic concentrations, we proposed a modification of this model based on independent ion hops in a 2-cell mode with second order hopping frequencies, opposed to the original 1-cell model. As we showed in this work, this model is able to correctly predict the high concentration deviations from the original model. Moreover, the model also predicts how does the conductivity change with temperature and brings new insights into the ion-size dependence. This models seems to be able to correctly predict the ionic conductivity of ionic mixtures throughout the whole concentration range.

The supplementary information for this work can be seen on appendix A.2.

The contribution of the author of this thesis to this publication, using the CRediT contribution classification,[94;95] was: Methodology, Software, Formal Analysis, Investigation, Data Curation, Writing - Original Draft, Writing - Review & Editing, Visualization.

USC
UNIVERSIDADE
DE SANTIAGO
DE COMPOSTELA

THE JOURNAL OF PHYSICAL CHEMISTRY C

pubs.acs.org/JPCC Article

Random-Alloy Model for the Conductivity of Ionic Liquid–Solvent Mixtures

Hadrian Montes-Campos, Svyatoslav Kondrat,* Esther Rilo, Oscar Cabeza, and Luis M. Varela*

Cite This: J. Phys. Chem. C 2020, 124, 11754−11759 Read Online

DOI: https://doi.org/10.1021/acs.jpcc.0c00531

USC
UNIVERSIDADE
DE SANTIAGO
DE COMPOSTELA

10- Structure of protic and aprotic ionic liquid inside carbon nanotubes and zeolite templated carbon structures

This last work is the culmination of all the previous studies on the properties of nanoconfined ILs presented in this thesis. In this study we present simulations of protic and aprotic ILs inside carbon nanotubes as a prior step to the study of their confinement inside a zeolite-templated carbon (ZTC) framework. The key difference between this systems and those presented in the previous studies is that they are made up only of interfaces, *i.e.* there is no region in which the bulk 3D structure of fluids can be adopted inside the confining structure. The zeolite-templated carbon framework is a structure with narrow interconnected pores in different spatial directions. This provides the structure with a high surface to volume ratio, which makes them ideal for their use in many electrochemical. However, in order to correctly characterize the properties of ILs confined in ZTC frameworks, we previously simulated the same ILs inside carbon nanotubes of different radii in order to use them for further predictions in the most complex ZTC structure.

ILs inside carbon nanotubes show a highly structured arrangement that goes from a purely 1D configuration in the narrowest nanotubes, to arrangements of higher dimensionality in the widest ones. This change in dimensionality appears when the radius of the nanotube is greater than the typical ion pair size and, therefore, multiple rings of IL appear inside the carbon nanotube. Using the results for the structural properties of ILs confined inside these nanotubes we were able to predict their properties when confined inside ZTC frameworks using its pore size distribution. In order to do that we modeled the structure as having a fraction of 1D regions and a fraction of 2D ones, which is equivalent to an effective non-integer dimensionality, corresponding to pores with a purely 1D arrangement and cavities formed where the pores meet which have a higher dimensionality. We showed that his model correctly predicts the structure of nanoconfined ILs, but it is not able to predict the

dynamics, but if combined with a model similar to the presented in the previous article with hopping probabilities between regions of different dimensionality. This method for calculating the structure opens the door to predicting the same properties in other carbon frameworks without the need of complex and time-consuming simulations.

The supplementary information for this article can be found in appendix A.3.

The contribution of the author of this thesis to this publication, using the CRediT contribution classification,[94;95] was: Conceptualization, Methodology, Software, Validation, Formal Analysis, Investigation, Data Curation, Writing - Original Draft, Writing - Review & Editing, Visualization.

Journal of Molecular Liquids 318 (2020) 114264

Contents lists available at ScienceDirect

Journal of Molecular Liquids

journal homepage: www.elsevier.com/locate/molliq

Ionic liquids nanoconfined in zeolite-templated carbon: A computational study

Hadrián Montes-Campos [a,*], Trinidad Méndez-Morales [b], Jose Manuel Otero-Mato [a], Oscar Cabeza [c], Luis Javier Gallego [a], Enrique Lomba [d], Luis Miguel Varela [a,*]

[a] Grupo de Nanomateriais, Fotónica e Materia Branda, Departamento de Física de Partículas, Universidade de Santiago de Compostela, Campus Vida s/n, E-15782 Santiago de Compostela, Spain
[b] Departamento de Física Aplicada, Facultade de Ciencias, Universidade de Vigo, E-36310 Vigo, Spain
[c] Mesturas Group, Department of Physics and Earth Sciences, University of A Coruña, 15071 A Coruña. Spain
[d] Instituto de Química Física Rocasolano, CSIC, Calle Serrano 119, E-28006 Madrid, Spain

DOI: https://doi.org/10.1016/j.molliq.2020.114264

USC
UNIVERSIDADE
DE SANTIAGO
DE COMPOSTELA

Part III

Conclusions

USC
UNIVERSIDADE
DE SANTIAGO
DE COMPOSTELA

11- Conclusions and Future Perspectives

11.1 Conclusions

The main conclusions from the studies presented in this thesis are:

1. It is possible to study the structure of ILs by using non-polarizable potentials, but the predicted dynamics will be only qualitatively correct. Our results show that even for a system with high charge densities the differences in the predicted structure between non-polarizable and polarizable force fields, while existent, are relatively minor. On the other hand, the single-particle dynamics is highly dependent on the inclusion of polarizability in the force field. The short time velocity autocorrelation function, and its Fourier transform, lead to shorter collision times and shorter characteristic times, while retaining a similar distribution of characteristic modes. This is compatible with a similar structure in both force fields but more intense interactions in the non-polarizable force field. On the other hand, the long time mean square displacement and cage correlation times showed large differences between force fields, with a slower dynamics always in the non-polarizable force field.

2. The structure of ILs is heavily conditioned by their nanoscopic arrangement into polar and apolar regions,which conditions also the location of solvated molecules in bulk ILs. When solvating neutral molecules with a similar polar character than one the IL ions the solute molecules are easily and selectively accommodated in the IL structure, with no significant changes in the bulk structure of the solvent.

3. We have proved that transport in bulk IL mixtures can be modeled by means of a pseudolattice of low mobility and high mobility

regions. In this model ionic transport takes place by hopping between these regions with different jumping frequencies depending on the types of the initial and final regions. This 2-cell model introduced in this thesis extends the original 1-cell model of Varela *et al.*,[90] and is able to predict the conductivity of ionic fluids (electrolite solutions, IL mixtures, …) throughout the whole concentration range.

4. ILs show a rich lateral structure at electrochemical interfaces, which had been scarcely studied in the literature compared to that in the perpendicular direction. This structure shows at least two different conformations for the ions at the interface, one with the ions arranged in an hexagonal pattern and one in a striped pattern.

5. ILs can undergo transitions between those conformations under changing internal or external parameters that couple the charge density at the interface. In particular, adding solvents to the IL and modifying characteristics of the electrode can have such effect.

6. Adding local variations of the charge density of the electrode, with e.g. point defects (vacancies), can modify the structure in the parallel direction to the interface without significantly modifying the structure in the perpendicular direction. This transition takes place after a critical fraction of defects is achieved. Moreover, this transition seems to be able to modify some macroscopical properties of the system.

7. Replacing a perfectly planar electrode (graphene) with one with an atomically rough one (borophene) seems to have negligible impact on the general properties of the IL. However, significant changes in the 2D conformation of the interface are registered.

8. When an IL is confined inside a one-dimensional pore with a radius of the order of the typical ion pair size, the structure is governed mainly by steric effects. This happens for both protic and

aprotic ILs, which show the same general structure. This structure is ruled by the ion pair size and does not seem to be altered by the existence of polar and apolar domains or the presence of hydrogen bonds. Only when the pore size increases, differences between protic and aprotic ILs appear.

9. ILs inside frameworks with multiple pores and pore sizes (e.g. ZTC frameworks) show structures closer to their bulk ones than to the structure inside one dimensional pores. These frameworks, however, disrupt the long range structure of ILs and affect the polar and apolar nanodomains. Moreover, protic ILs seem to have a structure closer to their bulk ones. This can be due to the appearance of the hydrogen-bond network, which quickly recovers the bulk structure.

10. This framework can be modeled as a mixture of one-dimensional and three-dimensional regions. This model results in a good prediction of the structure of the ILs inside ZTC. However, evaluating the transport of these systems using this model is quite challenging and a theoretical model for the interconnection of the regions with different dimensionality is required.

11.2 Future Perspectives

In the following years we expect to continue the research efforts that lead to this thesis opening or furtherly developing some of these research lines:

1. Development of specific force fields to model the hybrid solid-liquid interface, including details from quantum density functional theory.

2. Quantum study of the charge transfer and solid-liquid interaction at the interface.

3. Continuation of the study of IL inside nanoporous frameworks, specifically of mixtures of ILs with other substances.

4. Usage of artificial intelligence to predict properties of ILs in bulk and interface conditions.

A- Supplementary Information

In the following pages we include the Supplementary information for the following articles:

- Mixtures of Lithium Salts and Ionic Liquids at Defected Graphene Walls
- Random-alloy Model for the Conductivity of Ionic Liquid–Solvent Mixtures
- Ionic liquids nanoconfined in zeolite-templated carbon: a computational study

USC
UNIVERSIDADE
DE SANTIAGO
DE COMPOSTELA

Bibliography

[1] Álvaro García-Cerezo, Luis Baringo, and Raquel García-Bertrand. Representative days for expansion decisions in power systems. *Energies*, 13(2):335, 2020.

[2] Kristina Edström. Battery 2030+ roadmap: Inventing the sustainable batteries of the future, 2020.

[3] Tom Welton. Ionic liquids: a brief history. *Biophysical reviews*, 10(3):691–706, 2018.

[4] S. M. Urahata and M. C. C. Ribeiro. Structure of ionic liquids of 1-alkyl-3-methylimidazolium cations: A systematic computer simulation study. *J. Chem. Phys.*, 120(4):1855–1863, 2004.

[5] R. M. Lynden-Bell, N. A. Atamas, A. Vasilyuk, and C. G. Hanke. Chemical potentials of water and organic solutes in imidazolium ionic liquids: A simulation study. *Mol. Phys.*, 100(20):3225–3229, 2002.

[6] Jesús Carrete, Trinidad Méndez-Morales, Óscar Cabeza, Ruth M. Lynden-Bell, Luis J. Gallego, and Luis M. Varela. Investigation of the local structure of mixtures of an ionic liquid with polar molecular species through molecular dynamics: Cluster formation and angular distributions. *J. Phys. Chem. B*, 116(20):5941–5950, 2012. PMID: 22587330.

[7] A. A. H. Pádua, M. F. Costa Gomes, and J. N. A. Canongia-Lopes. Molecular solutes in ionic liquids: A structural perspective. *Acc. Chem. Res.*, 40(11):1087–1096, 2007.

[8] J. N. Canongia-Lopes, M. F. Costa-Gomes, and A. A. H. Pádua. Nonpolar, polar, and associating solutes in ionic liquids. *J. Phys. Chem. B*, 110(34):16816–16818, 2006.

[9] PA Hunt. The simulation of imidazolium-based ionic liquids. *Mol. Simulat*, 32(01):1–10, 2006.

[10] Tamar L Greaves and Calum J Drummond. Protic ionic liquids: properties and applications. *Chem. Rev.*, 108(1):206–237, 2008.

[11] Cinzia Chiappe and Daniela Pieraccini. Ionic liquids: solvent properties and organic reactivity. *J. Phys. Org. Chem.*, 18(4):275–297, 2005.

[12] Helen L Ngo, Karen LeCompte, Liesl Hargens, and Alan B McEwen. Thermal properties of imidazolium ionic liquids. *Thermochim Acta*, 357:97–102, 2000.

[13] S. Zhang, N. Sun, X. He, X. Lu, and X. Zhang. Physical properties of ionic liquids: Database and evaluation. *J. Phys. Chem. Ref. Data*, 35(4):1475–1517, 2006.

[14] K. R. Seddon, A. Stark, and M. J. Torres. Influence of chloride, water, and organic solvents on the physical properties of ionic liquids. *Pure Appl. Chem.*, 72(12):2275–2287, 2000.

[15] Maggel Deetlefs, Kenneth R Seddon, and Michael Shara. Predicting physical properties of ionic liquids. *Phys. Chem. Chem. Phys.*, 8(5):642–649, 2006.

[16] José MSS Esperança, José N Canongia Lopes, Mohd Tariq, Luís MNBF Santos, Joseph W Magee, and Luís Paulo N Rebelo. Volatility of aprotic ionic liquids: A review. *Journal of Chemical & Engineering Data*, 55(1):3–12, 2010.

[17] M. G. Freire, C. M. S. S. Neves, P. J. Carvalho, R. L. Gardas, A. M. Fernandes, I. M. Marrucho, L. M. Santos, and J. A. P. Coutinho. Mutual solubilities of water and hydrophobic ionic liquids. *J. Phys. Chem. B*, 111(45):13082–13089, 2007.

[18] M. Z. Bazant, B. D. Storey, and A. A. Kornyshev. Double layer in ionic liquids: Overscreening versus crowding. *Phys. Rev. Lett.*, 106(4):046102(1)–046102(4), 2011.

[19] V Ivaništšev, MV Fedorov, and RM Lynden-Bell. Screening of ion–graphene electrode interactions by ionic liquids: the effects of liquid structure. *J. Phys. Chem. C*, 118(11):5841–5847, 2014.

[20] Maxim V. Fedorov and Alexei A. Kornyshev. Ionic liquids at electrified interfaces. *Chem. Rev.*, 114(5):2978–3036, 2014.

[21] S. A. Kislenko, I. S. Samoylov, and R. H. Amirov. Molecular dynamics simulation of the electrochemical interface between a graphite surface and the ionic liquid [BMIM][PF_6]. *Phys. Chem. Chem. Phys.*, 11(27):5584–5590, 2009.

[22] R. M. Lynden-Bell, A. I. Frolov, and M. V. Fedorov. Electrode screening by ionic liquids. *Phys. Chem. Chem. Phys.*, 14(8):2693–2701, 2012.

[23] A. A. Kornyshev. Double-layer in ionic liquids: Paradigm change? *J. Phys. Chem. B*, 111(20):5545–5557, 2007.

[24] G. Feng, J. S. Zhang, and R. Qiao. Microstructure and capacitance of the electrical double layers at the interface of ionic liquids and planar electrodes. *J. Phys. Chem. C*, 113(11):4549–4559, 2009.

[25] S. Wang, S. Li, Z. Cao, and T. Yan. Molecular dynamic simulations of ionic liquids at graphite surface. *J. Phys. Chem. C*, 114(2):990–995, 2010.

[26] Q. Dou, M. L. Sha, H. Y. Fu, and G. Z. Wu. Molecular dynamics simulation of the interfacial structure of [$C_n$mim][PF_6] adsorbed on a graphite surface: effects of temperature and alkyl chain length. *J. Phys.: Condens. Matter*, 23(17):175001(1)–175001(8), 2011.

[27] Alexei A Kornyshev and Rui Qiao. Three-dimensional double layers, 2014.

[28] Céline Merlet, David T Limmer, Mathieu Salanne, René Van Roij, Paul A Madden, David Chandler, and Benjamin Rotenberg. The electric double layer has a life of its own. *J. Phys. Chem. C*, 118(32):18291–18298, 2014.

[29] Benjamin Rotenberg and Mathieu Salanne. Structural transitions at ionic liquid interfaces. *J. Phys. Chem. Lett.*, 6(24):4978–4985, 2015.

[30] José M Otero-Mato, Hadrián Montes-Campos, Oscar Cabeza, Diddo Diddens, Alina Ciach, Luis J Gallego, and Luis M Varela. 3D structure of the electric double layer of ionic liquid–alcohol mixtures at the electrochemical interface. *Phys. Chem. Chem. Phys.*, 20(48):30412–30427, 2018.

[31] B Docampo-Álvarez, V Gómez-González, H Montes-Campos, J M Otero-Mato, T Méndez-Morales, O Cabeza, L J Gallego, R M Lynden-Bell, V B Ivaništšev, M V Fedorov, and L M Varela. Molecular dynamics simulation of the behaviour of water in nano-confined ionic liquids□water mixtures. *J. Phys.: Condens. Matter*, 28(46):464001, 2016.

[32] Manish Pratap Singh, Rajendra Kumar Singh, and Suresh Chandra. Ionic liquids confined in porous matrices: physicochemical properties and applications. *Prog. Mater. Sci.*, 64:73–120, 2014.

[33] Guoping Wang, Lei Zhang, and Jiujun Zhang. A review of electrode materials for electrochemical supercapacitors. *Chem. Soc. Rev.*, 41(2):797–828, 2012.

[34] Yong Zhang, Hui Feng, Xingbing Wu, Lizhen Wang, Aiqin Zhang, Tongchi Xia, Huichao Dong, Xiaofeng Li, and Linsen Zhang. Progress of electrochemical capacitor electrode materials: A review. *Int. J. Hydrogen Energ.*, 34(11):4889–4899, 2009.

[35] Lihong Wang, Takahiro Morishita, Masahiro Toyoda, and Michio Inagaki. Asymmetric electric double layer capacitors using car-

bon electrodes with different pore size distributions. *Electrochim Acta*, 53(2):882–886, 2007.

[36] Marcus Rose, Yair Korenblit, Emanuel Kockrick, Lars Borchardt, Martin Oschatz, Stefan Kaskel, and Gleb Yushin. Hierarchical micro-and mesoporous carbide-derived carbon as a high-performance electrode material in supercapacitors. *Small*, 7(8):1108–1117, 2011.

[37] John Chmiola, Celine Largeot, Pierre-Louis Taberna, Patrice Simon, and Yury Gogotsi. Monolithic carbide-derived carbon films for micro-supercapacitors. *Science*, 328(5977):480–483, 2010.

[38] Tuan Ngoc Phan, Min Kyung Gong, Ranjith Thangavel, Yun Sung Lee, and Chang Hyun Ko. Enhanced electrochemical performance for edlc using ordered mesoporous carbons (CMK-3 and CMK-8): Role of mesopores and mesopore structures. *J. Alloy. Compd.*, 780:90–97, 2019.

[39] Zhibin Lei, Zonghuai Liu, Huanjing Wang, Xiuxia Sun, Li Lu, and XS Zhao. A high-energy-density supercapacitor with graphene–CMK-5 as the electrode and ionic liquid as the electrolyte. *J. Mater. Chem. A*, 1(6):2313–2321, 2013.

[40] Nicholas P Stadie, Shutao Wang, Kostiantyn V Kravchyk, and Maksym V Kovalenko. Zeolite-templated carbon as an ordered microporous electrode for aluminum batteries. *ACS nano*, 11(2):1911–1919, 2017.

[41] Celine Largeot, Cristelle Portet, John Chmiola, Pierre-Louis Taberna, Yury Gogotsi, and Patrice Simon. Relation between the ion size and pore size for an electric double-layer capacitor. *J. Am. Chem. Soc.*, 130(9):2730–2731, 2008.

[42] Joshua Monk, Ramesh Singh, and Francisco R Hung. Effects of pore size and pore loading on the properties of ionic liquids confined inside nanoporous CMK-3 carbon materials. *J. Phys. Chem. C*, 115(7):3034–3042, 2011.

[43] Xiaoxia He, Joshua Monk, Ramesh Singh, and Francisco R Hung. Molecular modelling of ionic liquids in the ordered mesoporous carbon CMK-5. *Mol. Simulat*, 42(9):753–763, 2016.

[44] Philippe Hapiot and Corinne Lagrost. Electrochemical reactivity in room-temperature ionic liquids. *Chem. Rev.*, 108(7):2238–2264, 2008.

[45] J. S. Wilkes. A short history of ionic liquids - from molten salts to neoteric solvents. *Green Chem.*, 4(2):73–80, 2002.

[46] T. Welton. Room-temperature ionic liquids. solvents for synthesis and catalysis. *Chem. Rev.*, 99(8):2071–2084, 1999.

[47] J. D. Holbrey and K. R. Seddon. Ionic liquids. *Clean Prod. Proc.*, 1:223–236, 1999.

[48] P. Wasserscheid and M. Keim. Ionic liquids—new "solutions" for transition metal catalysis. *Angew. Chem. Int. Ed. Engl.*, 39(21):3772–3789, 2000.

[49] P. Wasserscheid and T. Welton. *Ionic liquids in synthesis*. Wiley Online Library, 2003.

[50] Michiko Hirao, Hiromi Sugimoto, and Hiroyuki Ohno. Preparation of novel room-temperature molten salts by neutralization of amines. *J. Electrochem Soc.*, 147(11):4168, 2000.

[51] Masahiro Yoshizawa, Wataru Ogihara, and Hiroyuki Ohno. Design of new ionic liquids by neutralization of imidazole derivatives with imide-type acids. *Electrochem Solid St.*, 4(6):E25, 2001.

[52] R. Hayes, S. Imberti, G. G. Warr, and R. Atkin. The nature of hydrogen bonding in protic ionic liquids. *Angew. Chem. Int. Ed.*, 52(17):4623–4627, 2013.

[53] Marisa AA Rocha, Carlos FRAC Lima, Lígia R Gomes, Bernd Schröder, Joao AP Coutinho, Isabel M Marrucho, José MSS

Esperança, Luís PN Rebelo, Karina Shimizu, José N Canongia Lopes, et al. High-accuracy vapor pressure data of the extended [c n c1im][ntf2] ionic liquid series: trend changes and structural shifts. *J. Phys. Chem. B*, 115(37):10919–10926, 2011.

[54] Ortrud Aschenbrenner, Somsak Supasitmongkol, Marie Taylor, and Peter Styring. Measurement of vapour pressures of ionic liquids and other low vapour pressure solvents. *Green Chem.*, 11(8):1217–1221, 2009.

[55] Kathryn M Docherty and Charles F Kulpa Jr. Toxicity and antimicrobial activity of imidazolium and pyridinium ionic liquids. *Green Chem.*, 7(4):185–189, 2005.

[56] R. Sheldon. Catalytic reactions in ionic liquids. *Chem. Commun.*, 2001(23):2399–2407, 2001.

[57] Sheila N Baker, Gary A Baker, Maureen A Kane, and Frank V Bright. The cybotactic region surrounding fluorescent probes dissolved in 1-butyl-3-methylimidazolium hexafluorophosphate: effects of temperature and added carbon dioxide. *J. Phys. Chem. B*, 105(39):9663–9668, 2001.

[58] M. Armand, F. Endres, D. R. MacFarlane, H. Ohno, and B. Scrosati. Ionic-liquid materials for the electrochemical challenges of the future. *Nat. Mater.*, 8:621–629, 2009.

[59] LM Varela, T Méndez-Morales, J Carrete, V Gómez-González, B Docampo-Álvarez, LJ Gallego, O Cabeza, and O Russina. Solvation of molecular cosolvents and inorganic salts in ionic liquids: A review of molecular dynamics simulations. *J. Mol. Liq.*, 210:178–188, 2015.

[60] Trinidad Mendez-Morales, Jesus Carrete, Oscar Cabeza, Luis J Gallego, and Luis M Varela. Molecular dynamics simulation of the structure and dynamics of water–1-alkyl-3-methylimidazolium ionic liquid mixtures. *J. Phys. Chem. B*, 115(21):6995–7008, 2011.

[61] R. Hayes, S. Imberti, G. G. Warr, and R. Atkin. How water dissolves in protic ionic liquids. *Angew. Chem. Int. Ed.*, 51(30):7468–7471, 2012.

[62] Jörg Aichelin and G Bertsch. Numerical simulation of medium energy heavy ion reactions. *Phys. Rev. C*, 31(5):1730, 1985.

[63] Masaru Shibata and Kōji Uryū. Gravitational waves from the merger of binary neutron stars in a fully general relativistic simulation. *Prog. of Theor. Phys.*, 107(2):265–303, 2002.

[64] Herman JC Berendsen, David van der Spoel, and Rudi van Drunen. Gromacs: a message-passing parallel molecular dynamics implementation. *Comput. Phys. Commun.*, 91(1-3):43–56, 1995.

[65] Mark James Abraham, Teemu Murtola, Roland Schulz, Szilárd Páll, Jeremy C Smith, Berk Hess, and Erik Lindahl. GROMACS: High performance molecular simulations through multi-level parallelism from laptops to supercomputers. *SoftwareX*, 1:19–25, 2015.

[66] Steve Plimpton. Fast parallel algorithms for short-range molecular dynamics. *J. Comput. Phys.*, 117(1):1–19, 1995.

[67] William L Jorgensen and Julian Tirado-Rives. The OPLS [optimized potentials for liquid simulations] potential functions for proteins, energy minimizations for crystals of cyclic peptides and crambin. *J. Am. Chem. Soc.*, 110(6):1657–1666, 1988.

[68] William L Jorgensen, David S Maxwell, and Julian Tirado-Rives. Development and testing of the opls all-atom force field on conformational energetics and properties of organic liquids. *J. Am. Chem. Soc.*, 118(45):11225–11236, 1996.

[69] J. N. Canongia-Lopes, J. Deschamps, and A. H. Pádua. Modeling ionic liquids using a systematic all-atom force field. *J. Phys. Chem. B*, 108(6):2038–2047, 2004.

[70] O. Borodin. Polarizable force field development and molecular dynamics simulations of ionic liquids. *J. Phys. Chem. B*, 113(33):11463–11478, 2009.

[71] W. R. P. Scott, P. H. Hünenberger, I. G. Tironi, A. E. Mark, S. R. Billeter, J. Fennen, A. E. Torda, T. Huber, P. Krüger, and W. F. Van Gunsteren. The GROMOS biomolecular simulation program package. *J. Phys. Chem. A*, 103(19):3596–3607, 1999.

[72] W. D. Cornell, P. Cieplak, C. I. Bayly, I. R. Gould andK. M. Merz, D. M. Ferguson, D. C. Spellmeyer, T. Fox, J. W. Caldwell, and P. A. Kollman. A second generation force field for the simulation of proteins, nucleic acids, and organic molecules. *J. Am. Chem. Soc.*, 117(19):5179–5197, 1995.

[73] Alex D MacKerell Jr, Donald Bashford, MLDR Bellott, Roland Leslie Dunbrack Jr, Jeffrey D Evanseck, Martin J Field, Stefan Fischer, Jiali Gao, H Guo, Sookhee Ha, et al. All-atom empirical potential for molecular modeling and dynamics studies of proteins. *J. Phys. Chem. B*, 102(18):3586–3616, 1998.

[74] W. L. Jorgensen, D. S. Maxwell, and J. Tirado-Rives. Development and testing of the opls all-atom force field on conformational energetics and properties of organic liquids. *J. Am. Chem. Soc.*, 118(45):11225–11236, 1996.

[75] B Th Thole. Molecular polarizabilities calculated with a modified dipole interaction. *Chem. Phys.*, 59(3):341–350, 1981.

[76] T. Darden, D. York, and L. Pedersen. Particle mesh ewald: An $n\ log(n)$ method for ewald sums in large systems. *J. Chem. Phys.*, 98(12):10089–10094, 1993.

[77] Markus Deserno and Christian Holm. How to mesh up ewald sums. ii. an accurate error estimate for the particle–particle–particle-mesh algorithm. *J. Chem. Phys.*, 109(18):7694–7701, 1998.

[78] R Martin. Electronic structure–basic theory and practical methods, cambridge univ. *Pr., West Nyack, NY*, 2004.

[79] Walter Kohn. Nobel lecture: Electronic structure of matter—wave functions and density functionals. *Rev. Mod. Phys.*, 71(5):1253, 1999.

[80] Axel D Becke. Density-functional exchange-energy approximation with correct asymptotic behavior. *Phys. Rev. A*, 38(6):3098, 1988.

[81] Chengteh Lee, Weitao Yang, and Robert G Parr. Development of the colle-salvetti correlation-energy formula into a functional of the electron density. *Phys. Rev. B*, 37(2):785, 1988.

[82] Seymour H Vosko, Leslie Wilk, and Marwan Nusair. Accurate spin-dependent electron liquid correlation energies for local spin density calculations: a critical analysis. *Can. J. Phys.*, 58(8):1200–1211, 1980.

[83] Georg Kresse and Jürgen Furthmüller. Efficient iterative schemes for ab initio total-energy calculations using a plane-wave basis set. *Phys. Rev. B*, 54(16):11169, 1996.

[84] Georg Kresse and J Hafner. Ab initio molecular dynamics for open-shell transition metals. *Phys. Rev. B*, 48(17):13115, 1993.

[85] John P Perdew, Kieron Burke, and Matthias Ernzerhof. Generalized gradient approximation made simple. *Phys. Rev. Lett.*, 77(18):3865, 1996.

[86] Axel D Becke. A new mixing of hartree–fock and local density-functional theories. *J. Chem. Phys.*, 98(2):1372–1377, 1993.

[87] Nicholas Metropolis, Arianna W Rosenbluth, Marshall N Rosenbluth, Augusta H Teller, and Edward Teller. Equation of state calculations by fast computing machines. *J. Chem. Phys.*, 21(6):1087–1092, 1953.

[88] W Keith Hastings. Monte carlo sampling methods using markov chains and their applications. 1970.

[89] Kristen A Fichthorn and W Hh Weinberg. Theoretical foundations of dynamical monte carlo simulations. *J. Chem. Phys.*, 95(2):1090–1096, 1991.

[90] L M Varela, J Carrete, M García, L J Gallego, M Turmine, E Rilo, and O Cabeza. Pseudolattice theory of charge transport in ionic solutions: Corresponding states law for the electric conductivity. *Fluid Phase Equilibr*, 298(2):280–286, 2010.

[91] P Debye and E Hückel. De la theorie des electrolytes. i. abaissement du point de congelation et phenomenes associes. *Phys. Z.*, 24(9):185–206, 1923.

[92] Frederick Seitz. *The modern theory of solids*, volume 548. McGraw-Hill New York, 1940.

[93] T. Méndez-Morales, J. Carrete, O. Cabeza, O. Russina, A. Triolo, L. J. Gallego, and L. M. Varela. Solvation of lithium salts in protic ionic liquids: a molecular dynamics study. *J. Phys. Chem. B*, 118:761–770, 2014.

[94] Amy Brand, Liz Allen, Micah Altman, Marjorie Hlava, and Jo Scott. Beyond authorship: attribution, contribution, collaboration, and credit. *Learned Publishing*, 28(2):151–155, 2015.

[95] Liz Allen, Alison O'Connell, and Veronique Kiermer. How can we ensure visibility and diversity in research contributions? how the contributor role taxonomy (CRediT) is helping the shift from authorship to contributorship. *Learned Publishing*, 32(1):71–74, 2019.

[96] R. D. Rogers and K. R. Seddon. Ionic liquids–solvents of the future? *Science*, 302(5646):792–793, 2003.

[97] J. Dupont, R. F. de Souza, and P. A. Z. Suarez. Ionic liquid (molten salt) phase organometallic catalysis. *Chem. Rev.*, 102(10):3667–3692, 2002.

[98] S. Seki, Y. Kobayashi, H. Miyashiro, Y. Ohno, A. Usami, Y. Mita, N. Kihira, M. Watanabe, and N. Terada. Lithium secondary batteries using modified-imidazolium room-temperature ionic liquid. *J. Phys. Chem. B*, 110(21):10228–10230, 2006.

[99] Giovanni B Appetecchi, Maria Montanino, Andrea Balducci, Simon F Lux, Martin Winterb, and Stefano Passerini. Lithium insertion in graphite from ternary ionic liquid-lithium salt electrolytes: I. electrochemical characterization of the electrolytes. *J. Power Sources*, 192(2):599–605, 2009.

[100] J. Lassègues, J. Grondin, C. Aupetit, and P. Johansson. Spectroscopic identification of the lithium ion transporting species in LiTFSI-doped ionic liquids. *J. Phys. Chem. A*, 113(1):305–314, 2009.

[101] Franca Castiglione, Enzio Ragg, Andrea Mele, Giovanni Battista Appetecchi, Maria Montanino, and Stefano Passerini. Molecular environment and enhanced diffusivity of Li^+ ions in lithium-salt-doped ionic liquid electrolytes. *J. Phys. Chem. Lett.*, 2(3):153–157, 2011.

[102] Zhe Li, Grant D. Smith, and Dmitry Bedrov. Li^+ solvation and transport properties in ionic liquid/lithium salt mixtures: A molecular dynamics simulation study. *J. Phys. Chem. B*, 116(42):12801–12809, 2012.

[103] T. Méndez-Morales, J. Carrete, S. Bouzón-Capelo, M. Pérez-Rodríguez, O. Cabeza, L. J. Gallego, and L. M. Varela. MD simulations of the formation of stable clusters in mixtures of alkaline salts and imidazolium-based ionic liquids. *J. Phys. Chem. B*, 117(11):3207–3220, 2013.

[104] Volker Lesch, Sebastian Jeremias, Arianna Moretti, Stefano Passerini, Andreas Heuer, and Oleg Borodin. A combined theoretical and experimental study of the influence of different anion ratios on lithium ion dynamics in ionic liquids. *J. Phys. Chem. B*, 118(26):7367–7375, 2014.

[105] Zhe Li, Oleg Borodin, Grant D. Smith, and Dmitry Bedrov. Effect of organic solvents on Li^+ ion solvation and transport in ionic liquid electrolytes: A molecular dynamics simulation study. *J. Phys. Chem. B*, 119(7):3085–3096, 2015.

[106] Volker Lesch, Zhe Li, Dmitry Bedrov, Oleg Borodin, and Andreas Heuer. The influence of cations on lithium ion coordination and transport in ionic liquid electrolytes: a MD simulation study. *Phys. Chem. Chem. Phys.*, 18(1):382–392, 2016.

[107] O. Borodin. Molecular dynamics simulations of ionic liquids: Influence of polarization on il structure and ion transport. *Mater. Res. Soc. Proc.*, 1082:Q06–04, 2008.

[108] José N Canongia Lopes and Agílio AH Pádua. Cl&p: A generic and systematic force field for ionic liquids modeling. *Theor. Chem. Acc.*, 131(3):1–11, 2012.

[109] Florian Dommert, Katharina Wendler, Robert Berger, Luigi Delle Site, and Christian Holm. Force fields for studying the structure and dynamics of ionic liquids: a critical review of recent developments. *ChemPhysChem*, 13(7):1625–1637, 2012.

[110] O. Russina, R. Caminiti, T. Méndez-Morales, J. Carrete, O. Cabeza, L.J. Gallego, L.M. Varela, and A. Triolo. How does lithium nitrate dissolve in a protic ionic liquid? *J. Mol. Liq.*, 205(0):16 – 21, 2015.

[111] Dmitry Bedrov, Oleg Borodin, Zhe Li, and Grant D. Smith. Influence of polarization on structural, thermodynamic, and dynamic properties of ionic liquids obtained from molecular dy-

namics simulations. *J. Phys. Chem. B*, 114(15):4984–4997, 2010. PMID: 20337454.

[112] T. Yan, C. J. Burnham, M. G. Del Pópolo, and G. A. Voth. Molecular dynamics simulation of ionic liquids: The effect of electronic polarizability. *J. Phys. Chem. B*, 108(32):11877–11881, 2004.

[113] O. Borodin, G. D. Smith, and W. Henderson. Li^+ cation environment, transport, and mechanical properties of the litfsi doped n-methyl-n-alkylpyrrolidinium+$TFSI^-$ ionic liquids. *J. Phys. Chem. B*, 110(34):16879–16886, 2006.

[114] G. D. Smith, O. Borodin, S. P. Russo, R. J. Rees, and A. F. Hollenkamp. A molecular dynamics simulation study of $LiFePO_4$/electrolyte interfaces: structure and Li^+ transport in carbonate and ionic liquid electrolytes. *Phys. Chem. Chem. Phys.*, 11(42):9884–9897, 2009.

[115] C. J. F. Solano, S. Jeremias, E. Paillard, D. Beljonne, and R. Lazzaroni. A joint theoretical/experimental study of the structure, dynamics, and li^+ transport in bis([tri]fluoro[methane]sulfonyl)imide [t]fsi-based ionic liquids. *J. Chem. Phys.*, 139(3):034502, 2013.

[116] C. Schröder, T. Sonnleitner, R. Buchner, and O. Steinhauser. The influence of polarizability on the dielectric spectrum of the ionic liquid 1-ethyl-3-methylimidazolium triflate. *Phys. Chem. Chem. Phys.*, 13:12240–12248, 2011.

[117] Michael Schmollngruber, Volker Lesch, Christian Schröder, Andreas Heuer, and Othmar Steinhauser. Comparing induced point-dipoles and drude oscillators. *Phys. Chem. Chem. Phys.*, 17:14297–14306, 2015.

[118] C. Schröder. Comparing reduced partial charge models with polarizable simulations of ionic liquids. *Phys. Chem. Chem. Phys.*, 14:3089–3102, 2012.

[119] W. L. Jorgensen. Optimized intermolecular potential functions for liquid alcohols. *J. Phys. Chem.*, 90(7):1276–1284, 1986.

[120] Trinidad Mendez-Morales, Jesus Carrete, Julio R. Rodriguez, Oscar Cabeza, Luis J. Gallego, Olga Russina, and Luis M. Varela. Nanostructure of mixtures of protic ionic liquids and lithium salts: effect of alkyl chain length. *Phys. Chem. Chem. Phys.*, 17:5298–5307, 2015.

[121] Anthony Stone. *The theory of intermolecular forces*. Oxford University Press, 2013.

[122] Haibo Yu and Wilfred F van Gunsteren. Accounting for polarization in molecular simulation. *Comput. Phys. Comm.*, 172(2):69–85, 2005.

[123] Christian Schröder and Othmar Steinhauser. Simulating polarizable molecular ionic liquids with drude oscillators. *J. Chem. Phys.*, 133(15):154511, 2010.

[124] D. V. D. Spoel, E. Lindahl, B. Hess, A. R. V. Buuren, E. Apol, P. J. Meulenhoff, D. P. Tieleman, A. L. T. M. Sijbers, K. A. Feenstra, R. V. Drunen, and H. J. C. Berendsen. *Gromacs User Manual version 4.6.7*. http://www.Gromacs.org, 2014.

[125] J. N. Canongia-Lopes and A. A. H. Pádua. Molecular force field for ionic liquids composed of triflate or bistriflylimide anions. *J. Phys. Chem. B*, 108(43):16893–16898, 2004.

[126] B. Hess, H. Bekker, H. J. C. Berendsen, and J. G. E. M. Fraaije. Lincs: A linear constraint solver for molecular simulations. *J. Comp. Chem.*, 18(12):1463–1472, 1997.

[127] B. Hess. P-lincs: A parallel linear constraint solver for molecular simulation. *J. Chem. Theory Comp.*, 4(1):116–122, 2007.

[128] Giovanni Bussi, Davide Donadio, and Michele Parrinello. Canonical sampling through velocity rescaling. *J. Chem. Phys.*, 126(1):014101, 2007.

[129] M. Parrinello and A. Rahman. Polymorphic transitions in single crystals: A new molecular dynamics method. *J. Appl. Phys.*, 52(12):7182–7190, 1981.

[130] D. A. Case, T. A. Darden, T. E. III Cheatham, C. L. Simmerling, J. Wang, R. E. Duke, R. Luo, M. Crowley, R. C. Walker, W. Zhang, et al. AMBER 10, 2008.

[131] S. Niu, Z. Cao, S. Li, and T. Yan. Structure and transport properties of the $LiPF_6$ doped 1-ethyl-2,3-dimethyl-imidazolium hexafluorophosphate ionic liquids: A molecular dynamics study. *J. Phys. Chem. B*, 114(2):877–881, 2010.

[132] Daniel M. Seo, Oleg Borodin, Sang-Don Han, Paul D. Boyle, and Wesley A. Henderson. Electrolyte solvation and ionic association ii. acetonitrile-lithium salt mixtures: Highly dissociated salts. *J. Electrochem. Soc.*, 159(9):A1489–A1500, 2012.

[133] Jagath Pitawala, Anna Martinelli, Patrik Johansson, Per Jacobsson, and Aleksandar Matic. Coordination and interactions in a li-salt doped ionic liquid. *J. Non-Cryst. Solids*, 407(0):318 – 323, 2015.

[134] Volker Lesch, Andreas Heuer, Christian Holm, and Jens Smiatek. Solvent effects of 1-ethyl-3-methylimidazolium acetate: solvation and dynamic behavior of polar and apolar solutes. *Phys. Chem. Chem. Phys.*, 17(13):8480–8490, 2015.

[135] C. Schröder. Collective translational motions and cage relaxations in molecular ionic liquids. *J. Chem. Phys.*, 135:024502, 2011.

[136] M. G. Del Pópolo and G. A. Voth. On the structure and dynamics of ionic liquids. *J. Phys. Chem. B*, 108(5):1744–1752, 2004.

[137] T. Méndez-Morales, J. Carrete, O. Cabeza, L. J. Gallego, and L. M. Varela. Molecular dynamics simulation of the structure and dynamics of water-1-alkyl-3-methylimidazolium ionic liquid mixtures. *J. Phys. Chem. B*, 115(21):6995–7008, 2011.

[138] Daan Frenkel and Berend Smit. *Understanding molecular simulation: from algorithms to applications*, volume 1. Academic press, 2001.

[139] T. Kato, K. Machida, M. Oobatake, and S. Hayashi. Ionic dynamics in computer simulated molten $lino_3$. i. translational and reorientational motion. *J. Chem. Phys.*, 89:3211, 1988.

[140] K. Wendler, M. Brehm, F. Malberg, B. Kirchner, and L. delle Sitte. Short time dynamics of ionic liquids in AIMD-based power spectra. *J. Chem. Theory Comput.*, 8:1570, 2012.

[141] R. Ramírez, T. López-Ciudad, P. Padma Kumar, and D. Marx. Quantum corrections to classical time-correlation functions: hydrogen bonding and anharmonic floppy modes. *J. Chem. Phys.*, 121:3973, 2004.

[142] HJ Parkhurst Jr and J Jonas. Dense liquids. i. the effect of density and temperature on self-diffusion of tetramethylsilane and benzene-d6. *J. Chem. Phys.*, 63(6):2698–2704, 1975.

[143] Liyuan Sun, Oscar Morales-Collazo, Han Xia, and Joan F. Brennecke. Effect of structure on transport properties (viscosity, ionic conductivity, and self-diffusion coefficient) of aprotic heterocyclic anion (aha) room-temperature ionic liquids. 1. variation of anionic species. *J. Phys. Chem. B*, 119(48):15030–15039, 2015.

[144] M. Freemantle. *An Introduction to Ionic Liquids*. RSC Publishing, 2009.

[145] Suojiang Zhang, Xingmei Lu, Qing Zhou, Xiaohua Li, Xiangping Zhang, and Shucai Li. *Ionic Liquids: Physicochemical Properties*. Elsevier, 2009.

[146] Natalia V Plechkova and Kenneth R Seddon. Applications of ionic liquids in the chemical industry. *Chem. Soc. Rev.*, 37(1):123–150, 2008.

[147] D. Zhao, M. Wu, Y. Kou, and E. Min. Ionic liquids: applications in catalysis. *Catalysis Today*, 74(1–2):157–189, 2002.

[148] R. D. Rogers and K. R. Seddon. *Ionic liquids: industrial applications for green chemistry*. American Chemical Society, 2002.

[149] Olga Russina, Alessio Sferrazza, Ruggero Caminiti, and Alessandro Triolo. Amphiphile meets amphiphile: Beyond the polar–apolar dualism in ionic liquid/alcohol mixtures. *J. of phys. chem. letters*, 5(10):1738–1742, 2014.

[150] Olga Russina, Alessandro Mariani, Ruggero Caminiti, and Alessandro Triolo. Structure of a binary mixture of ethylammonium nitrate and methanol. *J. Solution Chem.*, 44(3-4):669–685, 2015.

[151] Olga Russina, Marina Macchiagodena, Barbara Kirchner, Alessandro Mariani, Bachir Aoun, Margarita Russina, Ruggero Caminiti, and Alessandro Triolo. Association in ethylammonium nitrate–dimethyl sulfoxide mixtures: First structural and dynamical evidences. *J. Non-Cryst. Solids*, 407(0):333 – 338, 2015. 7th IDMRCS: Relaxation in Complex Systems.

[152] Borja Docampo-Álvarez, Víctor Gómez-González, Trinidad Méndez-Morales, Jesús Carrete, Julio R. Rodríguez, Óscar Cabeza, Luis J. Gallego, and Luis M. Varela. Mixtures of protic ionic liquids and molecular cosolvents: A molecular dynamics simulation. *J. Chem. Phys*, 140(21):214502, 2014.

[153] Martin Allen, D Fennell Evans, and Rufus Lumry. Thermodynamic properties of the ethylammonium nitrate+ water system: Partial molar volumes, heat capacities, and expansivities. *J. Solution Chem.*, 14(8):549–560, 1985.

[154] Tristan JV Findlay and Martyn CR Symons. Solvation spectra. part 50.—spectrophotometric studies of the solvation of nitrate ions in protic and aprotic media. *J. Chem. Soc. Farad. Trans. 2*, 72:820–826, 1976.

[155] RG Horn, DF Evans, and BW Ninham. Double-layer and solvation forces measured in a molten salt and its mixtures with water. *J. Phys. Chem.*, 92(12):3531–3537, 1988.

[156] Ibrahim Bou Malham, Pierre Letellier, Alain Mayaffre, and Mireille Turmine. Part i: Thermodynamic analysis of volumetric properties of concentrated aqueous solutions of 1-butyl-3-methylimidazolium tetrafluoroborate, 1-butyl-2, 3-dimethylimidazolium tetrafluoroborate, and ethylammonium nitrate based on pseudo-lattice theory. *J. Chem. Thermodyn.*, 39(8):1132–1143, 2007.

[157] Sabbah Bouguerra, Ibrahim Bou Malham, Pierre Letellier, Alain Mayaffre, and Mireille Turmine. Part 2: Limiting apparent molar volume of organic and inorganic 1: 1 electrolytes in (water+ ethylammonium nitrate) mixtures at 298k–thermodynamic approach using bahe–varela pseudo-lattice theory. *J. Chem. Thermodyn*, 40(2):146–154, 2008.

[158] T Heimburg, SZ Mirzaev, and U Kaatze. Heat capacity behavior in the critical region of the ionic binary mixture ethylammonium nitrate–n-octanol. *Phys. Rev. E*, 62(4):4963, 2000.

[159] A Chagnes, A Tougui, B Carré, N Ranganathan, and D Lemordant. Abnormal temperature dependence of the viscosity of ethylammonium nitrate–methanol ionic mixtures. *J. Solution Chem.*, 33(3):247–255, 2004.

[160] T. Méndez-Morales, J. Carrete, O. Cabeza, L. J. Gallego, and L. M. Varela. Molecular dynamics simulations of the structural and thermodynamic properties of imidazolium-based ionic liquid mixtures. *J. Phys. Chem. B*, 115(38):11170–11182, 2011.

[161] T. Méndez-Morales, J. Carrete, M. García, O. Cabeza, L. J. Gallego, and L. M. Varela. Dynamical properties of alcohol + 1-hexyl-3-methylimidazolium ionic liquid mixtures: A computer simulation study. *J. Phys. Chem. B*, 115(51):15322–15322, 2011.

[162] T. L. Greaves, D. F. Kennedy, A. Weerawardena, N. M. K. Tse, N. Kirby, and C. J. Drummond. Nanostructured protic ionic liquids retain nanoscale features in aqueous solution while precursor brønsted acids and bases exhibit different behavior. *J. Phys. Chem. B*, 115(9):2055–2066, 2011.

[163] Tamar L Greaves, Danielle F Kennedy, Nigel Kirby, and Calum J Drummond. Nanostructure changes in protic ionic liquids (pils) through adding solutes and mixing pils. *Phys. Chem. Chem. Phys.*, 13(30):13501–13509, 2011.

[164] Mark James Abraham, Teemu Murtola, Roland Schulz, Szilárd Páll, Jeremy C Smith, Berk Hess, and Erik Lindahl. Gromacs: High performance molecular simulations through multi-level parallelism from laptops to supercomputers. *SoftwareX*, 1:19–25, 2015.

[165] D. V. D. Spoel, E. Lindahl, B. Hess, A. R. V. Buuren, E. Apol, P. J. Meulenhoff, D. P. Tieleman, A. L. T. M. Sijbers, K. A. Feenstra, R. V. Drunen, and H. J. C. Berendsen. *Gromacs User Manual version 4.0*. http://www.Gromacs.org, 2005.

[166] Herman JC Berendsen, David van der Spoel, and Rudi van Drunen. Gromacs: a message-passing parallel molecular dynamics implementation. *Comput. Phys. Commun.*, 91(1):43–56, 1995.

[167] Marcus D Hanwell, Donald E Curtis, David C Lonie, Tim Vandermeersch, Eva Zurek, and Geoffrey R Hutchison. Avogadro: an advanced semantic chemical editor, visualization, and analysis platform. *J. Cheminformatics*, 4(1):1, 2012.

[168] Víctor Gómez-González, Borja Docampo-Álvarez, Oscar Cabeza, Maxim Fedorov, Ruth M Lynden-Bell, Luis J Gallego, and Luis M Varela. Molecular dynamics simulations of the structure and single-particle dynamics of mixtures of divalent salts and ionic liquids. *J. Chem. Phys.*, 143(12):124507, 2015.

[169] Rep Kubo. The fluctuation-dissipation theorem. *Rep. Prog. Phys.*, 29(1):255, 1966.

[170] Haihui Joy Jiang, Paul A FitzGerald, Andrew Dolan, Rob Atkin, and Gregory G Warr. Amphiphilic self-assembly of alkanols in protic ionic liquids. *J. Phys. Chem. B*, 118(33):9983–9990, 2014.

[171] Wolffram Schroer, Alessandro Triolo, and Olga Russina. Nature of mesoscopic organization in protic ionic liquid–alcohol mixtures. *J. Phys. Chem. B*, 120(9):2638–2643, 2016.

[172] M. J. Earle and K. R. Seddon. Ionic liquids. green solvents for the future. *Pure Appl. Chem.*, 72(7):1391–1398, 2000.

[173] Robin D Rogers and Kenneth R Seddon. Ionic liquids–solvents of the future? *Science*, 302(5646):792–793, 2003.

[174] Maciej Galiński, Andrzej Lewandowski, and Izabela Stępniak. Ionic liquids as electrolytes. *Electrochim. Acta*, 51(26):5567–5580, 2006.

[175] Vasile I Pârvulescu and Christopher Hardacre. Catalysis in ionic liquids. *Chem. Rev.*, 107(6):2615–2665, 2007.

[176] Hermann Weingärtner. Understanding ionic liquids at the molecular level: facts, problems, and controversies. *Angew. Chem. Int. Ed.*, 47(4):654–670, 2008.

[177] Maxym Dudka, Svyatoslav Kondrat, Alexei Kornyshev, and Gleb Oshanin. Phase behaviour and structure of a superionic liquid in nonpolarized nanoconfinement. *J. Phys.: Condens. Matter*, 28(46):464007, 2016.

[178] Z. Liu, X. Wu, and W. Wang. A novel united-atom force field for imidazolium-based ionic liquids. *Phys. Chem. Chem. Phys.*, 8(9):1096–1104, 2006.

[179] Daniel Ebeling, Stephan Bradler, Bernhard Roling, and André Schirmeisen. 3-dimensional structure of a prototypical

ionic liquid–solid interface: Ionic crystal-like behavior induced by molecule–substrate interactions. *J. Phys. Chem. C*, 120(22):11947–11955, 2016.

[180] David T Limmer. Interfacial ordering and accompanying divergent capacitance at ionic liquid-metal interfaces. *Phys. Rev. Lett.*, 115(25):256102, 2015.

[181] Víctor Gómez-Gonzalez, Borja Docampo-Álvarez, Trinidad Méndez-Morales, Oscar Cabeza, Vladislav B. Ivaništšev, Maxim V. Fedorov, Luis J. Gallego, and Luis M. Varela. Molecular dynamics simulation of the structure and interfacial free energy barriers of mixtures of ionic liquids and divalent salts near a graphene wall. *Phys. Chem. Chem. Phys.*, 19:846–853, 2017.

[182] SA Brazovskii. Phase transition of an isotropic system to a nonuniform state. *J. Exp. Theor. Phys.*, 41:85, 1975.

[183] Ludwik Leibler. Theory of microphase separation in block copolymers. *Macromolecules*, 13(6):1602–1617, 1980.

[184] Glenn H Fredrickson and Eugene Helfand. Fluctuation effects in the theory of microphase separation in block copolymers. *J. Chem. Phys.*, 87(1):697–705, 1987.

[185] Michael Seul and David Andelman. Domain shapes and patterns: the phenomenology of modulated phases. *Science*, 267(5197):476, 1995.

[186] G. Gompper, C. Domb, M.S. Green, M. Schick, and J.L. Lebowitz. Self-assembling amphiphilic systems. Phase Transitions and Critical Phenomena. Vol. 16. Academic: London, 1994.

[187] Alina Ciach and W. T. Góźdź. 7 nonelectrolyte solutions exhibiting structure on the nanoscale. *Annu. Rep. Prog. Chem., Sect. C: Phys. Chem.*, 97:269–314, 2001.

[188] William Humphrey, Andrew Dalke, and Klaus Schulten. VMD: visual molecular dynamics. *J. Mol. Graph. Model.*, 14(1):33–38, 1996.

[189] Leandro Martínez, Ricardo Andrade, Ernesto G Birgin, and José Mario Martínez. Packmol: a package for building initial configurations for molecular dynamics simulations. *J. Comp. Chem.*, 30(13):2157–2164, 2009.

[190] Paulo T Araujo, Mauricio Terrones, and Mildred S Dresselhaus. Defects and impurities in graphene-like materials. *Mater. Today*, 15(3):98–109, 2012.

[191] Humberto Terrones, Ruitao Lv, Mauricio Terrones, and Mildred S Dresselhaus. The role of defects and doping in 2d graphene sheets and 1d nanoribbons. *Rep. Progr. Phys.*, 75(6):062501, 2012.

[192] KR Mecke. Morphological characterization of patterns in reaction-diffusion systems. *Phys. Rev. E*, 53(5):4794, 1996.

[193] Nobuyuki Otsu. A threshold selection method from gray-level histograms. *Automatica*, 11(285-296):23–27, 1975.

[194] J Pękalski, A Ciach, and N. G. Almarza. Periodic Ordering of Clusters and Stripes in a Two-Dimensional Lattice Model. I. Ground State, Mean-Field Phase Diagram and Structure of the Disordered Phases. *J. Chem. Phys.*, 140(11):114701, 2014.

[195] N. G. Almarza, J Pękalski, and A Ciach. Periodic Ordering of Clusters and Stripes in a Two-dimensional Lattice Model. II. Results of Monte Carlo Simulation. *J. Chem. Phys.*, 140(16):164708, 2014.

[196] T.L. Hill. *An Introduction to Statistical Thermodynamics*. Addison-Wesley: Reading, Mass., 1960.

[197] Ilya Prigogine, André Bellemans, and Victor Mathot. *The Molecular Theory of Solutions*, volume 4. North-Holland: Amsterdam, 1957.

[198] A Ciach and W. T. Góźdź. Mesoscopic description of network-forming clusters of weakly charged colloids. *Condens. Matter Phys.*, 13:23603, 2010.

[199] Daniel G Barci, Alejandro Mendoza-Coto, and Daniel A Stariolo. Nematic phase in stripe-forming systems within the self-consistent screening approximation. *Phys. Rev. E*, 88(6):062140, 2013.

[200] A Imperio and L Reatto. Microphase separation in two-dimensional systems with competing interactions. *J. Chem. Phys.*, 124(16):164712, 2006.

[201] Andrew J Archer. Two-dimensional fluid with competing interactions exhibiting microphase separation: Theory for bulk and interfacial properties. *Phys. Rev. E*, 78(3):031402, 2008.

[202] A Ciach, J Pękalski, and W. T. Góźdź. Origin of similarity of phase diagrams in amphiphilic and colloidal systems with competing interactions. *Soft Matter*, 9(27):6301–6308, 2013.

[203] Markus Edelmann and Roland Roth. Gyroid phase of fluids with spherically symmetric competing interactions. *Phys. Rev. E*, 93(6):062146, 2016.

[204] Yuan Zhuang, Kai Zhang, and Patrick Charbonneau. Equilibrium phase behavior of a continuous-space microphase former. *Phys. Rev. Lett.*, 116(9):098301, 2016.

[205] Alina Ciach. Mesoscopic theory for inhomogeneous mixtures. *Mol. Phys.*, 109(7-10):1101–1119, 2011.

[206] Danuta Kruk, Milosz Wojciechowski, Szczepan Brym, and Rajendra Kumar Singh. Dynamics of ionic liquids in bulk and in confinement by means of 1h nmr relaxometry - bmim-ocso4 in an sio2 matrix as an example. *Phys. Chem. Chem. Phys.*, 18:23184–23194, 2016.

[207] Daniel Walgraef. Nanostructure initiation during the early stages of thin film growth. *Phys. Rev. E*, 15(1):33–40, 2002.

[208] MG Clerc, E Tirapegui, and M Trejo. Pattern formation and localized structures in reaction-diffusion systems with non-fickian transport. *Phys. Rev. Lett.*, 97(17):176102, 2006.

[209] Rohit L Vekariya. a review of ionic liquids: applications towards catalytic organic transformations. *J. Mol. Liq.*, 227:44–60, 2017.

[210] Tamar L Greaves and Calum J Drummond. Protic ionic liquids: evolving structure–property relationships and expanding applications. *Chem. Rev.*, 115(20):11379–11448, 2015.

[211] Robert Hayes, Gregory G Warr, and Rob Atkin. Structure and nanostructure in ionic liquids. *Chem. Rev.*, 115(13):6357–6426, 2015.

[212] Samuel W Coles, Maksim Mishin, Susan Perkin, Maxim V Fedorov, and Vladislav B Ivaništšev. The nanostructure of a lithium glyme solvate ionic liquid at electrified interfaces. *Phys. Chem. Chem. Phys.*, 19(18):11004–11010, 2017.

[213] Robert Hayes, Gregory G Warr, and Rob Atkin. At the interface: solvation and designing ionic liquids. *Phys. Chem. Chem. Phys.*, 12(8):1709–1723, 2010.

[214] Vladislav Ivaništšev, Trinidad Méndez-Morales, Ruth M Lynden-Bell, Oscar Cabeza, Luis J Gallego, Luis M Varela, and Maxim V Fedorov. Molecular origin of high free energy barriers for alkali metal ion transfer through ionic liquid–graphene electrode interfaces. *Phys. Chem. Chem. Phys.*, 18(2):1302–1310, 2016.

[215] D Borissov, CL Aravinda, and W Freyland. Comparative investigation of underpotential deposition of ag from aqueous and ionic electrolytes: an electrochemical and in situ stm study. *J. Phys. Chem. B*, 109(23):11606–11615, 2005.

[216] Ge-Bo Pan and Werner Freyland. 2d phase transition of pf 6 adlayers at the electrified ionic liquid/au (111) interface. *Chem. Phys. Lett.*, 427(1):96–100, 2006.

[217] Yaodong Liu, Yi Zhang, Guozhong Wu, and Jun Hu. Coexistence of liquid and solid phases of Bmim-PF_6 ionic liquid on mica surfaces at room temperature. *J. Am. Chem. Soc.*, 128(23):7456–7457, 2006.

[218] Yongchun Fu and Alexander V Rudnev. Scanning probe microscopy of an electrode/ionic liquid interface. *Current Opinion in Electrochemistry*, 1:59–65, 2017.

[219] Jiale Ma, Qiangqiang Meng, Chun Chan, Zhen Li, Yonghui Zhang, and Jun Fan. Alkyl tail aggregations break long range ordering of ionic liquids confined in sub-nanometer pores. *J. Phys. Chem. C*, 122:27314–27322, 2018.

[220] Víctor Gómez-González, Borja Docampo-Álvarez, Trinidad Méndez-Morales, Oscar Cabeza, Vladislav B Ivaništšev, Maxim V Fedorov, Luis J Gallego, and Luis M Varela. Molecular dynamics simulation of the structure and interfacial free energy barriers of mixtures of ionic liquids and divalent salts near a graphene wall. *Phys. Chem. Chem. Phys.*, 19(1):846–853, 2017.

[221] Hadrian Montes-Campos, Jose Manuel Otero-Mato, Trinidad Mendez-Morales, Oscar Cabeza, Luis J. Gallego, Alina Ciach, and Luis M. Varela. Two-dimensional pattern formation in ionic liquids confined between graphene walls. *Phys. Chem. Chem. Phys.*, 19:24505–24512, 2017.

[222] Wu Zhou, Jaekwang Lee, Jagjit Nanda, Sokrates T Pantelides, Stephen J Pennycook, and Juan-Carlos Idrobo. Atomically localized plasmon enhancement in monolayer graphene. *Nat. Nanotechnol*, 7(3):161–165, 2012.

[223] RR Nair, M Sepioni, I-Ling Tsai, O Lehtinen, J Keinonen, AV Krasheninnikov, T Thomson, AK Geim, and IV Grigorieva. Spin-half paramagnetism in graphene induced by point defects. *Nat. Phys.*, 8(3):199–202, 2012.

[224] AA El-Barbary, RH Telling, CP Ewels, MI Heggie, and PR Briddon. Structure and energetics of the vacancy in graphite. *Phys. Rev. B*, 68(14):144107, 2003.

[225] Chi-Cheng Lee, Yukiko Yamada-Takamura, and Taisuke Ozaki. Competing magnetism in π-electrons in graphene with a single carbon vacancy. *Phys. Rev. B*, 90(1):014401, 2014.

[226] Jenel Vatamanu, Liulei Cao, Oleg Borodin, Dmitry Bedrov, and Grant D Smith. On the influence of surface topography on the electric double layer structure and differential capacitance of graphite/ionic liquid interfaces. *J. Phys. Chem. Lett.*, 2(17):2267–2272, 2011.

[227] Peter E Blöchl. Projector augmented-wave method. *Phys. Rev. B*, 50(24):17953, 1994.

[228] Hendrik J Monkhorst and James D Pack. Special points for brillouin-zone integrations. *Phys. Rev. B*, 13(12):5188, 1976.

[229] Kostya S Novoselov, Andre K Geim, Sergei V Morozov, D Jiang, Y_ Zhang, Sergey V Dubonos, Irina V Grigorieva, and Alexandr A Firsov. Electric field effect in atomically thin carbon films. *Science*, 306(5696):666–669, 2004.

[230] Volker Lesch, Hadrián Montes-Campos, Trinidad Méndez-Morales, Luis Javier Gallego, Andreas Heuer, Christian Schröder, and Luis M Varela. Molecular dynamics analysis of the effect of electronic polarization on the structure and single-particle dynamics of mixtures of ionic liquids and lithium salts. *J. Chem. Phys.*, 145(20):204507, 2016.

[231] Tianying Yan, Shu Li, Wei Jiang, Xueping Gao, Bing Xiang, and Gregory A Voth. Structure of the liquid- vacuum interface of room-temperature ionic liquids: A molecular dynamics study. *J. Phys. Chem. B*, 110(4):1800–1806, 2006.

[232] Oleg V Yazyev and Lothar Helm. Defect-induced magnetism in graphene. *Phys. Rev. B*, 75(12):125408, 2007.

[233] Graeme Henkelman, Andri Arnaldsson, and Hannes Jónsson. A fast and robust algorithm for Bader decomposition of charge density. *Comput. Mater. Sci.*, 36(3):354–360, 2006.

[234] Kenneth R Seddon. Ionic liquids: a taste of the future. *Nat. Mater.*, 2(6):363–365, 2003.

[235] Natalia V. Plechkova and Kenneth R. Seddon. *Ionic Liquids: "Designer" Solvents for Green Chemistry*, pages 103–130. John Wiley & Sons, Inc., 2007.

[236] Douglas R MacFarlane, Maria Forsyth, Patrick C Howlett, Jennifer M Pringle, Jiazeng Sun, Gary Annat, Wayne Neil, and Ekaterina I Izgorodina. Ionic liquids in electrochemical devices and processes: managing interfacial electrochemistry. *Acc. Chem. Res.*, 40(11):1165–1173, 2007.

[237] Xunyu Lu, Geoff Burrell, Frances Separovic, and Chuan Zhao. Electrochemistry of Room Temperature Protic Ionic Liquids: A Critical Assessment for Use as Electrolytes in Electrochemical Applications. *J. Phys. Chem. B.*, 116(30):9160–9170, 2012.

[238] M. C. Buzzeo, R. G. Evans, and R. G. Compton. Non-haloaluminate room-temperature ionic liquids in electrochemistry–a review. *Chem. Phys. Chem.*, 5(8):1106–1120, 2004.

[239] F. Endres and S. Z. El Abedin. Air and water stable ionic liquids in physical chemistry. *Phys. Chem. Chem. Phys.*, 8(18):2101–2116, 2006.

[240] M. Galiński, A. Lewandowski, and I. Stepniak. Ionic liquids as electrolytes. *Electrochim. Acta*, 51:5567–5580, 2006.

[241] H. Sakaebe and H. Matsumoto. N-methyl-n-propylpiperidinium bis(trifluoromethanesulfonyl)imide (pp13-tfsi) - novel electrolyte base for li battery. *Electrochem. Commun.*, 5(7):594–598, 2003.

[242] B. García, S. Lavallée, G. Perron, C. Michot, and M. Armand. Room temperature molten salts as lithium battery electrolyte. *Electrochim. Acta*, 49(26):4583–4588, 2004.

[243] W. A. Henderson and S. Passerini. Phase behavior of ionic liquid-lix mixtures: Pyrrolidinium cations and tfsi-anions. *Chem. Mater.*, 16(15):2881–2885, 2004.

[244] M. Diaw, A. Chagnes, B. Carré, P. Willmann, and D. Lemordant. Mixed ionic liquid as electrolyte for lithium batteries. *J. Power Sources*, 146(1–2):682–684, 2005.

[245] Q. Zhou, W. A. Henderson, G. B. Appetecchi, and S. Passerini. Phase behavior and thermal properties of ternary ionic liquid−lithium salt (il−il−lix) electrolytes. *J. Phys. Chem. C*, 114(3):6201–6204, 2010.

[246] S. Y. Lee, H. H. Yong, Y. J. Lee, S. K. Kim, and S. Ahn. Two-cation competition in ionic-liquid-modified electrolytes for lithium ion batteries. *Green Chem.*, 109(28):13663–13667, 2005.

[247] I. Nicotera, C. Oliviero, W. A. Henderson, G. B. Appetecchi, and S. Passerini. Nmr investigation of ionic liquid−lix mixtures: pyrrolidinium cations and tfsi- anions. *J. Phys. Chem. B*, 109(48):22814–22819, 2005.

[248] M. Castriota, T. Caruso, R. G. Agostino, E. Cazzanelli, W. A. Henderson, and S. Passerini. Raman investigation of the ionic liquid n-methyl-n-propylpyrrolidinium bis(trifluoromethanesulfonyl)imide and its mixture with $LiN(SO_2CF_3)_2$. *J. Phys. Chem. A*, 109(1):92–96, 2005.

[249] J. Lassègues, J. Grondin, and D. Talaga. Lithium solvation in bis(trifluoromethanesulfonyl)imide-based ionic liquids. *Phys. Chem. Chem. Phys.*, 8(48):5629–5632, 2006.

[250] E. Markevich, V. Baranchugov, and D. Aurbach. On the possibility of using ionic liquids as electrolyte solutions for rechargeable 5v li ion batteries. *Electrochem. Commun.*, 8(8):1331–1334, 2006.

[251] J. Xu, J. Yang, Y. NuLi, J. Wang, and Z. Zhang. Additive-containing ionic liquid electrolytes for secondary lithium battery. *J. Power Sources*, 160(1):621–626, 2006.

[252] M. Egashira, H. Todo, N. Yoshimoto, M. Morita, and J. Yamaki. Functionalized imidazolium ionic liquids as electrolyte components of lithium batteries. *J. Power Sources*, 174(2):560–564, 2007.

[253] Y. Saito, T. Umecky, J. Niwa, T. Sakai, and S. Maeda. Existing condition and migration property of ions in lithium electrolytes with ionic liquid solvent. *J. Phys. Chem. B*, 111(40):11794–11802, 2007.

[254] V. Borgel, E. Markevich, D. Aurbach, G. Semrau, and M. Schmidt. On the application of ionic liquids for rechargeable li batteries: High voltage systems. *J. Power Sources*, 189(1):331–336, 2009.

[255] B. G. Nicolau, A. Sturlaugson, K. Fruchey, M. C. C. Ribeiro, and M. D. Fayer. Room temperature ionic liquid-lithium salt mixtures: Optical Kerr effect dynamical measurements. *J. Phys. Chem. B*, 114(25):8350–8356, 2010.

[256] Q. Zhou, K. Fitzgerald, P. D. Boyle, and W. A. Henderson. Phase behavior and crystalline phases of ionic liquid-lithium salt mixtures with 1-alkyl-3-methylimidazolium salts. *Chem. Mater.*, 22(3):1203–1208, 2010.

[257] Hyun Yoon, GH Lane, Youssof Shekibi, PC Howlett, Maria Forsyth, AS Best, and DR MacFarlane. Lithium electrochemistry and cycling behaviour of ionic liquids using cyano based anions. *Energy Environ. Sci.*, 6(3):979–986, 2013.

[258] Franca Castiglione, Antonino Famulari, Guido Raos, Stefano V Meille, Andrea Mele, Giovanni Battista Appetecchi, and Stefano Passerini. Pyrrolidinium-Based Ionic Liquids Doped with Lithium Salts: How Does Li^+ Coordination Affect Its Diffusivity? *J. Phys. Chem. B*, 118(47):13679–13688, 2014.

[259] Luis Aguilera, Johannes Völkner, Ana Labrador, and Aleksandar Matic. The effect of lithium salt doping on the nanostructure of ionic liquids. *Phys. Chem. Chem. Phys.*, 17(40):27082–27087, 2015.

[260] Abhishek Lahiri, Guozhu Li, Mark Olschewski, and Frank Endres. Influence of Polar Organic Solvents in an Ionic Liquid Containing Lithium Bis (fluorosulfonyl) amide: Effect on the Cation–Anion Interaction, Lithium Ion Battery Performance, and Solid Electrolyte Interphase. *ACS Appl. Mater. Interfaces*, 8(49):34143–34150, 2016.

[261] S. Menne, J. Pires, M. Anouti, and A. Balducci. Protic ionic liquids as electrolytes for lithium-ion batteries. *Electrochem. Commun.*, 31:39–41, 2013.

[262] T Vogl, C Vaalma, D Buchholz, M Secchiaroli, R Marassi, S Passerini, and A Balducci. The use of protic ionic liquids with cathodes for sodium-ion batteries. *J. Mater. Chem. A*, 4(27):10472–10478, 2016.

[263] G. T. Cheek, W. E. O'Grady, S. Zein El Abedin, E. M. Moustafa, and F. Endres. Studies on the electrodeposition of magnesium in ionic liquids. *J. Electrochem. Soc.*, 155(1):D91–D95, 2008.

[264] Guinevere A. Giffin, Arianna Moretti, Sangsik Jeong, and Stefano Passerini. Complex nature of ionic coordination in mag-

nesium ionic liquid-based electrolytes: Solvates with mobile mg2+ cations. *J. Phys. Chem. C*, 118(19):9966–9973, 2014.

[265] Gulin Vardar, Alice E. S. Sleightholme, Junichi Naruse, Hidehiko Hiramatsu, Donald J. Siegel, and Charles W. Monroe. Electrochemistry of magnesium electrolytes in ionic liquids for secondary batteries. *ACS Applied Materials & Interfaces*, 6(20):18033–18039, 2014. PMID: 25248147.

[266] Shimul Saha, Takuho Taguchi, Naoki Tachikawa, Kazuki Yoshii, and Yasushi Katayama. Electrochemical behavior of cadmium in 1-butyl-1-methylpyrrolidinium bis(trifluoromethylsulfonyl)amide room-temperature ionic liquid. *Electrochim. Acta*, 183:42 – 48, 2015.

[267] Meng-Chang Lin, Ming Gong, Bingan Lu, Yingpeng Wu, Di-Yan Wang, Mingyun Guan, Michael Angell, Changxin Chen, Jiang Yang, Bing-Joe Hwang, et al. An ultrafast rechargeable aluminium-ion battery. *Nature*, 520(7547):324, 2015.

[268] Víctor Gómez-González, Borja Docampo-Álvarez, J Manuel Otero-Mato, Oscar Cabeza, Luis J Gallego, and Luis M Varela. Molecular dynamics simulations of the structure of mixtures of protic ionic liquids and monovalent and divalent salts at the electrochemical interface. *Phys. Chem. Chem. Phys.*, 20(18):12767–12776, 2018.

[269] V. Gómez-González, B. Docampo-Álvarez, H. Montes-Campos, J. C. Otero, E. López Lago, O. Cabeza, L. J. Gallego, and L. M. Varela. Solvation of Al^{3+} cations in bulk and confined protic ionic liquids: a computational study. *Phys. Chem. Chem. Phys.*, 20:19071–19081, 2018.

[270] M. V. Fedorov and R. M. Lynden-Bell. Probing the neutral graphene–ionic liquid interface: insights from molecular dynamics simulations. *Phys. Chem. Chem. Phys.*, 14(8):2552–2556, 2012.

[271] Sungsik Jo, Sang-Won Park, Chanwoo Noh, and YounJoon Jung. Computer simulation study of differential capacitance and charging mechanism in graphene supercapacitors: Effects of cyano-group in ionic liquids. *Electrochim. Acta*, 284:577–586, 2018.

[272] Yuanbo Zhang, Angel Rubio, and Guy Le Lay. Emergent elemental two-dimensional materials beyond graphene. *J. Phys. D: Appl. Phys.*, 50(5):053004, 2017.

[273] Ihsan Boustani. New quasi-planar surfaces of bare boron. *Surf. Sci.*, 370(2-3):355–363, 1997.

[274] Andrew J Mannix, Xiang-Feng Zhou, Brian Kiraly, Joshua D Wood, Diego Alducin, Benjamin D Myers, Xiaolong Liu, Brandon L Fisher, Ulises Santiago, Jeffrey R Guest, et al. Synthesis of borophenes: Anisotropic, two-dimensional boron polymorphs. *Science*, 350(6267):1513–1516, 2015.

[275] Andrew J Mannix, Zhuhua Zhang, Nathan P Guisinger, Boris I Yakobson, and Mark C Hersam. Borophene as a prototype for synthetic 2D materials development. *Nat. Nanotechnol.*, 13(6):444, 2018.

[276] Hui Tang and Sohrab Ismail-Beigi. Novel precursors for boron nanotubes: the competition of two-center and three-center bonding in boron sheets. *Phys. Rev. Lett.*, 99(11):115501, 2007.

[277] Xiang-Feng Zhou, Xiao Dong, Artem R Oganov, Qiang Zhu, Yongjun Tian, and Hui-Tian Wang. Semimetallic two-dimensional boron allotrope with massless dirac fermions. *Phys. Rev. Lett.*, 112(8):085502, 2014.

[278] Jesús Carrete, Wu Li, Lucas Lindsay, David A Broido, Luis J Gallego, and Natalio Mingo. Physically founded phonon dispersions of few-layer materials and the case of borophene. *Mater. Res. Lett.*, 4(4):204–211, 2016.

[279] Amador García-Fuente, J Carrete, A Vega, and LJ Gallego. What will freestanding borophene nanoribbons look like? an analysis of their possible structures, magnetism and transport properties. *Phys. Chem. Chem. Phys.*, 19(2):1054–1061, 2017.

[280] Süleyman Er, Gilles A de Wijs, and Geert Brocks. Dft study of planar boron sheets: a new template for hydrogen storage. *J. Phys. Chem. C*, 113(43):18962–18967, 2009.

[281] Lele Li, Hong Zhang, and Xinlu Cheng. The high hydrogen storage capacities of Li-decorated borophene. *Comp. Mater. Sci.*, 137:119–124, 2017.

[282] A Lebon, RH Aguilera-del Toro, LJ Gallego, and A Vega. Li-decorated pmmn8 phase of borophene for hydrogen storage. a van der Waals corrected density-functional theory study. *Int. J. Hydrogen Energ.*, 44(2):1021–1033, 2019.

[283] Xiaoming Zhang, Junping Hu, Yingchun Cheng, Hui Ying Yang, Yugui Yao, and Shengyuan A Yang. Borophene as an extremely high capacity electrode material for Li-ion and Na-ion batteries. *Nanoscale*, 8(33):15340–15347, 2016.

[284] G Kresse and J Furthmüller. Software VASP, Vienna (1999); G. Kresse, J. Hafner. *Phys. Rev. B*, 47:R558, 1993.

[285] Georg Kresse and Jürgen Furthmüller. Efficiency of ab-initio total energy calculations for metals and semiconductors using a plane-wave basis set. *Comput. Mater. Sci.*, 6(1):15–50, 1996.

[286] Georg Kresse and D Joubert. From ultrasoft pseudopotentials to the projector augmented-wave method. *Phys. Rev. B*, 59(3):1758, 1999.

[287] Edward Sanville, Steven D Kenny, Roger Smith, and Graeme Henkelman. Improved grid-based algorithm for Bader charge allocation. *J. Comput. Chem.*, 28(5):899–908, 2007.

[288] W Tang, E Sanville, and G Henkelman. A grid-based Bader analysis algorithm without lattice bias. *J. Phys. Condens. Matter*, 21(8):084204–084210, 2009.

[289] Min Yu and Dallas R Trinkle. Accurate and efficient algorithm for Bader charge integration. *J. Chem. Phys.*, 134(6):064111–064118, 2011.

[290] B. Hess, C. Kutzner, D. V. D. Spoel, and E. Lindahl. Gromacs 4: Algorithms for highly efficient, load-balanced, and scalable molecular simulation. *J. Chem. Theory Comput.*, 4(3):435–447, 2008.

[291] Trinidad Mendez-Morales, Jesus Carrete, Martin Perez-Rodriguez, Oscar Cabeza, Luis J. Gallego, Ruth M. Lynden-Bell, and Luis M. Varela. Molecular dynamics simulations of the structure of the graphene-ionic liquid/alkali salt mixtures interface. *Phys. Chem. Chem. Phys.*, 16:13271–13278, 2014.

[292] Nobuyuki Otsu. A threshold selection method from gray-level histograms. *IEEE Trans. Syst., Man, Cybern. B*, 9(1):62–66, 1979.

[293] Alejandro Lopez-Bezanilla and Peter B Littlewood. Electronic properties of 8-Pmmn borophene. *Phys. Rev. B*, 93(24):241405, 2016.

[294] Claude Elwood Shannon. A mathematical theory of communication. *Bell Labs Tech. J.*, 27(3):379–423, 1948.

[295] Mathieu Salanne. Simulations of room temperature ionic liquids: from polarizable to coarse-grained force fields. *Phys. Chem. Chem. Phys.*, 17(22):14270–14279, 2015.

[296] Sonja Gabl, Christian Schröder, and Othmar Steinhauser. Computational studies of ionic liquids: Size does matter and time too. *J. Chem. Phys.*, 137(9):094501, 2012.

[297] Gota Kikugawa, Shotaro Ando, Jo Suzuki, Yoichi Naruke, Takeo Nakano, and Taku Ohara. Effect of the computational domain size and shape on the self-diffusion coefficient in a Lennard-Jones liquid. *J. Chem. Phys.*, 142(2):024503, 2015.

[298] Alexandru Botan, Virginie Marry, and Benjamin Rotenberg. Diffusion in bulk liquids: finite-size effects in anisotropic systems. *Mol. Phys.*, 113(17-18):2674–2679, 2015.

[299] Pauline Simonnin, Benoît Noetinger, Carlos Nieto-Draghi, Virginie Marry, and Benjamin Rotenberg. Diffusion under confinement: hydrodynamic finite-size effects in simulation. *J. Chem. Theory Comput.*, 13(6):2881–2889, 2017.

[300] Dmitry Bedrov, Jean-Philip Piquemal, Oleg Borodin, Alexander D MacKerell Jr, Benoît Roux, and Christian Schröder. Molecular dynamics simulations of ionic liquids and electrolytes using polarizable force fields. *Chem. Rev.*, 2019.

[301] Jia Le Ma, Qiangqiang Meng, and Jun Fan. Charge driven lateral structural evolution of ions in electric double layer capacitors strongly correlates with differential capacitance. *Phys. Chem. Chem. Phys.*, 20(12):8054–8063, 2018.

[302] Vladislav B Ivaništšev, Kathleen Kirchner, and Maxim V Fedorov. Double layer in ionic liquids: capacitance vs temperature. *arXiv preprint arXiv:1711.06854*, 2017.

[303] Douglas R MacFarlane, Naoki Tachikawa, Maria Forsyth, Jennifer M Pringle, Patrick C Howlett, Gloria D Elliott, James H Davis, Masayoshi Watanabe, Patrice Simon, and C Austen Angell. Energy applications of ionic liquids. *Energy & Environmental Science*, 7(1):232–250, 2014.

[304] Ander González, Eider Goikolea, Jon Andoni Barrena, and Roman Mysyk. Review on supercapacitors: Technologies and materials. *Renewable and Sustainable Energy Reviews*, 58:1189–1206, 2016.

[305] Masayoshi Watanabe, Morgan L Thomas, Shiguo Zhang, Kazuhide Ueno, Tomohiro Yasuda, and Kaoru Dokko. Application of ionic liquids to energy storage and conversion materials and devices. *Chem. Rev.*, 117(10):7190–7239, 2017.

[306] Liumin Suo, Oleg Borodin, Tao Gao, Marco Olguin, Janet Ho, Xiulin Fan, Chao Luo, Chunsheng Wang, and Kang Xu. "water-in-salt" electrolyte enables high-voltage aqueous lithium-ion chemistries. *Science*, 350(6263):938–943, 2015.

[307] Jason P Hallett and Tom Welton. Room-temperature ionic liquids: solvents for synthesis and catalysis. 2. *Chem. Rev.*, 111(5):3508–3576, 2011.

[308] E Hückel and P Debye. Zur theorie der elektrolyte. i. gefrierpunktserniedrigung und verwandte erscheinungen. *Phys. Zeitschrift*, 24:185, 1923.

[309] P Debye, E Hückel, and II Zur Theorie der Elektrolyte. Das grenzgesetz für die elektrische leitfähigkeit. *Phys. Z.*, 24:305–325, 1923.

[310] Lars Onsager. Zur theorie der electrolyte. i. *Phys. Z.*, 27:388–392, 1926.

[311] Lars Onsager. Zur theorie der electrolyte. ii. *Phys. Z.*, 28:277–298, 1927.

[312] J. O'M. Bockris and A.K.N. Reddy. Modern electrochemistry, vol. 1. *MacDonald, London*, 125.

[313] Luis M Varela, Manuel García, and Víctor Mosquera. Exact mean-field theory of ionic solutions: non-debye screening. *Physics reports*, 382(1-2):1–111, 2003.

[314] CA Angell and RD Bressel. Fluidity and conductance in aqueous electrolyte solutions. approach from the glassy state and high-concentration limit. i. calcium nitrate solutions. *J. Phys. Chem-Us*, 76(22):3244–3253, 1972.

[315] John G Kirkwood. Statistical mechanics of liquid solutions. *Chem. Rev.*, 19(3):275–307, 1936.

[316] Ronald Lovett and Frank H Stillinger Jr. Ion-pair theory of concentrated electrolytes. ii. approximate dielectric response calculation. *J. Chem. Phys.*, 48(9):3869–3884, 1968.

[317] JS Ho/ye, JL Lebowitz, and G Stell. Generalized mean spherical approximations for polar and ionic fluids. *J. Chem. Phys.*, 61(8):3253–3260, 1974.

[318] Roland Kjellander and Stjepan Marcelja. Double-layer interaction in the primitive model and the corresponding poisson-boltzmann description. *J. Phys. Chem-Us*, 90(7):1230–1232, 1986.

[319] Michael E Fisher and Yan Levin. Criticality in ionic fluids: Debye-hückel theory, bjerrum, and beyond. *Phys. Rev. Lett.*, 71(23):3826, 1993.

[320] L. M. Varela, M. Garcia, F. Sarmiento, D. Attwood, and V. Mosquera. Pseudolattice theory of strong electrolyte solutions. *J. Chem. Phys.*, 107(16):6415–6419, 1997.

[321] LM Varela, T Méndez-Morales, J Carrete, V Gómez-González, B Docampo-Álvarez, LJ Gallego, O Cabeza, and O Russina. Solvation of molecular cosolvents and inorganic salts in ionic liquids: a review of molecular dynamics simulations. *J. Mol. Liq.*, 210:178–188, 2015.

[322] Juan C Araque, Jeevapani J Hettige, and Claudio J Margulis. Modern room temperature ionic liquids, a simple guide to understanding their structure and how it may relate to dynamics. *J. Phys. Chem. B*, 119(40):12727–12740, 2015.

[323] E. Rilo, J. Vila, S. García-Garabal, L. M. Varela, and O. Cabeza. Electrical conductivity of seven binary systems containing 1-ethyl-3-methyl imidazolium alkyl sulfate ionic liquids with water

or ethanol at four temperatures. *J. Phys. Chem. B*, 117(5):1411–1418, 2013. PMID: 23301957.

[324] M. Trulsson, J. Algotsson, J. Forsman, and C. E. Woodward. Differential capacitance of room temperature ionic liquids: The role of dispersion forces. *J. Phys. Chem. Lett.*, 1:1191–1195, 2010.

[325] Jerry F Casteel and Edward S Amis. Specific conductance of concentrated solutions of magnesium salts in water-ethanol system. *J. Chem. Eng. Data*, 17(1):55–59, 1972.

[326] Chae-Ho Yim and Yaser A Abu-Lebdeh. Connection between phase diagram, structure and ion transport in liquid, aqueous electrolyte solutions of lithium chloride. *J. Electrochem Soc.*, 165(3):A547–A556, 2018.

[327] Terrell L Hill. An introduction to statistical thermodynamics (paperback). 1987.

[328] A. Sher, Mark van Schilfgaarde, An-Ban Chen, and William Chen. Quasichemical approximation in binary alloys. *Phys. Rev. B*, 36:4279, 1987.

[329] Yanfang Geng, Siliu Chen, Tengfang Wang, Dahong Yu, Changjun Peng, Honglai Liu, and Ying Hu. Density, viscosity and electrical conductivity of 1-butyl-3-methylimidazolium hexafluorophosphate+ monoethanolamine and+ n, n-dimethylethanolamine. *J. Mol. Liq.*, 143(2-3):100–108, 2008.

[330] J Vila, E Rilo, L Segade, O Cabeza, and LM Varela. Electrical conductivity of aqueous solutions of aluminum salts. *Phys. Rev. E*, 71(3):031201, 2005.

[331] Rika Hagiwara and Je Seung Lee. Ionic liquids for electrochemical devices. *Electrochemistry*, 75(1):23–34, 2007.

[332] Douglas R MacFarlane, Maria Forsyth, Patrick C Howlett, Jennifer M Pringle, Jiazeng Sun, Gary Annat, Wayne Neil, and Ekaterina I Izgorodina. Ionic liquids in electrochemical devices and processes: managing interfacial electrochemistry. *Accounts Chem. Res.*, 40(11):1165–1173, 2007.

[333] Xuan Wu, Guang He, and Yi Ding. Dealloyed nanoporous materials for rechargeable post-lithium batteries. *ChemSusChem*, 2020.

[334] Céline Merlet, Benjamin Rotenberg, Paul A Madden, Pierre-Louis Taberna, Patrice Simon, Yury Gogotsi, and Mathieu Salanne. On the molecular origin of supercapacitance in nanoporous carbon electrodes. *Nat. Mater.*, 11(4):306–310, 2012.

[335] Kyoungsoo Kim, Taekyoung Lee, Yonghyun Kwon, Yongbeom Seo, Jongchan Song, Jung Ki Park, Hyunsoo Lee, Jeong Young Park, Hyotcherl Ihee, Sung June Cho, et al. Lanthanum-catalysed synthesis of microporous 3D graphene-like carbons in a zeolite template. *Nature*, 535(7610):131–135, 2016.

[336] Ling Zhang, Jiarun Zhang, Heyun Fu, Haipeng Zhang, Hui Liu, Yuqiu Wan, Shourong Zheng, and Zhaoyi Xu. Microporous zeolite-templated carbon as an adsorbent for the removal of long alkyl-chained imidazolium-based ionic liquid from aqueous media. *Micropor Mesopor Mat.*, 260:59–69, 2018.

[337] Irena Deroche, Lucia Gaberova, Guillaume Maurin, Philip Llewellyn, Maria Castro, and Paul Wright. Adsorption of carbon dioxide in SAPO STA-7 and AlPO-18: Grand canonical Monte Carlo simulations and microcalorimetry measurements. *Adsorption*, 14(2-3):207–213, 2008.

[338] Haruka Kyakuno, Kazuyuki Matsuda, Yusuke Nakai, Tomoko Fukuoka, Yutaka Maniwa, Hirotomo Nishihara, and Takashi Kyotani. Amorphous water in three-dimensional confinement of zeolite-templated carbon. *Chem. Phys. Lett.*, 571:54–60, 2013.

[339] Santiago Aparicio and Mert Atilhan. Choline-based ionic liquids on graphite surfaces and carbon nanotubes solvation: a molecular dynamics study. *J. Phys. Chem. C*, 116(22):12055–12065, 2012.

[340] Vitaly V Chaban and Oleg V Prezhdo. Nanoscale carbon greatly enhances mobility of a highly viscous ionic liquid. *ACS nano*, 8(8):8190–8197, 2014.

[341] Youngseon Shim and Hyung J Kim. Solvation of carbon nanotubes in a room-temperature ionic liquid. *Acs Nano*, 3(7):1693–1702, 2009.

[342] Kun Dong, Guohui Zhou, Xiaomin Liu, Xiaoqian Yao, Suojiang Zhang, and Alexander Lyubartsev. Structural evidence for the ordered crystallites of ionic liquid in confined carbon nanotubes. *J. Phys. Chem. C*, 113(23):10013–10020, 2009.

[343] Ramesh Singh, Joshua Monk, and Francisco R Hung. A computational study of the behavior of the ionic liquid [BMIM+][PF6-] confined inside multiwalled carbon nanotubes. *J. Phys. Chem. C*, 114(36):15478–15485, 2010.

[344] Andrey I Frolov, Kathleen Kirchner, Tom Kirchner, and Maxim V Fedorov. Molecular-scale insights into the mechanisms of ionic liquids interactions with carbon nanotubes. *Faraday Discuss*, 154:235–247, 2012.

[345] Hirotomo Nishihara, Quan-Hong Yang, Peng-Xiang Hou, Masashi Unno, Seigo Yamauchi, Riichiro Saito, Juan I Paredes, Amelia Martínez-Alonso, Juan MD Tascón, Yohei Sato, et al. A possible buckybowl-like structure of zeolite templated carbon. *Carbon*, 47(5):1220–1230, 2009.

[346] Steven J Stuart, Alan B Tutein, and Judith A Harrison. A reactive potential for hydrocarbons with intermolecular interactions. *J. Chem. Phys.*, 112(14):6472–6486, 2000.

[347] Lev Sarkisov and Alex Harrison. Computational structure characterisation tools in application to ordered and disordered porous materials. *Mol. Simulat*, 37(15):1248–1257, 2011.

[348] Mark James Abraham, Teemu Murtola, Roland Schulz, Szilárd Páll, Jeremy C Smith, Berk Hess, and Erik Lindahl. GROMACS: high performance molecular simulations through multi-level parallelism from laptops to supercomputers. *SoftwareX*, 1:19–25, 2015.

[349] David Van Der Spoel, Erik Lindahl, Berk Hess, Gerrit Groenhof, Alan E Mark, and Herman JC Berendsen. GROMACS: fast, flexible, and free. *J. Comput. Chem.*, 26(16):1701–1718, 2005.

[350] Herman JC Berendsen, David van der Spoel, and Rudi van Drunen. GROMACS: a message-passing parallel molecular dynamics implementation. *Comput. Phys. Commun.*, 91(1-3):43–56, 1995.

[351] Somisetti V Sambasivarao and Orlando Acevedo. Development of OPLS-AA force field parameters for 68 unique ionic liquids. *J. Chem. Theory Comput.*, 5(4):1038–1050, 2009.

[352] Borja Docampo-Álvarez, Víctor Gómez-González, Trinidad Méndez-Morales, Jesús Carrete, Julio R Rodríguez, Óscar Cabeza, Luis J Gallego, and Luis M Varela. Mixtures of protic ionic liquids and molecular cosolvents: A molecular dynamics simulation. *J. Chem. Phys.*, 140(21):214502, 2014.

[353] Hadrián Montes-Campos, José Manuel Otero-Mato, Roberto Carlos Longo, Oscar Cabeza, Luis Javier Gallego, and Luis Miguel Varela. Mixtures of lithium salts and ionic liquids at defected graphene walls. *J. Mol. Liq.*, 289:111083, 2019.

[354] Trinidad Mendez-Morales, Jesus Carrete, Silvia Bouzon-Capelo, Martin Perez-Rodriguez, Oscar Cabeza, Luis J Gallego, and Luis M Varela. MD simulations of the formation of stable clusters

in mixtures of alkaline salts and imidazolium-based ionic liquids. *J. Phys. Chem. B*, 117(11):3207–3220, 2013.

[355] Shimou Chen, Keita Kobayashi, Yasumitsu Miyata, Naoki Imazu, Takeshi Saito, Ryo Kitaura, and Hisanori Shinohara. Morphology and melting behavior of ionic liquids inside single-walled carbon nanotubes. *J. Am. Chem. Soc.*, 131(41):14850–14856, 2009.

[356] Gerald J Wang and Nicolas G Hadjiconstantinou. Why are fluid densities so low in carbon nanotubes? *Phys. Fluids*, 27(5):052006, 2015.

[357] Hongjun Liu and Stephen J Paddison. Direct calculation of the x-ray structure factor of ionic liquids. *Phys. Chem. Chem. Phys.*, 18(16):11000–11007, 2016.

[358] Chenlu Wang, Yanlei Wang, Yumiao Lu, Hongyan He, Feng Huo, Kun Dong, Ning Wei, and Suojiang Zhang. Height-driven structure and thermodynamic properties of confined ionic liquids inside carbon nanochannels from molecular dynamics study. *Phys. Chem. Chem. Phys.*, 21(24):12767–12776, 2019.

[359] Jason K Holt, Hyung Gyu Park, Yinmin Wang, Michael Stadermann, Alexander B Artyukhin, Costas P Grigoropoulos, Aleksandr Noy, and Olgica Bakajin. Fast mass transport through sub-2-nanometer carbon nanotubes. *Science*, 312(5776):1034–1037, 2006.

[360] Giancarlo Cicero, Jeffrey C Grossman, Eric Schwegler, Francois Gygi, and Giulia Galli. Water confined in nanotubes and between graphene sheets: A first principle study. *J. Am. Chem. Soc.*, 130(6):1871–1878, 2008.

[361] C Iacob, JR Sangoro, WK Kipnusu, R Valiullin, J Kärger, and F Kremer. Enhanced charge transport in nano-confined ionic liquids. *Soft Matter*, 8(2):289–293, 2012.

[362] Stephan Thürmer, Yoshikazu Kobayashi, Tomonori Ohba, and Hirofumi Kanoh. Pore-size dependent effects on structure and vibrations of 1-ethyl-3-methylimidazolium tetrafluoroborate in nanoporous carbon. *Chem. Phys. Lett.*, 636:129–133, 2015.

[363] Seiji Tsuzuki, Wataru Shinoda, Md Shah Miran, Hiroshi Kinoshita, Tomohiro Yasuda, and Masayoshi Watanabe. Interactions in ion pairs of protic ionic liquids: Comparison with aprotic ionic liquids. *J. Chem. Phys.*, 139(17):174504, 2013.

[364] Koichi Fumino, Alexander Wulf, and Ralf Ludwig. The potential role of hydrogen bonding in aprotic and protic ionic liquids. *Phys. Chem. Chem. Phys.*, 11(39):8790–8794, 2009.

[365] Yunxia Yang, Craig M Brown, Chunxia Zhao, Alan L Chaffee, Burke Nick, Dongyuan Zhao, Paul A Webley, Jacob Schalch, Jason M Simmons, Yun Liu, et al. Micro-channel development and hydrogen adsorption properties in templated microporous carbons containing platinum nanoparticles. *Carbon*, 49(4):1305–1317, 2011.

[366] Joshua D Moore, Jeremy C Palmer, Ying-Chun Liu, Thomas J Roussel, John K Brennan, and Keith E Gubbins. Adsorption and diffusion of argon confined in ordered and disordered microporous carbons. *Appl. Surf. Sci.*, 256(17):5131–5136, 2010.